

**DYNAMIC ANALYSIS INCLUDING STABILITY OF INFINITELY  
LONG FLEXIBLY SUPPORTED JOURNAL BEARINGS WITH  
MICROPOLAR LUBRICANT**

**A**

**Thesis Report**

**Submitted in partial fulfillment of the requirement for the award of  
degree**

**MASTER OF ENGINEERING  
IN  
CAD/CAM & ROBOTICS**

**Submitted By**

**ANIRBAN DAS**

**Roll No. 800881025**

**Under the Guidance of**

**Dr. A.K.CHATTOPADHYAY**

**Professor & H.O.D.**

**Mechanical Engineering Department  
Mody Institute of Technology & Science  
Lakshmangarh, Rajasthan**



**DEPARTMENT OF MECHANICAL ENGINEERING  
THAPAR UNIVERSITY  
PATIALA-147004, INDIA**

## CERTIFICATE

This is to certify that the work which is being presented in this thesis report entitled "*Dynamic analysis including stability of infinitely long flexibly supported journal bearings with micropolar lubricant*" in partial fulfillment of requirement for the award of the master degree in CAD/CAM & Robotics submitted in the mechanical engineering department, Thapar University, Patiala, is an authentic record of the initial work carried out by me under the guidance of **Dr. A.K.CHATTOPADHYAY**, Professor & H.O.D., Mechanical Engineering Department, Mody Institute of Technology & Science, Lakshmangarh, Rajasthan.

The matter embodied in this report has not been submitted in part or full to any other university or institute for the award of any degree.

Dated: 9<sup>th</sup> July, 2010


  
Anirban Das


This is to certify that above declaration made by the student concerned is correct to the best of my knowledge & belief.



**Dr. A.K.CHATTOPADHYAY**  
Professor & H.O.D.  
Mechanical Engineering Department  
Mody Institute of Technology & Science,  
Lakshmangarh, Rajasthan

Countersigned by

  
**Dr. S.K. MOHAPATRA**  
Professor and H.O.D.  
Mechanical Engineering Department  
Thapar University, Patiala

  
**Dr. R.K. SHARMA**  
Dean of Academic Affairs  
Thapar University  
Patiala

## ACKNOWLEDGEMENT

I am highly grateful to the authorities of Thapar University, Patiala for providing this opportunity to carry out the thesis work.

I would like to express a deep sense of gratitude and thank profusely to my thesis guide **Dr.A.K.Chattopadhyay** for his sincere & invaluable guidance, suggestions and attitude which inspired me to submit thesis report in the present form.

I am especially thankful to **Mr.J.S.Saini, Mr.Anirban Bhattacharya, Mr. Ravinder Kumar Duvedi** assistant professors, Mechanical Engg. Department, TU, Patiala for their invaluable guidance.

I am also thankful to other faculty members of Mechanical Department, TU, Patiala for their intellectual support. My special thanks are due to my family members and friends who constantly encouraged me to complete this study.



Anirban Das

## ABSTRACT

The aim of the present thesis is to study theoretically, using finite difference techniques, the stability characteristics of infinitely long flexibly supported hydrodynamic journal bearings lubricated with micropolar fluid. The theoretical study has been presented using the linear analysis based on the perturbation method. Parametric studies have been conducted and stability characteristics have been obtained and a comparison of the results of newtonian and micropolar fluid analyses for different parameters have been compared and presented. A modified Reynolds equation has been obtained using micropolar lubrication theory and the solution of pressure obtained from this equation is used in the governing differential equations of motion for external stiffness and damping, to arrive at a stability threshold.

## NOTATIONS

C	Radial clearance (m)
$C_B$	Body couple per unit mass of micropolar fluid ( $m^2/s^2$ )
D	journal diameter (m)
$D_{ij}$	damping co-efficient of micropolar fluid film, for $i=R, \varphi$ and $j=R, \varphi$ (Ns/m)
$\bar{D}_{ij}$	dimensionless damping co-efficient of micropolar fluid film
$F_B$	body force per unit mass of micropolar fluid ( $m/s^2$ )
$F_i$	force component along the R and $\varphi$ direction
h	local film thickness (m)
$\bar{h}$	non-dimensional film thickness = $h/C$
$l_m$	non-dimensional characteristic length of the micropolar fluid = $\Lambda/C$
M	mass parameter (kg)
$\bar{m}$	non-dimensional parameter = $MC\omega^2/W_0$
$\bar{M}_c$	critical value of non-dimensional parameter
N	coupling number = $[\chi/(2\mu+\chi)]^{1/2}$
P	micropolar film pressure in the film region in the non-linear analysis (Pa)
$\bar{p}$	Non-dimensional micropolar film pressure in the film region in the non-linear analysis.
$p_i$	local micropolar film pressure in the film region , $i=0,1$ and $2$ for the steady State & first order perturbed film pressure along the $\varepsilon_0$ and $\varphi$ directions (Pa)

$\bar{p}_i$	non-dimensional local micropolar film pressure in the film region , $i=0,1$ and $2$ for the steady state and first Order perturbed film pressure along the $\varepsilon_0$ and $\varphi$ directions (Pa)
$S_{ij}$	stiffness of the micropolar fluid film for $i=R,\varphi$ and $j=R, \varphi$ (N/m)
$\bar{S}_{ij}$	dimensionless damping co-efficient of the micropolar fluid film $= 2C^3 S_{ij} / (\mu\omega R^3 L)$ For $i=R, \varphi$ and $j=R, \varphi$
T	time (s)
U	velocity of journal= $\omega R$ (m/s)
$v$	microrotational velocity vector
V	velocity vector (m/s)
$W_0$	steady state load in the bearing (N)
$\bar{W}_0$	non-dimensional steady state load in the bearing $= 2C^2 W_0 / (\mu\omega R^3 L)$
x	Cartesian coordinate axis along the circumferential direction= $R\theta$ (m)
z	Cartesian coordinate axis along the bearing axis (m)
$\bar{z}$	non-dimensional Cartesian coordinate axis along the bearing axis $= 2z / L$
$\alpha, \beta, \gamma$	viscosity co-efficient of the micropolar fluid (kg m/s)
$\varepsilon_i$	perturbed eccentricity for $i=R$ and $\varphi$
$\varepsilon_0$	steady state eccentricity ratio
$\theta$	circumferential coordinate (rad)
$\lambda_R$	whirl ratio
$\Lambda$	characteristic length of the micropolar fluid= $[\gamma/(4\mu)]^{1/2}$ (m)

$\mu, \lambda$	Newtonian viscosity co-efficient (Pa s)
$\mu_v$	effective viscosity coefficient of the micropolar fluid $= (2\mu + \chi)/2$ (Pa s)
$\pi^*$	thermodynamic pressure
$\rho$	mass density ( $\text{kg/m}^3$ )
$\tau$	non-dimensional time $= \omega t$
$\Phi$	attitude angle (rad)
$\Phi_0$	steady state attitude angle (rad)
$\chi$	spin viscosity coefficients of the micropolar fluid (Pa s)
$\omega$	angular velocity of the journal (rad/s)
$\omega_p$	angular velocity of the orbital motion of the journal centre (rad/s)
d	Damping co-efficient of the support
$\bar{d}$	Non-dimensional damping co-efficient of the support
K	Stiffness co-efficient of the support
$\bar{K}$	Non-dimensional stiffness co-efficient of the support

### **ABBREVIATION USED**

SRR=Stiffness in r-direction due to disturbance in r-direction= $S_{rr}$

SPP= Stiffness in  $\phi$ -direction due to disturbance in  $\phi$ -direction= $S_{\phi\phi}$

SRP= Stiffness in  $\phi$ -direction due to disturbance in r-direction = $S_{r\phi}$

SPR= Stiffness in r-direction due to disturbance in  $\phi$ -direction = $S_{\phi r}$

DRR= Damping co-efficient in r-direction due to disturbance in r-direction = $D_{rr}$

DPP= Damping co-efficient in  $\phi$ -direction due to disturbance in  $\phi$ -direction = $D_{\phi\phi}$

DRP= Damping co-efficient in  $\phi$ -direction due to disturbance in r-direction = $D_{r\phi}$

DPR= Damping co-efficient in r-direction due to disturbance in  $\phi$ -direction =  $D_{\phi r}$

$\bar{d}$  = Non-dimensional damping co-efficient of the support= $\overline{DBAR}$

$\bar{K}$  = Non-dimensional stiffness co-efficient of the support= $\overline{KBAR}$

$\bar{z}$  = non-dimensional Cartesian coordinate axis along the bearing axis= $\overline{ZBAR}$

## LIST OF FIGURES

Fig .1: Schematic diagram of flexibly supported hydrodynamic journal bearing.	13
Fig 3.1: Bearing configuration for the derivation of Reynolds equation.	40
Fig 4.1: Schematic diagram of hydrodynamic journal bearing under steady state condition.	47
Fig.4.1.1: Variation of load parameter with $l_m$ for various values of $N$ (AN).	48
Fig.4.1.2: Variation of load parameter with $l_m$ for various values of $\epsilon_0$ .	48
Fig.4.1.3: Variation of attitude angle with $l_m$ for various values of $N$ (AN).	49
Fig.4.1.4: Variation of attitude angle with $l_m$ for various values of $\epsilon_0$ .	49
Fig 4.2: Schematic diagram of hydrodynamic journal bearings under dynamic Operating Condition.	56
Fig.4.2.1: Variation of $\overline{S}_{RR}$ with $l_m$ for various values of $N$ (AN).	69
Fig.4.2.2: Variation of $\overline{S}_{PR}$ with $l_m$ for various values of $N$ (AN).	70
Fig.4.2.3: Variation of $\overline{S}_{RP}$ with $l_m$ for various values of $N$ (AN).	70
Fig.4.2.4: Variation of $\overline{S}_{PP}$ with $l_m$ for various values of $N$ (AN).	71
Fig.4.2.5: Variation of $\overline{D}_{RR}$ with $l_m$ for various values of $N$ (AN).	71
Fig.4.2.6: Variation of $\overline{D}_{PR}$ with $l_m$ for various values of $N$ (AN).	72
Fig.4.2.7: Variation of $\overline{D}_{RP}$ with $l_m$ for various values of $N$ (AN).	72
Fig.4.2.8: Variation of $\overline{D}_{PP}$ with $l_m$ for various values of $N$ (AN).	73
Fig.4.2.9: Variation of $\overline{S}_{RR}$ with $l_m$ for various values of $\epsilon_0$ .	73
Fig.4.2.10: Variation of $\overline{S}_{PR}$ with $l_m$ for various values of $\epsilon_0$ .	74
Fig.4.2.11: Variation of $\overline{S}_{RP}$ with $l_m$ for various values of $\epsilon_0$ .	74
Fig.4.2.12: Variation of $\overline{S}_{PP}$ with $l_m$ for various values of $\epsilon_0$ .	75
Fig.4.2.13: Variation of $\overline{D}_{RR}$ with $l_m$ for various values of $\epsilon_0$ .	75
Fig.4.2.14: Variation of $\overline{D}_{PR}$ with $l_m$ for various values of $\epsilon_0$ .	76

Fig.4.2.15: Variation of $\bar{D}_{RP}$ with $l_m$ for various values of $\epsilon_0$ .	76
Fig.4.2.16: Variation of $\bar{D}_{PP}$ with $l_m$ for various values of $\epsilon_0$ .	77
Fig 4.3: Schematic diagram of co-ordinate system.	60
Fig.4.3.1: Variation of $\bar{M}_C$ with $l_m$ for various values of $N$ (AN).	77
Fig.4.3.2: Variation of $\bar{M}_C$ with $l_m$ for various values of $\epsilon_0$ .	78
Fig.4.3.3: Variation of $\bar{M}_C$ with $\bar{K}$ for various values of $\epsilon_0$ .	78
Fig.4.3.4: Variation of $\bar{M}_C$ with $\bar{K}$ for various values of $\bar{d}$	79
Fig.4.3.5: Variation of $\lambda_R$ with $l_m$ for various values of $N$ (AN).	79
Fig.4.3.6: Variation of $\lambda_R$ with $l_m$ for various values of $\epsilon_0$ .	80
Fig.4.3.7: Variation of $\lambda_R$ with $l_m$ for various values of $\epsilon_0$ .	81

# INDEX

SL.NO.	TOPIC	PAGE NO.
	<b>Certificate</b>	<b>1</b>
	<b>Acknowledgement</b>	<b>2</b>
	<b>Abstract</b>	<b>3</b>
	<b>Notations</b>	<b>4</b>
	<b>List of figures</b>	<b>8</b>
	<b>CHAPTER 1 :Introduction and aim</b>	
1.1	Introduction	14
1.2	About the thesis	18
	<b>CHAPTER 2 : Literature Review</b>	
2.1	Introduction	19
2.2	Theory of micropolar fluid	21
2.3	Flexibly supported bearings with micropolar lubrication	23
	<b>CHAPTER 3 : Problem Formulation</b>	
3.1	<b>Work procedure</b>	26
3.2	<b>Basic Governing Equation</b>	
3.2.1	Introduction	27
3.2.2	Field equations	27
3.2.3	Derivation of modified Reynolds equation	28
3.2.4	Study of non-dimensional parameters	33

3.2.5	Velocity and microrotational velocity vectors	35
	<b>CHAPTER 4 : Theoretical Analysis</b>	
4.1	<b>Theoretical analysis of the steady state characteristics</b>	
4.1.1	Introduction	41
4.1.2	Theoretical analysis	41
4.1.2.1	Governing equation	41
4.1.2.2	Numerical solution for pressures	43
4.1.2.3	Pressure Profiles	44
4.1.3	Results and discussion	45
4.1.3.1	Load carrying capacity ( $\overline{W}_0$ )	45
4.1.3.2	Attitude angle ( $\phi_0$ )	46
4.2	<b>Dynamic analysis</b>	
4.2.1	Introduction	50
4.2.2	Theoretical analysis	51
4.2.2.1	Governing equation	51
4.2.3	Perturbation technique	52
4.2.3.1	Numerical solution for pressures	54
4.2.3.2	Perturbed Pressure Equations	54
4.2.4	Stiffness and damping coefficients	56
4.2.5	Equation of motion	58
4.2.6	Results and discussion	66

4.2.6.1	Non-dimensional components of stiffness and damping coefficients.	66
4.2.6.2	Critical mass parameter ( $\bar{M}_c$ )	67
4.2.6.3	Whirl ratio ( $\lambda_R$ )	68
	<b>CHAPTER 5 : Conclusion And Scope For Future Work</b>	
5.1	Conclusion	82
5.2	Scope For Future Work	83
	<b>CHAPTER 6 : References</b>	
6.1	References	84
	<b>CHAPTER 7 : Appendices</b>	
7.1	Appendix-I: Programme For Calculating Load Carrying Capacity, Attitude Angle, Stiffness & Damping Of Infinitely Long Hydrodynamic Journal Bearings With Micropolar Lubricants.	89
7.2	Appendix-II: Programme For Calculating Load Carrying Capacity, Attitude Angle, Stiffness & Damping Of Infinitely Long Hydrodynamic Journal Bearings With Newtonian fluids.	96
7.3	Appendix-III: Programme For Calculating Bearing Stability Parameter of Infinitely Long Flexibly Supported Hydrodynamic Journal Bearings.	104
7.4	Appendix-IV: Additional Literature Review	107
7.5	Appendix-V: Reference of Additional Literature Review	109

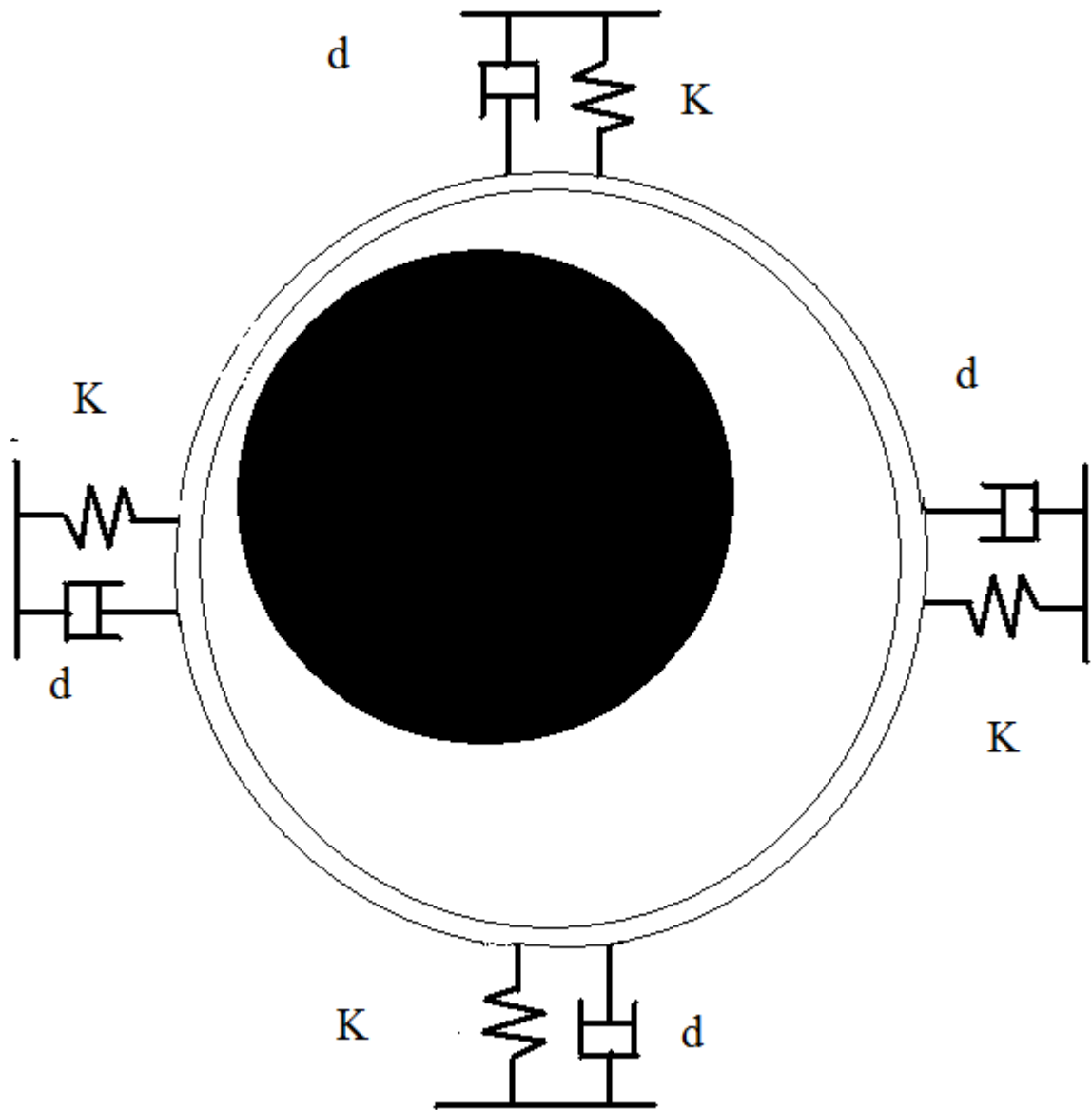


Fig .1: Schematic diagram of flexibly supported hydrodynamic journal bearing.

# 1. INTRODUCTION & AIM

## 1.1 Introduction

A *bearing* is a mechanical element which locates two machine parts relative to each other and permits a relative motion between them. The use of bearings is in vogue for centuries, but the recent developments in science and technology demands critical designs of bearings with high precision and optimum performance even in the most adverse working conditions. The rapid developments in the fields of rocketry and missile technology, cryogenics, aeronautics and space engineering, nuclear engineering, electronics, computer sciences and technologies, bio-medical engineering and a lot more fields in science and technology make the aspects of designing bearings more and more challenging and innovative. Moreover, the mode, time and place of operations demand exploration of new materials, lubricants and even lubrication theories and technologies.

However, all bearings used today are categorized into two main classes depending on their functions— (1) rolling contact bearings and (2) sliding contact bearings. As the name suggests the rolling contact bearings use rolling elements at the points of contact of the surfaces in relative motion and thus reduce the friction. They consist of different ball bearings and roller bearings. The sliding friction bearings are based upon two concepts of lubrication— (a) sliding friction thin film lubrication or boundary film lubrication and (b) sliding friction thick film lubrication. The sliding friction thick film lubrication is further categorized into two different groups, namely— (i) self-acting or hydrodynamic lubrication, and (ii) externally pressurized or hydrostatic lubrication.

In hydrodynamic lubrication the load carrying capacity is generated due to the development of positive pressure within the fluid film between two surfaces by virtue of relative motion of the surfaces. The load supporting pressure is developed due to the following mechanisms:

(i) Formation of a convergent wedge-shaped film due to the dragging of fluid into such a clearance space owing to the shape and mode of operation of the bearing. These types of bearings are particularly known as wedge film bearings.

(ii) The resistance of the viscous fluid being squeezed out from the space between two surfaces relatively approaching or oscillating with relative normal motion. The bearings operating under this principle are known as squeeze film bearings.

As the magnitude of hydrodynamic pressure depends upon the relative tangential or normal velocity, sometimes the developed pressure may not be sufficient for obtaining the desired load carrying capacity, particularly at the low relative velocity and thereby demands external supply of pressurized lubricants. This type of lubrication is called externally pressurized or hydrostatic lubrication. These bearings are also known as hybrid bearings as their operational principle includes both self-acting and external pressurization.

However, it has been observed that the hydrodynamic journal bearings can show excellent performances in withstanding static load, but fail easily under dynamic conditions if not critically designed for the specific purpose.

Though dry lubrication like lubrication with graphite, molybdenum disulphide etc. are used in some cases, *e.g.* in extrusion processes in cold and hot working, most of the above types of bearings are lubricated with fluids *i.e.* with liquids and gases. Under the general industrial operating conditions such Newtonian lubricating fluids become contaminated with microstructures like dust and worn out metal particles. As the classical continuum theory becomes erroneous in the analysis of such lubrication, microcontinuum approach seems to be more appropriate.

The characteristic behavior of the substances under the influence of external forces can be best explained from two distinct viewpoints. According to the first one, which is commonly known as atomistic or discrete viewpoint, every material is considered to be a large number of molecules and atoms held together by intermolecular and interatomic forces. The occurrences of different physical phenomena are considered as the results of various statistical averages of the individual motions of all these molecules or atoms, and different material properties are calculated in terms of parameters characterizing the basic geometrical orientation of such primitive elements and the molecular forces. As this model usually finds very limited scope due to the crude approximations that have to be made in calculation in order to simplify the mathematical difficulties involved, the second viewpoint, commonly known as continuum field approach, the fundamental concepts of which had its origin well over two centuries ago in the works of Euler and later Cauchy gradually finds its application. The basic assumption underlying the

classical theories of continuum mechanics is the existence of the continuity of mass *i.e.* the existence of a continuous mass density at every geometrical point, for which any volume element  $\Delta V$  can be taken to its limit  $dV$  without affecting the homogeneity of the mass distribution. Thus the identities of the material points in a volume element are lost and their individual motions are considered in a global sense coinciding with that of the centre of the mass of the volume element. This classical continuum theory has found wide acceptance as a physical theory. But the atomistic models of materials especially of the fluids having coarse structures and fibers (such as colloidal fluids, liquid crystals and fluids containing additives) have shown that the mass density can differ drastically from the continuum mass, when the size  $\Delta V$  falls below a certain critical limit but still in the macroscopic range. Hence the continuum approach for mass density is no longer applicable. The classical continuum theory is expected to break down either by avoiding certain physical phenomena completely or leading to gross approximations. The classical continuum theory is also likely to give erroneous results for the typical class of problems like flow through narrow passages or through fine capillaries, where the characteristic length scale is comparable to the average molecular or grain size contained in the fluid, as in such cases the molecular or granular constituents of the medium are excited individually and the intrinsic motion of the material constituents must have to be considered.

As the atomistic model indicates that the continuous mass density cannot prevail when the volume element  $\Delta V$  falls beyond a certain critical volume  $\Delta V^*$ , the continuum theory in general is applied considering that  $\Delta V \geq \Delta V^*$ , or extending in the region  $\Delta V < \Delta V^*$  with the consideration of deformation in the volume element.

The feasibility of deformation of the volume to an extent to the primitive element not only is debatable, but also makes the calculation more complex, in the region  $\Delta V < \Delta V^*$  which may occur in a hydrodynamic bearing in practical usage, where the volume of the contaminated sub-structures may be comparable to the film thickness, and the application of the microcontinuum approach becomes highly justified.

Based upon the microcontinuum approach, the first consistent theory of fluid microcontinua, was presented by **Eringen** [31]. The microfluid was considered to contain microstructures having individual mass and velocity, in as much as the macrovolume element contains the microvolume elements and those microstructures can translate, rotate and deform independently of the motion of the macrovolume. The theory

included the mechanism to support the local stress moments and body moments and to consider the influence of the spin inertia of each microelement. But this theory of microfluid is too complicated and the mathematical model is not so acquiescent to the solution of the non-trivial problems. **Eringen**, therefore, again simplified the theory [36], postulating a subclass of the microfluids, called micropolar fluids, considering the microrotational effects and ignoring the microdeformation effects of the substructures and permitting the surface and the body couples. The theory included two independent kinematic vector fields representing the translation velocities and the angular or spin velocities of the microstructures *i.e.* translation velocity vector and microrotational velocity vector. Although contemporary theories of fluid microcontinua were also presented by various authors, the basic field equations, however, remained similar to those of **Eringen** [31]. Physically the fluid consisting of bar like elements may be represented as micropolar fluid. The theory of micropolar fluid, thus, may be a satisfactory model for analyzing the flow behaviors of real fluid suspensions, polymeric fluids and fluid consisting of polymeric additives as is mixed with the engine oil for enhancing lubricating effectiveness, certain anisotropic fluids, *e.g.* liquid crystals consisting of dumbbell shaped molecules and possibly animal blood. Hence the theory of micropolar fluid has found its application as a refined model for studying the behavior of such fluid flows as in the field of lubrication, where the clearance in a bearing is comparable to the average grain size or molecular size of a non-Newtonian fluid *viz.* a polymeric fluid or in the practical usage where the lubricants under general operating conditions become fluid suspensions after being contaminated with dirt and worn out metal particles. For an important practical example, in the area of nuclear power plant, where sodium, which is used in a dual role of a heat transfer agent and a lubricant in the journal bearing supporting the mixing screw in the batch mixers exhibits the non-Newtonian micropolar characteristics. The microcontinuum theory finds another worth-mentioning application in the study of blood rheology because the sizes of the blood cells are comparable to the diameters of the arteries and thus, there may exist the possible rotation and deformation of each blood cell while flowing through arteries. Hydrodynamic bearings are generally used in cases when the relative velocity are high enough as a result of continuous increase in the sizes and speeds of the rotating machinery or due to use of fluids having kinematic viscosity, the oil film close in the bearings frequently becomes turbulent.

Again keeping in mind the extremely small radial clearance to facilitate ease of alignment flexibly supported bearings have come into vogue. Therefore, it is important to do a study on stability of such infinitely long flexibly supported journal bearing.

## **1.2 ABOUT THE THESIS**

The aim of the present thesis is to investigate and predict theoretically the static and dynamic characteristics including the stability of flexibly supported infinitely long hydrodynamic oil journal bearings lubricated with the micropolar fluids. The dissertation has been divided into some chapters.

A brief review of the relevant literature is included in Chapter 2.

In chapter 3, the derivation of Reynolds equation has been modified by the basic equations *i.e.* the equation of continuity of mass, the equations for the balance of linear momentum and the balance of angular momentum, which are coupled together due to the existence of two kinematic vector fields of the microstructures and characterizing the micropolar fluid.

In chapter 4, the theoretical prediction of hydrodynamic pressures in the bearing is obtained by the solution of modified Reynolds equation satisfying the appropriate boundary conditions. The steady state pressure profile is obtained easily by finite difference technique with successive over-relaxation scheme. The steady state parameters like load carrying capacity, attitude angle can be easily obtained once the pressure profile over the entire bearing surface has been found.

For dynamic pressure, using linearized analysis, first order perturbations of eccentricity ratio and attitude angle are used, and the resulting equations are solved by finite difference method with successive over-relaxation scheme. Knowledge of the perturbed pressures enables one to obtain the dynamic characteristics in terms of the components of stiffness and damping coefficients. Stiffness and damping coefficients aside, the dynamic characteristics also include the threshold stability and the whirl ratio for external stiffness and external damping co-efficient.

In addition to the linearized stability analysis have also been considered in the rotor bearing system to get actual threshold of stability and the values obtained in parametric study in which we will vary different parameters and check the stability.

Finally, important conclusions based on the work presented in the earlier chapters of this dissertation are summarized and scope for future work are reported in Chapter 5.

A list of references, and appendices are provided at the end of the dissertation.

## 2. LITERATURE REVIEW

### 2.1 INTRODUCTION

The first formulation of a hypothesis regarding the force necessary to overcome the viscous resistance of a fluid was derived by **Newton** [1] in 1668, **Petroff** [2] made the first significant contribution theoretically in 1883 with his consideration of the effect of viscous force in the fluid film lubrication.

**Tower's** [3] experiments for the determination of suitable methods of lubricating railway axle bearings, which were partial bearings lubricated from an oil bath, were the first significant experimental studies and the developed pressure distribution in the bearing clearance under the loaded condition as measured through a number of pressure gauges at the midplane in the circumferential direction was found to exhibit a peak, which was several times higher than the mean pressure calculated on the basis of the projected area. Just after three years of **Tower's** first experiments, **Reynolds** [4] presented a theoretical study to justify the experimental results of **Tower**. The experiments of **Tower** and the analysis of **Reynolds** may be considered as the entrance to the concept of hydrodynamic lubrication and the field of *Tribology*.

Since the development of the concept of the hydrodynamic lubrication about 120 years ago with the experiments of **Tower** [3] and theoretical study of **Reynolds** [4] lot of theoretical, experimental and analytical studies were presented by a number of authors. A few of them considered as benchmark work are only briefly reported.

At the age of infancy of tribology the experimental and theoretical analyses were based upon the use of liquid lubrication. But almost within a decade the science reached its maturity following the experiments of **Kingsbury** [5], who not only extended the concept of hydrodynamic lubrication to the gasses by using air as lubricant, but also developed an experimental set up to study the behaviours of gas bearings based on the concept of electrical analogy. The first exact solution of Reynolds equation for pressure distribution for a full journal bearing using full film boundary condition was presented by **Sommerfeld** [6] in 1904 alongwith the load and friction characteristics in terms of eccentricity ratio.

**Harrison** [7] in 1913 enriched the hydrodynamic lubrication through his experiments with special reference to air as lubricant. **Rayleigh** [8] first investigated the effect of film

shape on the operating characteristics of a bearing using the calculus of variations. **Christopherson** [9] pioneered in establishing the suitability of the Southwell's relaxation method for the lubrication problems and using the relaxation method **Cameron** and **Wood** [10] obtained the solution of finite bearings and presented bearing characteristics for two slenderness ratios using realistic boundary conditions. During the same time **Vogelpohl** [11] developed an approximate solution based on infinite series. **Ocvirk** [12] presented the solution of the Reynolds equation using narrow bearing approximation.

Theoretical research on the dynamic characteristics of impervious self-acting oil bearing was initiated by **Harrison** [13], who showed that hydrodynamic equations for a light rigid rotor, supported by a pair of infinitely long bearings with full film, are satisfied by an orbital motion of the journal axis under a constant load.

However, the derivation of Reynolds equation was based upon the assumptions relating to cavitations, fluid inertia forces and non-linear flow effects. Among the studies of the effect of the convective inertia forces on the hydrodynamic lubrication **Kahlert** [14] and **Osterle** and **Saibel** [15] are always cited for their pioneering studies. The investigation of cavitations in the lubricating film was initiated with the experiments of **Coles** and **Hughes** [16], which showed that the end of the pressure curve was coinciding with the position of zero pressure gradient, which however, conflicted with the experimental results of **Jacobson** and **Floberg** [17], which indicated that the pressure cavitated somewhere beyond the point observed. However, the experimental evidences since the early years of last century put forward the realization of the existence of a separate lubrication theory for fluid suspension and the effort for establishing a theory was intensified since mid of the last century. The early studies on such theories of fluid micro-continua have no concern with the research works of bearings. The theory was later simplified to an acceptable fluid film lubrication theory, called micropolar lubrication theory and in subsequent years this simplified micropolar lubrication theory was introduced in the analyses of bearings.

The present work has, therefore, been aimed at studying the lubrication effectiveness of hydrodynamic journal bearings using micropolar lubrication under the abovementioned operational situations. Hence, in what follow, an attempt has been made to present a brief review of the available literature in the following sequence:

- (a) A review of the theory of micropolar fluid.
- (b) A review of flexibly supported bearings with micropolar lubrication.

## **2.2 THEORY OF MICROPOLAR FLUID**

The development of the theory of micropolar fluid was initiated with the development of the theory on micro-continuum approach. For the application of the classical continuum theory in the field of film lubrication, the most practical importance is whether the deep molecular orientation results in any rheological abnormalities in the vicinity of the solid surfaces; and the significant differences in the behavior of the molecules of the liquid in intimate contact with and adhering to the surfaces or to absorbed layers on the surface from the behavior of the adjacent molecules of the fluid in the bulk are found obvious and the experimental evidences may be worth mentioning herein.

**Kingsbury [18]** observed such rheological abnormalities that varied from a small enhancement of viscosity to rigidity in the adhering layer ranging from 10–3 mm to 10–7 mm and attributed this difference in the behavior of the molecules to a possible intensified viscosity in that part of the fluid within the range of the attraction of the surface molecules of the metal. In 1909 **Cosserat** and **Cosserat [19]** developed the theories of oriented media in which there existed three directors at each point. The work of **Jeffery [20]** was the first to study the effect of the behavior of the Newtonian fluid of infinite extent in presence of a single ellipsoidal particle and the result indicated the enhancement of the viscosity of such fluid suspension than its base fluid. **Hardy** and **Nottage [21]** concluded that to be beyond the range of surface influence, the liquid film must be between 0.00762 to 0.01015 mm. in thickness. **Needs [22]**, through a series of experiments of the boundary surface influences on the viscosity of thin lubricating films squeezed in between two optically plane parallel circular disks approaching each other with no tangential velocity and film thickness down to 0.000635 mm, found an increasing time lag for the plates in their time of approach than that predicted by classical Newtonian theory for the film thickness below 0.00127 mm, indicating the increase in the effective viscosity of the film in that zone. He found the evidences where the effective viscosity in the boundary film increased nearly five times than that in the bulk. **Buckley's [23]** experiment showed the total loss of rigidity in clean liquid at a distance of  $0.3 \times 10^{-4}$  mm from a solid boundary. The unexpected behavior of the fluid containing oblong molecules in a shear field was recognized by **Anzeliuss [24]** and this

dependence of the stress and moment at each point of the fluid was expressed by him as a function of the usual rate of strain tensor and the orientation of the substructure. In an experiment of the Couette type flow performed on leuben oil containing additives of aluminum naphthenate up to 2%, **Henniker [25]** found an extensive tenfold increase in the viscosity within 50000A of the surface. Later by squeeze film experiments of various fluids (*e.g.* solutions of pure fatty acids in pure hydrocarbon solvents) between two plates submerged in the fluid and by measuring the gap between the plates as a function of time **Fuks [26,27]** found the existence of a residual film between the plates even after squeezing for a very long time, similar to those obtained by **Needs [28]** and also observed that the thickness of such residual film increased with the increase in fatty acid concentration, the chain length of the hydrocarbon in both solvent and fatty acid and the surface energy of the solid substrate. A few more experiments by **Hoyt and Fabula [29]** and by **Vogel and Patterson [30]** showed that the mixing of some extremely small amount of polymeric additives in the lubricating fluid reduced the skin friction near a rigid body than in such a fluid to an extent of 30-35%.

Subsequent to the introduction of micro-elastic solids, **Eringen [31]** in 1964 proposed a similar theory— the basic equations, jump conditions and constitutive equations of '*simple microfluent*' media, exhibiting similar micro-effects. These fluids, named as '*simple microfluids*' are considered to be a fluent medium and a generalization of the Stokesian fluids whose properties and behavior are affected by the local motions of the material particles contained in each of its volume element. Non-linear Stokesian fluids are considered to be a special class of simple micro-fluids. As these fluids possess local inertia, Eringen extended continuum theory to consider: (a) conservation of micro-inertia moments, and (b) balance of first stress moments, and developed and discussed the concepts of inertial spin, body moments, gyration tensors, stress moments, wherein the stresses and stress moments were expressed as the functions of deformation rate tensor and various microdeformation rate tensors. A simple microfluid in its simplest form has as many as twenty two viscosity coefficients and the fluids in which gyrational effects are important, such as anisotropic fluids, vortex fluids and fluid having surface tensions are guessed to fall in this group.

In 1965 **Eringen [32,33]** presented the theory of micromorphic material. As even the linear theory was too complicated for engineering application, **Eringen [34]** simplified it with the consideration of a subclass of micromorphic materials, named as micropolar

media. The study however presented the discussions on deformation and motion, laws of motion, constitutive equations, theory of micropolar media, micropolar viscoelasticity, micropolar materials with attenuating neighborhood and the problem of micropolar channel flow, with the assumptions of linear constitutive equations, microisotropic medium and negligible heat conduction. As an extension of the above study, the linear theory with basic equations, theory of micropolar elasticity, couple stress theory, non-negative internal energy and the Uniqueness theorem of micropolar elasticity were presented by **Eringen** [35] in the same year. Finally, the totality of the microcontinuum theory was achieved by **Eringen** [36], when he presented the laws of motion, constitutive equations of microfluids, the definition of micropolar fluids—the theories of its thermodynamics and field equations and the study of such a fluid flow in a circular pipe.

### **2.3 FLEXIBLY SUPPORTED BEARINGS WITH MICROPOLAR LUBRICATION**

Based on the theory of micropolar lubrication the first application of the theory was presented by **Eringen** [37] himself for the steady motion of micropolar fluids in a circular channel in which the profiles for the velocity, microrotational velocity, shear stress difference and the couple stress on the fluid surface adjacent to the wall were presented graphically. The velocity profile was found to lose its parabolic nature and was smaller than that of classical Navier-Stokes fluid. Though the shearing stress remained the same as that determined by classical theory, the surface shear was found to be reduced by an amount equivalent to the effect of the distributed couples aroused on the fluid surface in a thin layer adjacent to the surface thus, indicating the development of a boundary layer phenomenon not present in the Navier-Stokes theory.

**Balaram** [38] presented an analysis of micropolar squeeze films between two rectangular plates of infinite length along with the expressions for the pressure, the load carrying capacity of the squeeze film and the relationship of film thickness with time. The results showed an improvement in load carrying capacity with the increase in the density of the macromolecular volume but a decrease in load capacity with an increase in substructure particle size. The squeeze film action was also found to increase in micropolar fluid. **Prakash** and his co-workers presented a number of studies on different

types of lubrications and for different configurations of bearings using micropolar lubricants during 1975. **Prakash** and **Christensen** [39] developed the hydrodynamic theory for the two-dimensional micropolar lubrication of a rigid cylinder on a plane surface in order to make critical analysis of micropolar effects revealed in the results of **Fuks** [26, 27]. **Prakash** and **Sinha** [40] also presented a theoretical analysis of squeeze films in both full and half journal bearings with a steady, laminar, incompressible flow of micropolar fluid between two eccentric cylinders in relative normal motion along with the expressions for Reynolds equation, non-dimensional pressure distribution, load capacity and response time. The results supported the experimental results [22,25] of increase in the effective viscosity in narrow passages. In 1976, in another study, **Prakash** and **Sinha** [41] presented the Reynolds equation and the expressions for various bearing characteristics of squeeze films for the general case of dynamically loaded infinitely long journal bearing for steady incompressible two-dimensional micropolar fluid flow under a sinusoidal load with no journal rotation. The graphical representation of results exhibited decreasing velocity of approach with increasing micropolar effect. An analysis providing the expressions for different hydrodynamic characteristics such as the load carrying capacity, the volume flow flux and the frictional force, of one dimensional journal bearings, both infinitely long and infinitely short, with micropolar lubrication, was presented by **Zaheeruddin** and **Isa** [42]. The results showed that an increase in the equivalent viscosity of the micropolar fluid increased the load carrying capacity and the time of approach, but decreases the Co-efficient of friction.

**Zaheeruddin** [43] in another paper presented the generalized Reynolds equation in dynamically loaded one-dimensional, both infinitely long and infinitely short types of porous journal bearings operating under a cyclic load and lubricated with micropolar fluids. The analysis was to show the effects of microstructures present in the lubricants, the permeability of the bearing material and the bearing wall thickness on the operating eccentricity ratio. The three-dimensional Reynolds equation was first presented by **Singh** and **Sinha** [44], which the authors solved to yield the expressions for the velocity distribution, microrotational velocities flow flux and frictional torques.

**Huang** and **Weng** [45] in 1990 studied the dynamic characteristics of finite width journal bearing with micropolar lubrication using linear stability theory and graphically presented the stiffness, damping coefficients and the critical stability parameter of the journal bearings for width to diameter 30 ratio 1.0 and 10 under both Newtonian and

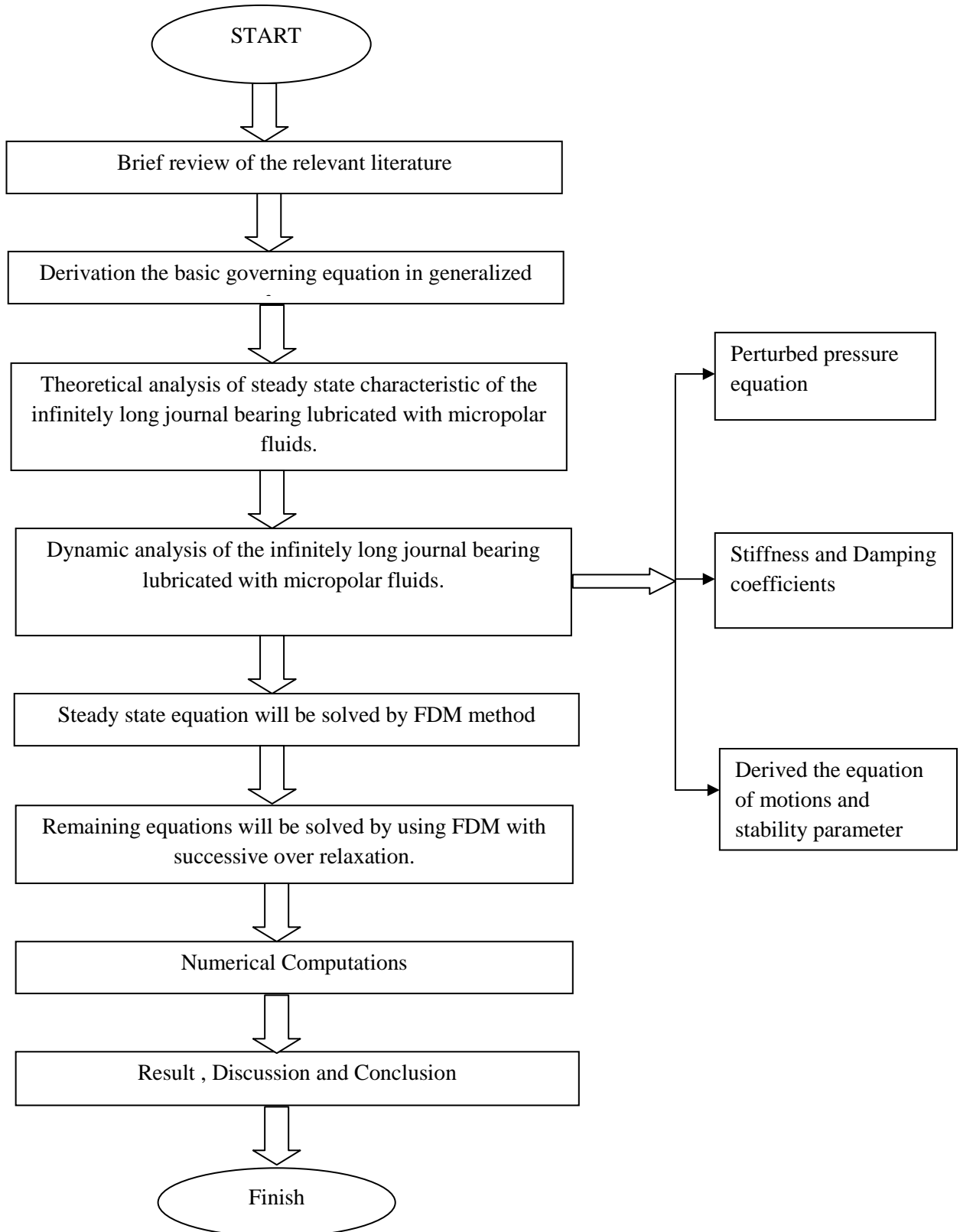
micropolar lubrication. The micropolar fluids exhibited larger normal stiffness coefficient but smaller normal damping coefficient, and comparatively narrower stable region of the journal. The features of increasing effective viscosity and load capacity under micropolar lubrication resulted in lower limit values of the Sommerfeld number for completely stable operation. A long journal was found to exhibit significant difference in the values of critical mass parameter for the Newtonian and micropolar fluids, whereas the short bearing was found to be almost equally stable in both types of lubrication. The steady flow of a micropolar fluid between two rotating disks of finite radius rotating at different same speeds was investigated by **Chaturani** and **Narasimman** [46] and the equations of motion were reduced to a set of ordinary non-linear coupled differential equations, which were then linearised by quasilinearisation technique. The numerical solutions were obtained using fourth order Runga-Kutta method via orthonormalisation. The work of **Marsh** [53] **Kerr** [54] has shown that the stability characteristic of this system are affected by both the stiffness and damping of the bearing support. **D.A.Boefey** [55] examine the stability characteristics of a bearing on a flexible damped support using a purely analytical approach. His analysis was based on the linearised solution to the time dependent Reynolds equation.

**Chattopadhyay. A.K., Karmakar, S.,** [47] in 1997 a theoretical analysis is presented investigating the stability of a symmetrical, rigid rotor on a flexibly supported journal bearing. Oil-film flow in the bearing is assumed to be turbulent and the dynamics of the system is studied by calculating the components of the fluid film force by solving the generalized Reynolds equation modified to include the effect of turbulence and using these in the non-linear equation of motion of the journal and the bearing. The modified Reynolds equation is solved for pressure distribution by using finite difference method with S.O.R. scheme.

**Das, S., Guha, S.K., and Chattopadhyay,A.K.** [48] Theoretical analysis of stability characteristic of hydrodynamic journal bearings lubricated with micropolar fluid.

# 3. PROBLEM FORMULATION

## 3.1 WORK PROCEDURE



## 3.2 BASIC GOVERNING EQUATION

### 3.2.1 INTRODUCTION

As the presence of the microstructures in the lubricating fluid, particularly in the hydrodynamic lubrication, imparts the microrotation and microdeformation of the particles with the attendant enhancement of the viscosity of the fluid, the analysis with such lubricants requires the concepts of conservation of the micro-inertia moments and the balance of the first stress moments in addition to the basic principle of the continuous media. As such a micro-fluid in its simplest form contains 22 viscosity coefficients, and as the micro-fluid theory is too complicated and not easily amenable to the solution of non-trivial problems in lubrication, the analysis has been limited to the micropolar fluid, in which micro-deformation effects are ignored. The basic field equations of the micropolar fluid were developed by **Eringen** [36], and later adopted by **Prakash** and **Sinha** [40] followed by the model of **Singh** and **Sinha** [44]. In this chapter, starting from the basic field equation and using certain assumptions, modified Reynolds equation has been derived and a brief discussion of the various non-dimensional parameters related to micropolar fluid has been made.

### 3.2.2 FIELD EQUATIONS

The field equations for micropolar fluids in vectorial form are [40]:

*Principle of conservation of mass*

$$\frac{\partial \rho}{\partial t} + \nabla \cdot (\rho \vec{V}) = 0 \quad (3.1)$$

*Conservation of linear momentum:*

$$(\lambda + 2\mu)\nabla(\nabla \cdot \vec{v}) - \frac{(2\mu + \chi)}{2}\nabla \times \nabla \times \vec{v} + \chi \nabla \times \vec{v} - \nabla \pi^* + \rho F_B = \rho \frac{D\vec{V}}{Dt} \quad (3.2)$$

*Conservation of angular momentum:*

$$(\alpha + \beta + \gamma)\nabla(\nabla \cdot \vec{v}) - \gamma \nabla \times \nabla \times \vec{v} + \chi \nabla \times \vec{v} - 2\chi \vec{v} + \rho C_B = \rho j \frac{Dv}{Dt} \quad (3.3)$$

where  $\rho$  is the mass density,  $\vec{V}$  is the velocity vector and  $\vec{v}$  is the microrotational velocity vector.  $\pi^*$  is the thermodynamic pressure and is to be replaced by the hydrodynamic film pressure,  $p$ , since,  $\pi^* = -\left[\frac{\partial E}{\partial \rho^{-1}}\right] = p$  where  $E$  is the internal energy [36] and  $p$  is to be determined by the boundary conditions.  $\mu$  and  $\lambda$  are the familiar viscosity coefficients of the classical fluid mechanics, while  $\alpha, \beta$  and  $\gamma$  are the new viscosity coefficients derived as the combinational effects of the gyroviscosities for micropolar fluid as defined by **Eringen** [36].  $\chi$  is also a new viscosity coefficient for micropolar fluid, termed as *spin viscosity*, which establishes the link between the velocity vector,  $\vec{V}$  and the microrotational velocity vector,  $\vec{v}$ .  $\mathbf{F}_B$  is the body force per unit mass,  $\mathbf{C}_B$  is the body couple (moment) per unit mass and  $j$  is the microinertia constant.  $\lambda, \mu$  and  $\chi$  are all of dimension  $[ML^{-1}T^{-1}]$ ,  $\alpha, \beta$  and  $\gamma$  are all of dimension  $[MLT^{-1}]$  and  $j$  is of dimension  $[L^2]$  [40]. If microrotation velocity and local fluid vorticity are considered to be identically equal and is imposed as a possible solution of the balance equations, which seems to be a natural solution and is desirable in reducing the number of constitutive coefficients, it can be shown that  $j = \Lambda^2$  [40].  $\frac{D}{Dt}$  indicates the material differentiation.

Constitutive equations for the stress tensor  $t_{kl}$  and the couple stress tensor  $m_{kl}$  are [40]:

$$t_{kl} = \left(-\pi^* + \lambda \vec{V}_{r,r}\right) \delta_{kl} + \left(\mu - \frac{1}{2} \chi\right) \left(\vec{V}_{k,1} + \vec{V}_{1,k}\right) + \chi \left(\vec{V}_{1,k} - \eta_{k1r} \vec{V}_r\right) \quad (3.4)$$

$$m_{kl} = \alpha \vec{v}_{r,r} \delta_{kl} + \beta \vec{v}_{k,1} + \gamma \vec{v}_{1,k}$$

Where,  $\eta_{k1r}$  is an alternating tensor. An index followed by a comma represents partial differentiation with respect to the space variable  $x_k$ .

### 3.2.3 DERIVATION OF MODIFIED REYNOLDS EQUATION

The above micropolar effects are then incorporated into the lubrication problem for a journal bearing to derive the modified Reynolds equation with certain simplifications.

### Basic assumptions

The basic assumptions in micropolar lubrication to a journal bearing include the usual lubrication assumptions in deriving Reynolds equation and the assumptions to generalize the micropolar effects [44]:

- (i) The flow is incompressible and steady, *i.e.*  $\rho = \text{constant}$  and  $\frac{\partial \rho}{\partial t} = 0$
- (ii) The flow is laminar *i.e.* free of vortices and turbulences.
- (iii) Body forces and body couples are negligible, *i.e.*  $F_B = 0$  and  $C_B = 0$ .
- (iv) The film is very thin in comparison to the length and the span of the bearing. Thus, the curvature effect of the fluid film may be ignored and the rotational velocities may be replaced by the translatory velocities.
- (v) No slip occurs at the bearing surfaces.
- (vi) Bearing surfaces are smooth, non-porous and rigid *i.e.* no effects of surface roughness or porosity and the surface can withstand infinite pressure and stress theoretically without having any deformation.
- (vii) No fluid flow exists across the fluid film, *i.e.* the lubrication characteristics are independent of  $y$ -direction.
- (viii) The micropolar properties are also independent of  $y$ -direction. The velocity vector, the microrotational velocity vector and the fluid film pressure are given as:

$$\left. \begin{aligned} \vec{V} &= [\vec{V}_x(x, y, z), \vec{V}_y(x, y, z), \vec{V}_z(x, y, z)] \\ \vec{v} &= [\vec{v}_1(x, y, z), \vec{v}_2(x, y, z), \vec{v}_3(x, y, z)] \\ p &= p(x, y, z) \end{aligned} \right\} \quad (3.5)$$

Note that for  $\alpha = \beta = \gamma = \chi = 0$  and for negligible body couple per unit mass equation (3.3) yields  $\mathbf{v} = 0$  and so, equation (3.2) reduces to the classical Navier-Stokes equation. For  $\chi = 0$  the velocity vector and the microrotational velocity vector are uncoupled and the global motion of the fluid becomes free of the microrotation and their effects.

## DIRECTIONAL FLOW EQUATIONS

With the above assumptions (3.1) reduces to

$$\left. \begin{aligned} \nabla \cdot \vec{V} &= 0 \\ \text{i.e., } \frac{\partial \vec{V}_x}{\partial x} + \frac{\partial \vec{V}_y}{\partial y} + \frac{\partial \vec{V}_z}{\partial z} &= 0 \end{aligned} \right\} \quad (3.6)$$

It can also be considered that,

$$\nabla \cdot \vec{v} = 0 \quad (3.7)$$

The explanation for equation (3.7) can be given following **Tipei [49]** as:

In case of a flow in thin layers bounded by solid surfaces, as in lubrication problem, the component of  $\mathbf{v}$  perpendicular to the boundaries becomes negligible with respect to the other two components. Since the derivatives with respect to the normal  $y$ -direction are

much larger than the other derivatives, *i.e.*  $\frac{\partial}{\partial y} \gg \frac{\partial}{\partial x}$  or  $\frac{\partial}{\partial z}$ , hence  $\nabla(\nabla \cdot \vec{v}) = \frac{\partial^2 \vec{v}_1}{\partial x \partial y} + \frac{\partial^2 \vec{v}_3}{\partial z \partial y}$ ,

while the other components are much smaller. The component of  $(\nabla \times \mathbf{v})$  upon  $y$ -coordinate *i.e.*  $\& \left[ \frac{\partial \vec{v}_1}{\partial z} - \frac{\partial \vec{v}_3}{\partial x} \right]$  is an order of magnitude smaller and may be neglected and

hence equation (3.3) as projected upon  $y$ -axis yields  $\nabla(\nabla \cdot \vec{v}) \approx 0$  This result can be obtained directly under usual approximations in lubrication theory **[50]** by considering  $\nabla^2 \vec{v} \gg \nabla(\nabla \cdot \vec{v})$  Now from the vector calculus  $(\nabla \times \nabla \times \vec{V})$  and  $(\nabla \times \nabla \times \vec{v})$  can be written as:

$$\nabla \times \nabla \times \vec{V} = \nabla(\nabla \cdot \vec{V}) - \nabla^2 \vec{V} \quad \text{and} \quad \nabla \times \nabla \times \vec{v} = \nabla(\nabla \cdot \vec{v}) - \nabla^2 \vec{v} \quad (3.8)$$

With the basic assumptions and equation (3.8), equation (3.2) yields the following three equations along  $x$ -,  $y$ - and  $z$ -directions respectively:

$$\frac{(2\mu + \chi)}{2} \left( \frac{\partial^2 \vec{V}_x}{\partial x^2} + \frac{\partial^2 \vec{V}_x}{\partial y^2} + \frac{\partial^2 \vec{V}_x}{\partial z^2} \right) + \chi \left( \frac{\partial \vec{v}_3}{\partial y} - \frac{\partial \vec{v}_2}{\partial z} \right) - \frac{\partial p}{\partial x} = \rho \left( \vec{V}_x \frac{\partial \vec{V}_x}{\partial x} + \vec{V}_y \frac{\partial \vec{V}_x}{\partial y} + \vec{V}_z \frac{\partial \vec{V}_x}{\partial z} \right) \quad (3.9)$$

$$\frac{(2\mu + \chi)}{2} \left( \frac{\partial^2 \vec{V}_y}{\partial x^2} + \frac{\partial^2 \vec{V}_y}{\partial y^2} + \frac{\partial^2 \vec{V}_y}{\partial z^2} \right) + \chi \left( \frac{\partial \vec{v}_1}{\partial y} - \frac{\partial \vec{v}_3}{\partial x} \right) - \frac{\partial p}{\partial y} = \rho \left( \vec{V}_x \frac{\partial \vec{V}_y}{\partial x} + \vec{V}_y \frac{\partial \vec{V}_y}{\partial y} + \vec{V}_z \frac{\partial \vec{V}_y}{\partial z} \right) \quad (3.10)$$

$$\frac{(2\mu+\chi)}{2}\left(\frac{\partial^2\vec{V}_z}{\partial x^2}+\frac{\partial^2\vec{V}_z}{\partial y^2}+\frac{\partial^2\vec{V}_z}{\partial z^2}\right)+\chi\left(\frac{\partial\vec{v}_2}{\partial x}-\frac{\partial\vec{v}_1}{\partial y}\right)-\frac{\partial p}{\partial z}=\rho\left(\vec{V}_x\frac{\partial\vec{v}_2}{\partial x}+\vec{V}_y\frac{\partial\vec{v}_2}{\partial y}+\vec{V}_z\frac{\partial\vec{v}_2}{\partial z}\right) \quad (3.11)$$

Similarly, with the basic assumptions and equation (3.8), equation (3.3) yields the following

three equations along  $x$ -,  $y$ - and  $z$ -directions respectively:

$$\gamma\left(\frac{\partial^2\vec{v}_1}{\partial x^2}+\frac{\partial^2\vec{v}_1}{\partial y^2}+\frac{\partial^2\vec{v}_1}{\partial z^2}\right)+\chi\left(\frac{\partial\vec{V}_z}{\partial y}-\frac{\partial\vec{V}_y}{\partial z}\right)-2\chi\vec{v}_1=\rho j\left(\vec{V}_x\frac{\partial\vec{v}_1}{\partial x}+\vec{V}_y\frac{\partial\vec{v}_1}{\partial y}+\vec{V}_z\frac{\partial\vec{v}_1}{\partial z}\right) \quad (3.12)$$

$$\gamma\left(\frac{\partial^2\vec{v}_2}{\partial x^2}+\frac{\partial^2\vec{v}_2}{\partial y^2}+\frac{\partial^2\vec{v}_2}{\partial z^2}\right)+\chi\left(\frac{\partial\vec{V}_x}{\partial z}-\frac{\partial\vec{V}_z}{\partial x}\right)-2\chi\vec{v}_2=\rho j\left(\vec{V}_x\frac{\partial\vec{v}_2}{\partial x}+\vec{V}_y\frac{\partial\vec{v}_2}{\partial y}+\vec{V}_z\frac{\partial\vec{v}_2}{\partial z}\right) \quad (3.13)$$

$$\gamma\left(\frac{\partial^2\vec{v}_3}{\partial x^2}+\frac{\partial^2\vec{v}_3}{\partial y^2}+\frac{\partial^2\vec{v}_3}{\partial z^2}\right)+\chi\left(\frac{\partial\vec{V}_y}{\partial x}-\frac{\partial\vec{V}_x}{\partial y}\right)-2\chi\vec{v}_3=\rho j\left(\vec{V}_x\frac{\partial\vec{v}_3}{\partial x}+\vec{V}_y\frac{\partial\vec{v}_3}{\partial y}+\vec{V}_z\frac{\partial\vec{v}_3}{\partial z}\right) \quad (3.14)$$

## NON-DIMENSIONAL SCHEME

Equations (3.9) to (3.14) when non-dimensionalised with the following substitutions

$$\left. \begin{aligned}
 \bar{x} &= \frac{x}{R}; \quad \bar{y} = \frac{y}{R}; \quad \bar{z} = \frac{z}{L/2}; \quad \delta_1 = \frac{C}{R}; \quad \delta_2 = \frac{C}{L/2}; \quad \delta_3 = \frac{h_{\min}}{R}; \quad \delta_4 = \frac{L/2}{R}; \\
 \bar{V}_i &= \frac{V_i}{U}, \text{ where } i = x, y, z; \quad \bar{v}_i = v_i \frac{C}{U}, \text{ where } i = 1, 2, 3; \quad \xi = \frac{h_{\min}}{C} \\
 \bar{p} &= \frac{ph_{\min}^2}{\left(\mu + \frac{\chi}{2}\right)UR}; \quad R_e = \frac{2\rho CU}{(2\mu + \chi)}; \quad R_R = \frac{\rho jUh}{4\mu\Lambda}; \quad N = \left(\frac{\chi}{2\mu + \chi}\right)^{1/2} \\
 l_m &= \frac{C}{\Lambda}; \quad L_R = \frac{h_{\min}}{\Lambda}; \quad \text{where } \Lambda = \left(\frac{\gamma}{4\mu}\right)^{1/2} \text{ and is of dimension of length.}
 \end{aligned} \right\} \quad (3.15)$$

The following equations will result:

$$\begin{aligned}
 &\left( \delta_1^2 \frac{\partial^2 \bar{V}_x}{\partial \bar{x}^2} + \frac{\partial^2 \bar{V}_x}{\partial \bar{y}^2} + \delta_2^2 \frac{\partial^2 \bar{V}_x}{\partial \bar{z}^2} \right) + 2N^2 \left( \frac{\partial \bar{v}_3}{\partial \bar{y}} - \delta_2 \frac{\partial \bar{v}_2}{\partial \bar{z}} \right) - \frac{1}{\xi^2} \frac{\partial \bar{p}}{\partial \bar{x}} \\
 &= R_e \left( \delta_1 \bar{V}_x \frac{\partial \bar{V}_x}{\partial \bar{x}} + \bar{V}_y \frac{\partial \bar{V}_x}{\partial \bar{y}} + \delta_2 \bar{V}_z \frac{\partial \bar{V}_x}{\partial \bar{z}} \right)
 \end{aligned} \quad (3.16)$$

$$\begin{aligned}
 &\xi \delta_3 \left( \delta_1^2 \frac{\partial^2 \bar{V}_y}{\partial \bar{x}^2} + \frac{\partial^2 \bar{V}_y}{\partial \bar{y}^2} + \delta_2^2 \frac{\partial^2 \bar{V}_y}{\partial \bar{z}^2} \right) + 2\xi \delta_3 N^2 \left( \delta_2 \frac{\partial \bar{v}_1}{\partial \bar{z}} - \delta_1 \frac{\partial \bar{v}_3}{\partial \bar{x}} \right) - \frac{\partial \bar{p}}{\partial \bar{y}} \\
 &= \xi \delta_3 R_e \left( \delta_1 \bar{V}_x \frac{\partial \bar{V}_y}{\partial \bar{x}} + \bar{V}_y \frac{\partial \bar{V}_y}{\partial \bar{y}} + \delta_2 \bar{V}_z \frac{\partial \bar{V}_y}{\partial \bar{z}} \right)
 \end{aligned} \quad (3.17)$$

$$\begin{aligned}
& \xi^2 \delta_4 \left( \delta_1^2 \frac{\partial^2 \bar{V}_z}{\partial \bar{x}^2} + \frac{\partial^2 \bar{V}_z}{\partial \bar{y}^2} + \delta_2^2 \frac{\partial^2 \bar{V}_z}{\partial \bar{z}^2} \right) + 2\xi^2 \delta_4 N^2 \left( \delta_1 \frac{\partial \bar{v}_2}{\partial \bar{x}} - \frac{\partial \bar{v}_1}{\partial \bar{y}} \right) - \frac{\partial \bar{p}}{\partial \bar{z}} \\
& = \xi^2 \delta_4 R_e \left( \delta_1 \bar{V}_x \frac{\partial \bar{V}_z}{\partial \bar{x}} + \bar{V}_y \frac{\partial \bar{V}_z}{\partial \bar{y}} + \delta_2 \bar{V}_z \frac{\partial \bar{V}_z}{\partial \bar{z}} \right)
\end{aligned} \tag{3.18}$$

$$\begin{aligned}
& \left( \delta_1^2 \frac{\partial^2 \bar{v}_1}{\partial \bar{x}^2} + \frac{\partial^2 \bar{v}_1}{\partial \bar{y}^2} + \delta_2^2 \frac{\partial^2 \bar{v}_1}{\partial \bar{z}^2} \right) + \frac{N^2 L_R^2}{2(1-N^2)\xi^2} \left( \frac{\partial \bar{V}_z}{\partial \bar{y}} - \delta_2 \frac{\partial \bar{V}_z}{\partial \bar{z}} \right) - \frac{N^2 L_R^2}{(1-N^2)\xi^2} \bar{v}_1 \\
& = R_R \left( \delta_1 \bar{V}_x \frac{\partial \bar{v}_1}{\partial \bar{x}} + \bar{V}_y \frac{\partial \bar{v}_1}{\partial \bar{y}} + \delta_2 \bar{V}_z \frac{\partial \bar{v}_1}{\partial \bar{z}} \right)
\end{aligned} \tag{3.19}$$

$$\begin{aligned}
& \left( \delta_1^2 \frac{\partial^2 \bar{v}_2}{\partial \bar{x}^2} + \frac{\partial^2 \bar{v}_2}{\partial \bar{y}^2} + \delta_2^2 \frac{\partial^2 \bar{v}_2}{\partial \bar{z}^2} \right) + \frac{N^2 L_R^2}{2(1-N^2)\xi^2} \left( \delta_2 \frac{\partial \bar{V}_x}{\partial \bar{z}} - \delta_1 \frac{\partial \bar{V}_z}{\partial \bar{x}} \right) - \frac{N^2 L_R^2}{(1-N^2)\xi^2} \bar{v}_2 \\
& = R_R \left( \delta_1 \bar{V}_x \frac{\partial \bar{v}_2}{\partial \bar{x}} + \bar{V}_y \frac{\partial \bar{v}_2}{\partial \bar{y}} + \delta_2 \bar{V}_z \frac{\partial \bar{v}_2}{\partial \bar{z}} \right)
\end{aligned} \tag{3.20}$$

$$\begin{aligned}
& \left( \delta_1^2 \frac{\partial^2 \bar{v}_3}{\partial \bar{x}^2} + \frac{\partial^2 \bar{v}_3}{\partial \bar{y}^2} + \delta_2^2 \frac{\partial^2 \bar{v}_3}{\partial \bar{z}^2} \right) + \frac{N^2 L_R^2}{2(1-N^2)\xi^2} \left( \delta_1 \frac{\partial \bar{V}_y}{\partial \bar{x}} - \frac{\partial \bar{V}_x}{\partial \bar{y}} \right) - \frac{N^2 L_R^2}{(1-N^2)\xi^2} \bar{v}_3 \\
& = R_R \left( \delta_1 \bar{V}_x \frac{\partial \bar{v}_3}{\partial \bar{x}} + \bar{V}_y \frac{\partial \bar{v}_3}{\partial \bar{y}} + \delta_2 \bar{V}_z \frac{\partial \bar{v}_3}{\partial \bar{z}} \right)
\end{aligned} \tag{3.21}$$

### 3.2.4 STUDY OF NON-DIMENSIONAL PARAMETERS

In this section the interpretations of the non-dimensional parameters are given briefly. As the current analysis is aimed at showing the micropolar effects on the hydrodynamic journal bearings, a separate importance is given in discussion of the micropolar properties at the end of this section

## ❖ MICROPOLAR PARAMETERS

$N$  and  $\Lambda$  are two parameters distinguishing a micropolar fluid from a Newtonian fluid.  $N$  is a non-dimensional parameter called the *coupling number*, which couples the linear and angular momentum equations arising out of the microrotational effect of the suspended particles in the fluid.  $\Lambda$ , a dimensional parameter represents the interaction between the micropolar fluid and the film gap.  $\Lambda$  is termed as the *characteristic length* of the micropolar fluid and has the dimension of the length.  $l_m$  is a non-dimensional quantity and is termed as the *non-dimensional characteristic length* of the micropolar fluid. For  $\chi = 0$ ,  $N = 0$  the equations representing linear and angular momentums are uncoupled and equation (3.2) reduces to that of classical Navier-Stokes equation. On the other hand the strong micropolar effect is exhibited with the increase in the value of  $\Lambda$  or decrease in clearance in between the journal and bearing *i.e.* when non-dimensional characteristic length  $l_m$  decreases. The second case is most likely here as  $C$  is usually very small in lubrication theory. Hence for  $N \rightarrow 0$  or for  $l_m \rightarrow \infty$ , (*i.e.* characteristic length of the microstructure is small), the micropolar characteristic is lost and the lubrication problem reduces to that of the classical hydrodynamic lubrication. Again, as the gradient of the microrotational velocity across the film thickness is very small, when  $l_m \rightarrow 0$ , the velocity and other flow characteristics will reduce to their equivalents in the Newtonian theory with  $\mu$  everywhere replaced by  $\left(\mu + \frac{1}{2}\chi\right)$  Hence  $\left(\mu + \frac{1}{2}\chi\right)$  togetherly may be considered as the *effective viscosity*,  $\mu_e$ , which arises due to the microrotational effect. The thermodynamic restrictions require that  $0 \leq N \leq 1$ .  $j$ , the microinertia constant is evolved due to the microrotational effects.

## ❖ OTHER NON-DIMENSIONAL PARAMETERS AND ORDER ANALYSIS

$L_R$ , a non-dimensional quantity, may be termed as *length ratio*. During the initial stage of the application of the micropolar theory to the lubrication flow problems, researchers [36, 49] used either  $NL_R$  or  $Nl_m$  as the parameter in discussing the micropolar fluid; but as these products characterize the combinational effects, later  $N$  and  $l_m$  were considered separately to study their effects as can be found in **Prakash** and **Sinha** [40].  $Re$  may be considered as the *modified Reynolds number*, where  $\mu$  has been replaced by effective

viscosity,  $\mu_e$ , *i.e.*  $\left(\mu + \frac{1}{2}\chi\right)$  and this number is always less than the classical Reynolds number. Generally for lubrication problem,  $Re \ll 1$  and is usually of the order of  $10^{-3}$ . As  $j$  is the square of a length typical of the microstructure as discussed earlier, it is reasonable to consider  $R_R \ll 1$ . Also with the assumptions that  $\delta_1, \delta_2, \delta_3$  are of the order of  $10^{-3}$  and  $\delta_4, \xi, L_R$  are of the order of 1, equations (3.16) to (3.21) will reduce to

$$\frac{\partial^2 \bar{V}_x}{\partial \bar{y}^2} + 2N^2 \frac{\partial \bar{v}_3}{\partial \bar{y}} - \frac{1}{\xi^2} \frac{\partial \bar{p}}{\partial \bar{x}} = 0 \quad (3.22)$$

$$\frac{\partial \bar{p}}{\partial \bar{y}} = 0 \quad (3.23)$$

$$\frac{\partial^2 \bar{V}_z}{\partial \bar{y}^2} - 2N^2 \frac{\partial \bar{v}_1}{\partial \bar{y}} - \frac{1}{\xi^2 \delta_4} \frac{\partial \bar{p}}{\partial \bar{z}} = 0 \quad (3.24)$$

$$\frac{\partial^2 \bar{v}_1}{\partial \bar{y}^2} + \frac{N^2 L_R^2}{2(1-N^2)\xi^2} \frac{\partial \bar{V}_z}{\partial \bar{y}} - \frac{N^2 L_R^2}{(1-N^2)\xi^2} \bar{v}_1 = 0 \quad (3.25)$$

$$\frac{\partial^2 \bar{v}_2}{\partial \bar{y}^2} - \frac{N^2 L_R^2}{(1-N^2)\xi^2} \bar{v}_2 = 0 \quad (3.26)$$

$$\frac{\partial^2 \bar{v}_3}{\partial \bar{y}^2} - \frac{N^2 L_R^2}{2(1-N^2)\xi^2} \frac{\partial \bar{V}_x}{\partial \bar{y}} - \frac{N^2 L_R^2}{(1-N^2)\xi^2} \bar{v}_3 = 0 \quad (3.27)$$

### 3.2.5 VELOCITY AND MICROROTATIONAL VELOCITY VECTORS

Now to solve the velocity components and the microrotational velocity components equations (3.22) to (3.27) are returned to their dimensional forms as follows:

$$\frac{(2\mu + \chi)}{2} \frac{\partial^2 \bar{V}_x}{\partial y^2} + \chi \frac{\partial \bar{v}_3}{\partial y} - \frac{\partial p}{\partial x} = 0 \quad (3.28)$$

$$\frac{\partial p}{\partial y} = 0 \quad (3.29)$$

$$\frac{(2\mu + \chi)}{2} \frac{\partial^2 \bar{V}_z}{\partial y^2} - \chi \frac{\partial \bar{v}_1}{\partial y} - \frac{\partial p}{\partial z} = 0 \quad (3.30)$$

$$\gamma \frac{\partial \bar{v}_1}{\partial y^2} + \chi \frac{\partial \bar{V}_z}{\partial y} - 2\chi \bar{v}_1 = 0 \quad (3.31)$$

$$\gamma \frac{\partial^2 \bar{v}_2}{\partial y^2} - 2\chi \bar{v}_2 = 0 \quad (3.32)$$

$$\gamma \frac{\partial^2 \bar{v}_3}{\partial y^2} - \chi \frac{\partial \bar{V}_x}{\partial y} - 2\chi \bar{v}_3 = 0 \quad (3.33)$$

As  $x = R\theta$ , equation (3.28) reduces to

$$\frac{(2\mu + \chi)}{2} \frac{\partial^2 \bar{V}_x}{\partial y^2} + \chi \frac{\partial \bar{v}_3}{\partial y} - \frac{1}{R} \frac{\partial p}{\partial \theta} = 0 \quad (3.34)$$

Solving equations (3.30) and (3.31) the expressions for  $v_1$  and  $V_z$  are evaluated as follows

$$v_1 = A_1 + A_2 e^{ay} + A_3 e^{-ay} + \left( \frac{1}{2\mu} \frac{\partial p}{\partial z} \right) y \quad (3.35)$$

$$\bar{V}_z = 2A_1 y + 2A_2 \frac{N^2}{a} e^{ay} - 2A_3 \frac{N^2}{a} e^{-ay} + A_4 + \left( \frac{1}{2\mu} \frac{\partial p}{\partial z} \right) y^2 \quad (3.36)$$

Where,  $A_1, A_2, A_3$  and  $A_4$  are four constants to be evaluated from the boundary conditions and

$$a \text{ is a non-dimensional quantity given by, } a = \frac{N}{\Lambda} = \sqrt{\frac{4\mu N^2}{\gamma}}$$

Boundary conditions for  $v_1$  and  $V_z$  are:

$$(i). \text{At } y=0 \quad v_1=0 \text{ and } V_z=0 \quad (3.37)$$

$$(ii). \text{At } y=h \quad v_1=0 \text{ and } V_z=0$$

Using the above boundary conditions in equations (3.35) and (3.36)  $A_1$ ,  $A_2$ ,  $A_3$  and  $A_4$  are evolved as

$$\begin{aligned} A_1 &= -\frac{h}{4\mu} \frac{\partial p}{\partial z}; & A_2 &= -\frac{h}{4\mu} \frac{\partial p}{\partial z} \frac{1}{(e^{ah} - 1)} \\ A_3 &= \frac{h}{4\mu} \frac{\partial p}{\partial z} \frac{1}{(1 - e^{-ah})}; & A_4 &= \frac{hN^2}{2\mu a} \frac{\partial p}{\partial z} \frac{(1 + e^{-ah})}{(1 - e^{-ah})} \end{aligned} \quad (3.38)$$

With the substitutions of  $A_1$ ,  $A_2$ ,  $A_3$  and  $A_4$  the expressions for  $v_1$  and  $V_z$  become

$$v_1 = \frac{h}{4\mu} (\sinh ay) \left\{ \frac{(\cosh ay - 1)}{\sinh ay} - \frac{(\cosh ah + 1)}{\sinh ah} \right\} \frac{\partial p}{\partial z} + \frac{y}{2\mu} \frac{\partial p}{\partial z} \quad (3.39)$$

$$\bar{V}_z = \frac{y(y-h)}{2\mu} \frac{\partial p}{\partial z} + \frac{h}{2\mu} \frac{N^2}{a} \left\{ \sinh ay - \frac{(\cosh ay - 1)(\cosh ah + 1)}{\sinh ah} \right\} \frac{\partial p}{\partial z} \quad (3.40)$$

Similarly, solving equations (3.33) and (3.34) with the following boundary conditions

$$(i). \text{At } y=0 \quad v_3=0 \text{ and } V_x=0 \quad (3.41)$$

$$(ii). \text{At } y=h \quad v_3=0 \text{ and } V_x=U$$

The following equations will result:

$$v_3 = -\frac{h}{4\mu R} (\sinh ay) \left\{ \frac{(\cosh ay - 1)}{\sinh ay} - \frac{(\cosh ah + 1)}{\sinh ah} \right\} \frac{\partial p}{\partial \theta} - \frac{y}{2\mu R} \frac{\partial p}{\partial \theta}$$

$$+ \frac{U}{2 \left[ \frac{2N^2}{a} - h \frac{(\cosh ah + 1)}{\sinh ah} \right]} \left\{ \sinh ay - \frac{(\cosh ay - 1)(\cosh ah + 1)}{\sinh ah} \right\} \quad (3.42)$$

$$\begin{aligned} \vec{V}_x = & \frac{y(y-h)}{2\mu R} \frac{\partial p}{\partial \theta} + \frac{h}{2\mu R} \frac{N^2}{a} \left\{ \sinh ay - \frac{(\cosh ay - 1)(\cosh ah + 1)}{\sinh ah} \right\} \frac{\partial p}{\partial \theta} - \\ & \frac{U}{2 \left[ \frac{2N^2}{a} - h \frac{(\cosh ah + 1)}{\sinh ah} \right]} \left[ \frac{2y(\cosh ah + 1)}{\sinh ah} + \frac{2N^2}{a} (\sinh ay) \left\{ \frac{(\cosh ay - 1)}{\sinh ay} - \frac{(\cosh ah + 1)}{\sinh ah} \right\} \right] \end{aligned} \quad (3.43)$$

Now, from the principle of conservation of mass as stated in equation (3.1), it follows that

$$\frac{\partial(\rho \vec{V}_y)}{\partial y} = - \frac{\partial \rho}{\partial t} - \frac{\partial(\rho \vec{V}_x)}{\partial x} - \frac{\partial(\rho \vec{V}_z)}{\partial z} \quad (3.44)$$

Integrating both sides with respect to  $y$  within the limit 0 and  $h$ , equation (3.43) becomes:

$$\rho(\vec{V}_h - \vec{V}_0) = - \int_0^h \frac{\partial \rho}{\partial t} dy - \int_0^h \frac{\partial(\rho \vec{V}_x)}{\partial x} dy - \int_0^h \frac{\partial(\rho \vec{V}_z)}{\partial z} dy \quad (3.45)$$

Where,  $(\vec{V}_y)_{y=h} = \vec{V}_h$  and  $(\vec{V}_y)_{y=0} = \vec{V}_0$

As the upper limit  $h$  is the function of the coordinates  $x, z$  the integration before differentiation can be performed by using Leibnitz's rule and using the boundary conditions that

$$(i). \text{ At } y=0 \quad V_x=0 \quad \text{and} \quad V_z=0 \quad (3.46)$$

$$(ii) \text{ At } y=h \quad V_x=U \quad \text{and} \quad V_z=0$$

And noting that  $V_h = U \frac{\partial h}{\partial x} + \frac{\partial h}{\partial t}$  and  $V_0=0$ , the following equation will result:

$$\begin{aligned} & \frac{\partial}{\partial x} \left[ \frac{\rho h}{12\mu} \left\{ h^2 + 12\Lambda^2 - 6N\Lambda h \coth \frac{Nh}{2\Lambda} \right\} \frac{\partial p}{\partial x} \right] + \frac{\partial}{\partial z} \left[ \frac{\rho h}{12\mu} \left\{ h^2 + 12\Lambda^2 - 6N\Lambda h \coth \frac{Nh}{2\Lambda} \right\} \frac{\partial p}{\partial z} \right] \\ &= \frac{\partial}{\partial x} \left( \frac{\rho U h}{2} \right) + \frac{\partial(\rho h)}{\partial t} \end{aligned} \quad (3.47)$$

For incompressible fluid flow equation (3.47) reduces to give the **Reynolds equation for incompressible fluid flow in micropolar lubrication**:

$$\frac{\partial}{\partial x} \left[ \frac{h^3}{\mu} \Phi(\Lambda, N, h) \frac{\partial p}{\partial x} \right] + \frac{\partial}{\partial z} \left[ \frac{h^3}{\mu} \Phi(\Lambda, N, h) \frac{\partial p}{\partial z} \right] = 6 \frac{\partial(Uh)}{\partial x} + 12 \frac{\partial h}{\partial t} \quad (3.48)$$

$$\text{Where, } \Phi(\Lambda, N, h) = \left\{ 1 + 12 \frac{\Lambda^2}{h^2} - 6 \frac{N\Lambda}{h} \coth \frac{Nh}{2\Lambda} \right\} \quad (3.49)$$

Introducing the rotating coordinate system and considering that the journal centre is rotating an angular velocity  $\omega_p$ , equation (3.48) becomes:

$$\frac{\partial}{\partial x} \left[ \frac{h^3}{\mu} \Phi(\Lambda, N, h) \frac{\partial p}{\partial x} \right] + \frac{\partial}{\partial z} \left[ \frac{h^3}{\mu} \Phi(\Lambda, N, h) \frac{\partial p}{\partial z} \right] = 6 \frac{\partial(Uh)}{\partial x} + 12 \frac{\partial h}{\partial t} - 12\omega_p \frac{\partial h}{\partial \theta} \quad (3.50)$$

Equation (3.50) represents the **modified Reynolds equation in rotating coordinate system in micropolar lubrication**.

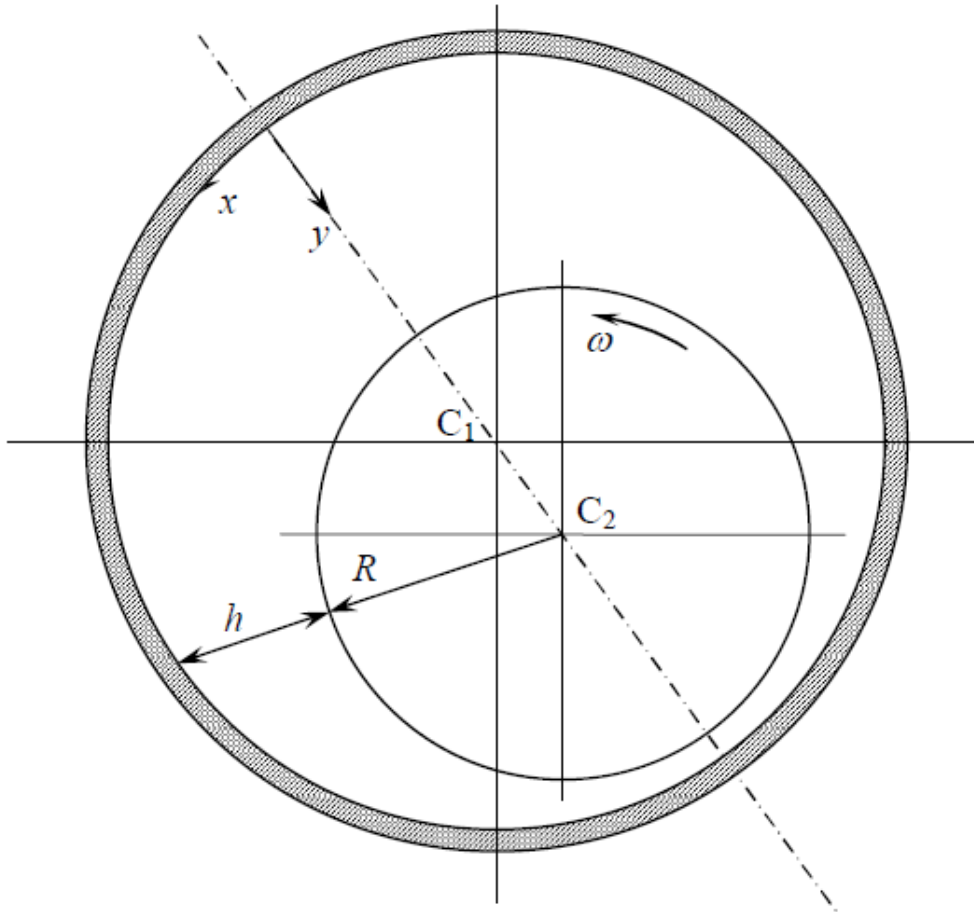


**Figure 3.1:** Bearing configuration for the derivation of Reynolds equation.

## 4. THEORETICAL ANALYSIS

### 4.1 THEORETICAL ANALYSIS OF THE STEADY STATE CHARACTERISTICS

#### 4.1.1 Introduction

This chapter deals with the theoretical analysis of the steady state characteristics of infinitely long journal bearings lubricated with micropolar fluids. The steady state analysis is important for the subsequent linear transient analysis for determining the threshold of instability of the journal bearings.

A good amount of work has been reported on the steady state characteristics of rotor/bearing systems lubricated with micropolar fluids. **Prakash** and **Sinha** [40] studied the steady state characteristics of an infinitely long journal bearing considering a two dimensional flow field. **Huang et al.** [51], **Khonsari** and **Brewe** [52] made same study on the steady state characteristics of journal bearing system lubricated with incompressible micropolar lubricant. In the present chapter a comprehensive parametric study has been made of the steady state characteristics viz. load parameter, attitude angle of the journal/bearing systems lubricated with micropolar fluids. In the analysis the governing modified Reynolds equation in the non-dimensional form satisfying the boundary conditions has been solved by finite difference technique with successive over-relaxation scheme. The steady state non-dimensional pressure profiles thus obtained is used to determine the steady state characteristics mentioned above. The results of the analysis are compared with the similar available results of earlier authors.

#### 4.1.2 Theoretical analysis

##### 4.1.2.1 Governing equation

A schematic diagram of a journal bearing in micropolar lubrication with the appropriate coordinate system used for the purpose of analysis is shown in *Fig.4.1*. The journal is considered to rotate with a steady angular velocity: about its axis. The governing modified Reynolds equation (3.47) for two-dimensional flow of micropolar lubricant under steady state condition is written as follows:

$$\frac{\partial}{\partial x} \left[ \frac{h_0^3}{\mu} \Phi(\Lambda, N, h_0) \frac{\partial p_0}{\partial x} \right] + \frac{\partial}{\partial z} \left[ \frac{h_0^3}{\mu} \Phi(\Lambda, N, h_0) \frac{\partial p_0}{\partial z} \right] = 6U \frac{\partial h_0}{\partial x} \quad (4.1)$$

With the following substitutions

$$\theta = \frac{x}{R}, \quad \bar{z} = \frac{2z}{L}, \quad \bar{h}_0 = \frac{h_0}{C}, \quad \bar{p}_0 = \frac{p_0 C^2}{\mu \omega R^2}, \quad l_m = \frac{C}{\Lambda}$$

equation (4.1) will reduce to its non-dimensional form as:

$$\frac{\partial}{\partial \theta} \left[ \bar{g}(l_m, N, \bar{h}_0) \frac{\partial \bar{p}_0}{\partial \theta} \right] + \left( \frac{D}{L} \right)^2 \frac{\partial}{\partial \bar{z}} \left[ \bar{g}(l_m, N, \bar{h}_0) \frac{\partial \bar{p}_0}{\partial \bar{z}} \right] = \frac{1}{2} \frac{\partial \bar{h}_0}{\partial \theta} \quad (4.2)$$

Where

$$\bar{\Phi}(l_m, N, \bar{h}_0) = \left\{ 1 + \frac{12}{\bar{h}_0^2 l_m^2} - 6 \frac{N}{\bar{h}_0 l_m} \coth \left( \frac{N l_m \bar{h}_0}{2} \right) \right\}$$

And

$$\bar{g}(l_m, N, \bar{h}_0) = \frac{\bar{h}_0^3}{12} \bar{\Phi}(l_m, N, \bar{h}_0) = \frac{\bar{h}_0^3}{12} + \frac{\bar{h}_0}{l_m^2} - \frac{N \bar{h}_0^2}{2 l_m} \coth \left( \frac{N l_m \bar{h}_0}{2} \right)$$

As  $\bar{h}_0 = 1 + \varepsilon_0 \cos \theta = \bar{h}_0(\theta)$  is a function of  $\theta$  only,  $\bar{g}(l_m, N, \bar{h}_0) = \bar{g}(\theta)$  is also a function of  $\theta$  only.

Equation (4.2) is further simplified to the following non-dimensional form under steady state condition for infinitely long journal bearings

$$C_A \frac{\partial \bar{h}_0}{\partial \theta} \cdot \frac{\partial \bar{P}_0}{\partial \theta} + C_B \frac{\partial^2 \bar{P}_0}{\partial \theta^2} = \frac{1}{2} \frac{\partial \bar{h}_0}{\partial \theta} \quad (4.3)$$

Where,

$$\left. \begin{aligned} C_A &= \frac{\bar{h}_0^2}{4} + \frac{1}{l_m^2} - \frac{N\bar{h}_0}{l_m} \coth\left(\frac{Nl_m\bar{h}_0}{2}\right) + \frac{N^2\bar{h}_0^2}{4} \operatorname{cosech}^2\left(\frac{Nl_m\bar{h}_0}{2}\right) \\ C_B &= \frac{\bar{h}_0^3}{12} + \frac{\bar{h}_0}{l_m^2} - \frac{N\bar{h}_0^2}{2l_m} \coth\left(\frac{Nl_m\bar{h}_0}{2}\right) \end{aligned} \right\} \quad (4.4)$$

Boundary conditions for equation (4.3) are as follows:

$$\left. \begin{aligned} &1. \text{The pressures at the ends of the bearing are zero} \\ &\quad \bar{p}_0(\theta, \pm 1) = 0 \\ &2. \text{The pressures distribution is symmetrical about the midplane of} \\ &\quad \text{the bearing} \\ &\quad \frac{\partial \bar{p}_0(\theta, 0)}{\partial \bar{z}} = 0 \\ &3. \text{Cavitation boundary condition} \\ &\quad \frac{\partial \bar{p}_0(\theta_2, \bar{z})}{\partial \theta} = 0, \quad \bar{p}_0(\theta, \bar{z}) = 0 \quad \text{for } \theta \geq \theta_2 \end{aligned} \right\} \quad (4.5)$$

where,  $\theta_2$  represents the angular coordinate at which the film cavitates.

#### 4.1.2.2 Numerical solution for pressures

Equation (4.3) is solved by using finite difference method with successive over-relaxation scheme as described explicitly to obtain the steady state pressure distribution  $\bar{P}_0$ , satisfying the boundary conditions as given in equation (4.5). Following the geometrical and operational symmetry of the bearing over its midplane, the half of the bearing length is considered and the bearing surface area is divided into a number of rectangular meshes of size  $\Delta\theta$  each. Representing a grid point as (i), where i and represent the coordinates along  $x(\theta)$  directions respectively, the first and second order derivatives of pressures are approximated by central difference method as follows:

$$\left. \begin{aligned} \frac{\partial \bar{p}_0}{\partial \theta} &= \frac{(\bar{p}_0)_{i+1} - (\bar{p}_0)_{i-1}}{2(\Delta\theta)} \\ \frac{\partial^2 \bar{p}_0}{\partial \theta^2} &= \frac{(\bar{p}_0)_{i+1} - 2(\bar{p}_0)_i + (\bar{p}_0)_{i-1}}{(\Delta\theta)^2} \end{aligned} \right\} \quad (4.6)$$

#### 4.1.2.3 Pressure Profiles

With the above representations equation (4.3) can be expressed in the finite difference form as

$$(\bar{p}_0)_i = C_1(\bar{p}_0)_{i+1} + C_2(\bar{p}_0)_{i-1} + C_3 \quad (4.7)$$

Where,

$$\left. \begin{aligned} C_1 &= \frac{1}{2} \left[ 1 - \frac{(C_A)_i \varepsilon_0 (\Delta\theta) \sin \theta_i}{2(C_B)_i} \right] \\ C_2 &= \frac{1}{2} \left[ 1 + \frac{(C_A)_i \varepsilon_0 (\Delta\theta) \sin \theta_i}{2(C_B)_i} \right] \\ C_3 &= \frac{(\Delta\theta)^2}{4(C_B)_i} \varepsilon_0 \sin \theta_i \quad \theta_i = i(\Delta\theta) \end{aligned} \right\} \quad (4.8)$$

where,  $(C_A)_i$  and  $(C_B)_i$  are to be evaluated using equation (4.4), in which

$$\bar{h}_0 = (\bar{h}_0)_i \quad \text{and} \quad \frac{\partial \bar{h}_0}{\partial \theta} = \left( \frac{\partial \bar{h}_0}{\partial \theta} \right)_i \quad \text{are to be calculated corresponding to each } \theta_i.$$

To compute the non-dimensional pressures numerically the number of divisions along  $\theta$ - and  $z$ -axes *i.e.* along bearing circumference and bearing length, considering half of the bearing length, are taken as 44 and 12 respectively. Since the pressure distribution is symmetrical about  $z=0$ , it is sufficient to solve the pressure distribution for one-half of the bearing length. Iteration is started considering initial pressures at all mesh points to be zero and the computed grid pressures are modified through successive over-relaxation

scheme. The convergence criterion for iteration is  $\left| \frac{\sum \bar{p}_0^{n+1} - \sum \bar{p}_0^n}{\sum \bar{p}_0^{n+1}} \right| \leq 0.001$ , where  $n$

represents the number of iterations. It is found that the rate of convergence is greatly influenced by the proper selection of the over-relaxation factor. The choice of the over-

relaxation factor is done on a trial basis. However for quick convergence in some cases the over-relaxation factor may be chosen as high as 1.30. In this particular analysis it is taken as 1.05.

### 4.1.3 Results and discussion

The schematic diagram of the journal is shown in *Fig.4.1*. Since the steady state characteristics *viz.*, load carrying capacity, attitude angle of the journal are dependent on the steady state film pressure  $\bar{p}_0$ , which, in turn, depends upon the micropolar parameters  $l_m$ ,  $N$ , eccentricity ratio  $\varepsilon_o$  and the slenderness ratio  $L/D$ , detailed parametric studies are done to show their effects in the respective non-dimensional form of steady state pressure profiles, steady state load, attitude angle and the results have been compared with the respective values for Newtonian fluid, thereby validating the methods and computer codes.

#### 4.1.3.1 Load carrying capacity

##### Effect of Coupling Number ( $N$ )

*Fig.4.1.1* shows the variation of the dimensionless load capacity of the journal bearings as a function of  $l_m$  for  $L/D = 1.0$  and;  $\varepsilon_o = 0.5$  when coupling number  $N$  is taken as a parameter. It is found from the figure that for any coupling number  $N$ , the load capacity reduces with  $l_m$  and approaches asymptotically to the Newtonian value as  $l_m \rightarrow \infty$  at a finite value of  $l_m$  the load parameter increases as coupling number is increased. Moreover, as  $l_m \rightarrow 0$  the load parameter increases rapidly as  $N$  increases. This is expected since the micropolar effect will be significant either when the characteristic material length is large or the clearance is small. The second case is very important here as  $C$  is usually very small in hydrodynamic journal bearing. As  $l_m \rightarrow 0$  the velocity and the other flow characteristics will reduce to their equivalents in the Newtonian theory with  $\mu$  everywhere replaced by  $\left(\mu + \frac{1}{2}\chi\right)$ , as gradient of microrotational velocity across film thickness is very small. Hence effectively the viscosity has been enhanced. So, when the non-dimensional load has been referred to the Newtonian viscosity, it is increased by a factor  $\left(\mu + \frac{1}{2}\chi\right)/\mu$  at  $l_m \rightarrow 0$ . The decrease in the load capacity to the asymptotic value at  $l_m \rightarrow \infty$  can be attributed to the same reason as given in the

explanation of steady state pressure.  $\left(\mu + \frac{1}{2}\chi\right)/\mu$  is equal to  $\left\{1/(1-N^2)\right\}$  by virtue of definition of  $N$ . So at  $l_m \rightarrow 0$  at higher value of  $N$ ,  $\left\{1/(1-N^2)\right\}$  is more and so  $\overline{W}_o$  is more. In between  $l_m \rightarrow 0$  and  $l_m \rightarrow \infty$ , at  $N \neq 0$ , the effect of angular momentum equation will modify Reynolds' equation through coupling number. Hence following the same explanation as that given for the steady state pressure, the enhanced pressure will increase the non-dimensional load carrying capacity.

#### **Effect of Eccentricity Ratio ( $\varepsilon_o$ )**

*Fig.4.1.2* shows the variation of load parameter with  $l_m$  for  $L/D = 1.0$  and  $N^2 = 0.5$ , when  $\varepsilon_o$  is considered as a parameter. It can be discerned that for a particular value of  $l_m$ , the non-dimensional load carrying capacity though increases in both types of lubrication as  $\varepsilon_o$  is increased, the rate of increase in  $\overline{W}_o$  in micropolar lubrication is found to be more rapid than that in the Newtonian lubrication. It is also found that the load parameter at any eccentricity ratio is considerably higher than that for Newtonian value at lower values of  $l_m$  and converges to that for Newtonian fluid as  $l_m \rightarrow \infty$ .

#### **4.1.3.2 Attitude angle**

##### **Effect of Coupling Number ( $N$ )**

*Fig.4.1.3* shows the variation of the attitude angle with micropolar parameter  $l_m$  for  $L/D = 1.0$  and  $\varepsilon_o = 0.5$  when coupling number  $N$  as treated a parameter. It can be seen from the figure that for a particular value of  $l_m$  attitude angle decreases as  $N$  is increased. Furthermore, as  $l_m$  increases the values of the attitude angle converge asymptotically to that for the Newtonian fluid. For any coupling number, attitude angle initially decreases with increase in  $l_m$  reaching a minimum and then reversing the trend as  $l_m$  is further increased. It is found that the optimum value of  $l_m$  at which  $\phi_o$  becomes a minimum increases with a decrease in  $N$ . It can be verified from the figure that the optimum value of  $l_m$  for minimum value of  $\phi_o$  shifts from around  $l_m = 6.0$  at  $N^2 = 0.9$  to around 16.0 at  $N^2 = 0.3$ . It can be demonstrated that to the left of the optimum  $l_m$ , micropolar effect becomes significant and to the right of this micropolar effect diminishes. Further at  $l_m = 0$ , the attitude angle remains the same as that for the Newtonian fluid. The reason is that components of non-dimensional forces along the line of centres and perpendicular to it

will be increased by the same factor  $\left(\mu + \frac{1}{2}\chi\right)/\mu$  and the attitude angle being the function of the ratio of the two will remain unaffected.

**Effect of Eccentricity Ratio ( $\epsilon_o$ )**

Effect of the eccentricity ratio on attitude angle has been shown in *Fig.4.1.4*, for  $L/D = 1.0$  and  $N^2 = 0.5$ . It is found from the figure that at any  $l_m$ , attitude angle decreases with increase in  $\epsilon_o$ . Furthermore, the effect of micropolar parameter  $l_m$  becomes more pronounced at higher  $\epsilon_o$ . The optimum micropolarity is found to be almost independent of  $\epsilon_o$  and occurs at  $l_m$  around 10.0.

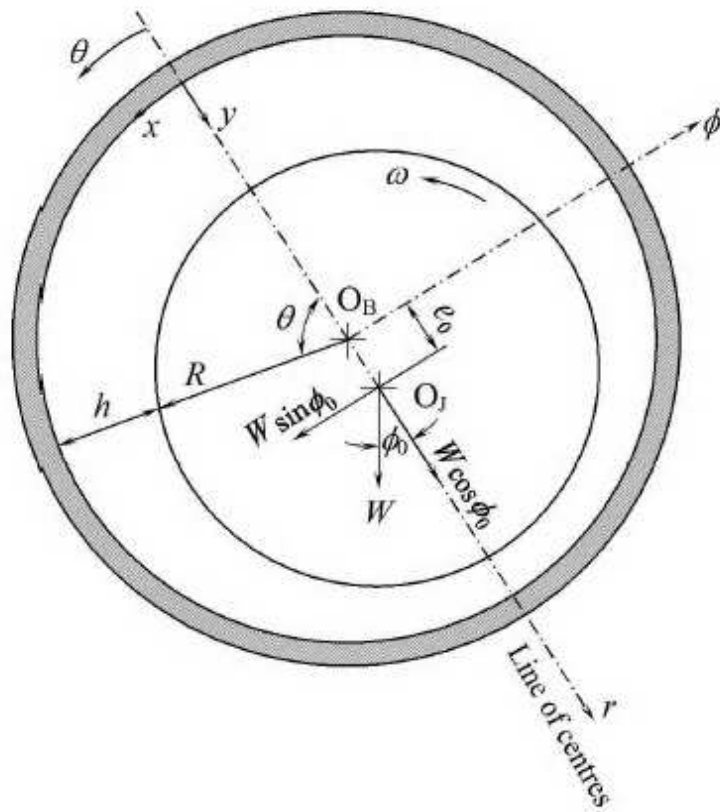


**Figure 4.1:** Schematic diagram of hydrodynamic journal bearing under steady state condition

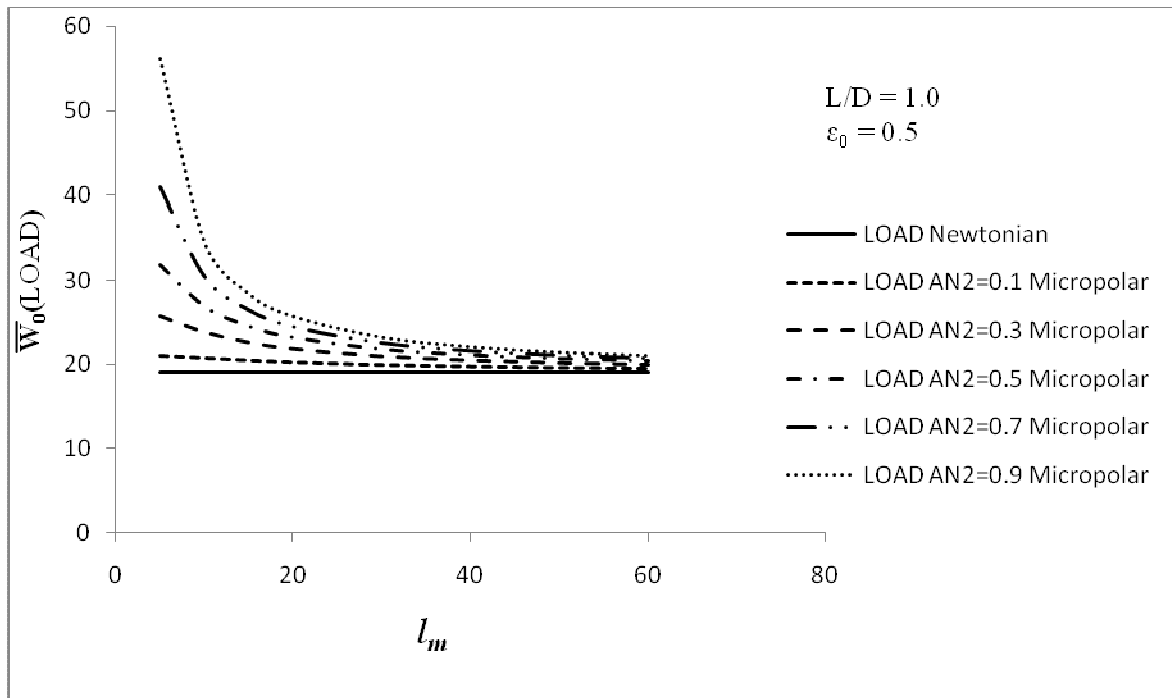


Fig.4.1.1: Variation of load parameter with  $l_m$  for various values of N (AN).

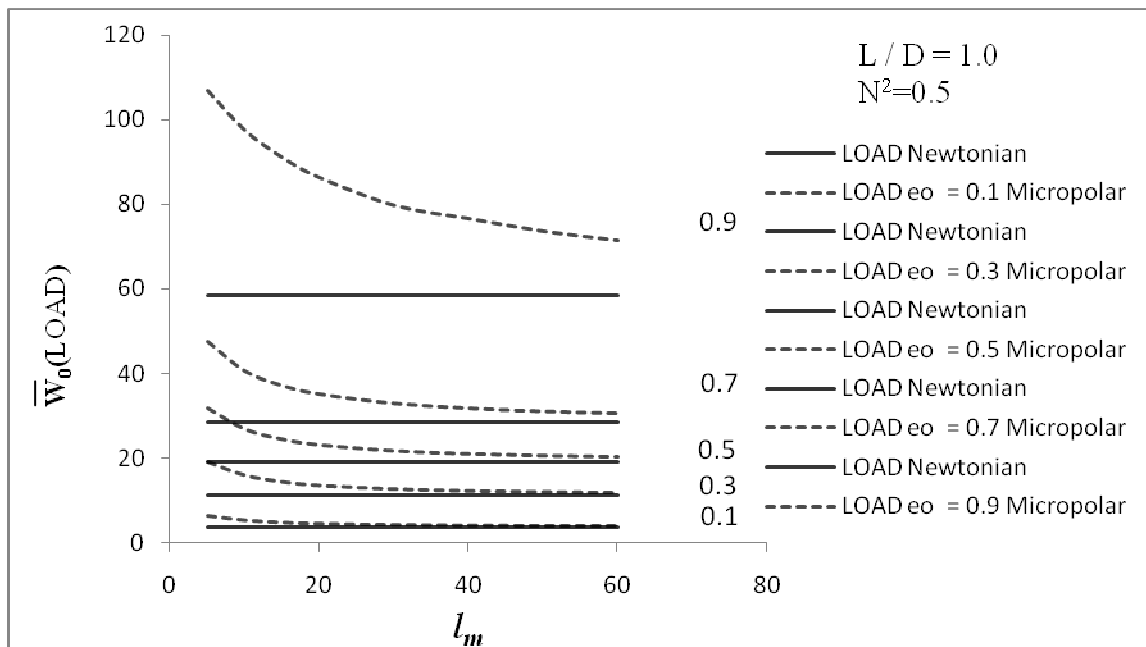


Fig.4.1.2: Variation of load parameter with  $l_m$  for various values of  $\epsilon_0$ .

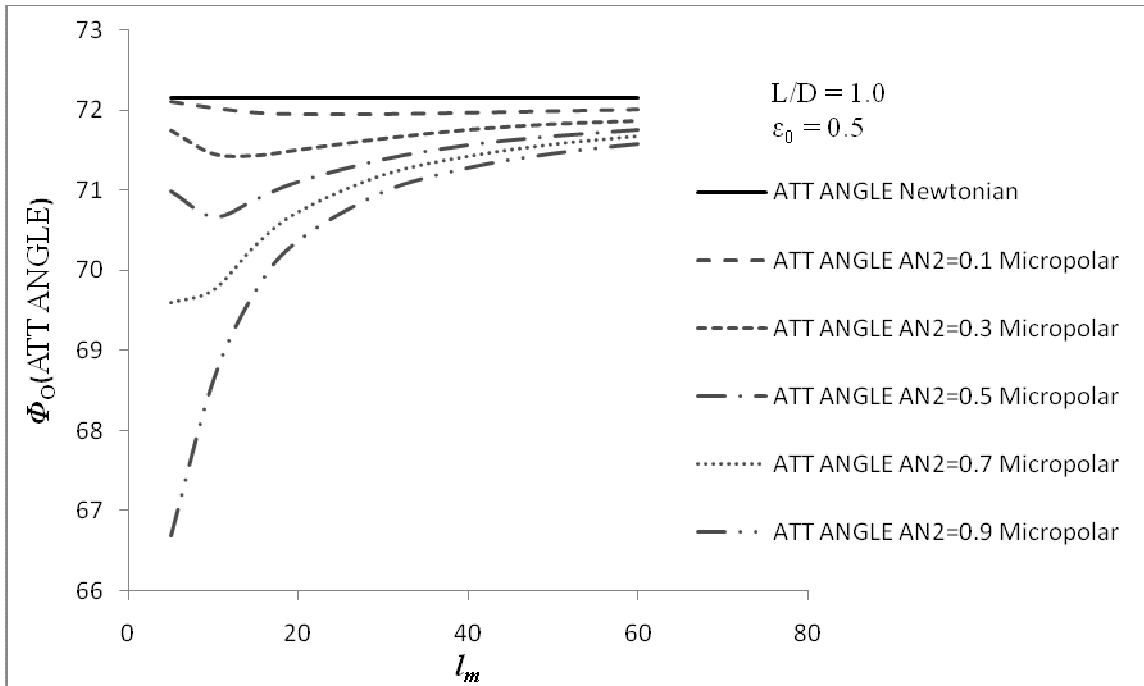


Fig.4.1.3: Variation of attitude angle with  $l_m$  for various values of N (AN).

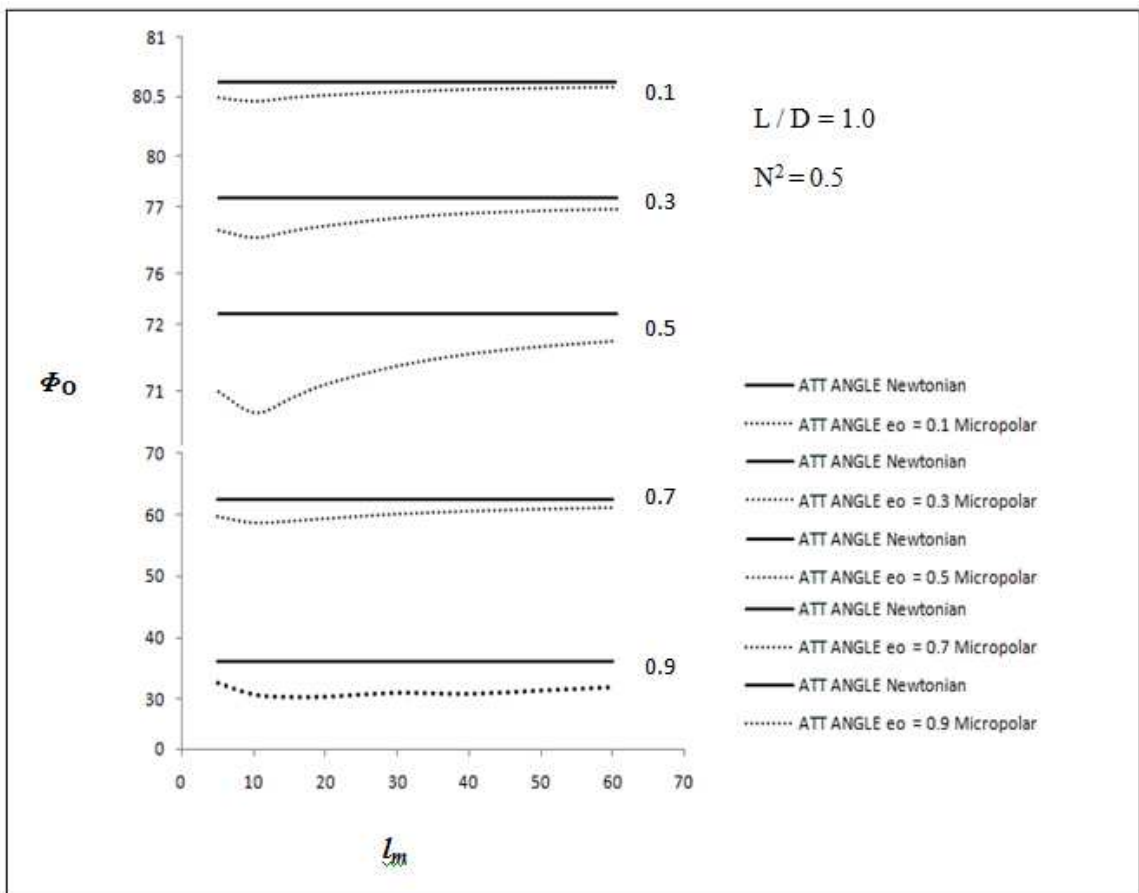


Fig.4.1.4: Variation of attitude angle with  $l_m$  for various values of  $\epsilon_0$ .

## **4.2 DYNAMIC ANALYSIS**

### **4.2.1 Introduction**

The present chapter deals with the dynamic analysis of infinitely long hydrodynamic journal bearings in micropolar lubrication regime. A linearised technique in the form of small order perturbations of eccentricity ratio and attitude angle has been adopted to simplify Reynolds equation and equations of motion. This method eliminates the time dependent terms and the dynamic pressure can be computed conveniently by using the finite difference method with successive over-relaxation scheme. Knowledge of the perturbed pressures enables one to compute the four components of stiffness and damping coefficients of the bearings by the numerical integration of the perturbed pressure fields along the line of centers and perpendicular to the line of centers. It will be shown subsequently that the real parts of these integrals will give to some scale the components of stiffness and the imaginary parts the components of damping coefficients. Apart from the stiffness and damping coefficients another dynamic quantity is the threshold of oil whirl stability, an important phenomenon exhibited by rotor/bearing system. Because of the oil whirl, the shaft center shifts away from the static equilibrium position, whirls in an orbit and may ultimately come in contact with the bearing surface, and the bearing may fail due to seizure. Therefore, a study of oil whirl instability is important in bearing design.

Keeping this in view, the threshold for oil whirl and external stiffness and damping for a rigid rotor in self acting cylindrical journal bearings of infinite length lubricated with micropolar fluid has been analyzed theoretically. In this analysis, the journal is also assumed to execute small harmonic oscillation about its static equilibrium position, such that first order perturbation can be applied without serious error. The equations of motion of the journal have been written using the oil stiffness and damping coefficients and external stiffness and damping coefficients, and the resulting equations have been investigated for oil whirl stability. The results of the analysis are shown in the form of graphs and the effects of various parameters like micropolar parameters, eccentricity ratio are studied and discussed.

## 4.2.2 Theoretical analysis

### 4.2.2.1 Governing equation

A schematic diagram of a journal bearing in micropolar lubrication with the appropriate coordinate system used for the purpose of analysis is shown in Fig 4.2. The journal is considered to rotate with a steady angular velocity: about its axis and it is further assumed that the journal undergoes a steady whirl in an elliptic orbit with a frequency  $\omega_p$  about its mean steady state position. The governing modified Reynolds equation (3.47) for two-dimensional flow of micropolar lubricant with the following substitutions

$$\theta = \frac{x}{R}, \quad \bar{z} = \frac{2z}{L}, \quad \bar{h} = \frac{h}{C}, \quad \bar{p} = \frac{pC^2}{\mu\omega R^2}, \quad l_m = \frac{C}{\Lambda}, \quad \tau = \omega t \quad (4.9)$$

will reduce to its non-dimensional form as

$$\frac{\partial}{\partial \theta} \left[ \bar{g}(l_m, N, \bar{h}) \frac{\partial \bar{p}}{\partial \theta} \right] + \left( \frac{D}{L} \right)^2 \frac{\partial}{\partial \bar{z}} \left[ \bar{g}(l_m, N, \bar{h}) \frac{\partial \bar{p}}{\partial \bar{z}} \right] = \frac{1}{2} (1 - 2\phi') \frac{\partial \bar{h}}{\partial \theta} + \frac{\partial \bar{h}}{\partial \tau} \quad (4.10)$$

Where,

$$\bar{\Phi}(l_m, N, \bar{h}) = \left\{ 1 + \frac{12}{\bar{h}^2 l_m^2} - 6 \frac{N}{\bar{h} l_m} \coth \left( \frac{N l_m \bar{h}}{2} \right) \right\}$$

$$\bar{g}(l_m, N, \bar{h}) = \frac{\bar{h}^3}{12} \bar{\Phi}(l_m, N, \bar{h}) = \frac{\bar{h}^3}{12} + \frac{\bar{h}}{l_m^2} - \frac{N \bar{h}^2}{2 l_m} \coth \left( \frac{N l_m \bar{h}}{2} \right)$$

And

$$\phi' = \frac{\partial \phi}{\partial \tau}$$

As  $\bar{h} = \bar{h}(\theta)$  is a function of  $\theta$  only.  $\bar{g}(l_m, N, \bar{h}) = \bar{g}(\theta)$  is also function of  $\theta$  only.

### 4.2.3 Perturbation Technique

The concept of the perturbation technique is to provide small order perturbation to the eccentricity ratio and attitude angle assuming the journal to execute small harmonic oscillation about its static equilibrium position, to eliminate the time dependent terms without serious error. First order perturbation method is utilized for non-dimensional pressure and local film thickness with assumption that the journal whirls about its mean steady state position given by the eccentricity ratio  $\varepsilon_0$  with amplitudes  $\mathbf{Re}(\varepsilon_1 e^{i\lambda_r t})$  and  $\mathbf{Re}(\varepsilon_0 e^{i\lambda_r t})$  along the line of centers and perpendicular to the line of centers respectively for which the non-dimensional pressure and local film thickness will be as follows

$$\left. \begin{aligned} \bar{p} &= \bar{p}_0 + \bar{p}_1 \varepsilon_1 e^{i\lambda_R \tau} + \bar{p}_2 \varepsilon_0 \phi_1 e^{i\lambda_R \tau} \\ \bar{h} &= \bar{h}_0 + \varepsilon_1 e^{i\lambda_R \tau} \cos \theta + \varepsilon_0 \phi_1 e^{i\lambda_R \tau} \sin \theta \end{aligned} \right\} \quad (4.11)$$

Where,

$$\bar{h}_0 = 1 + \varepsilon_0 \cos \theta ; \quad \varepsilon = \varepsilon_0 + \varepsilon_1 e^{i\lambda_R \tau} \quad ; \quad \phi = \phi_0 + \phi_1 e^{i\lambda_R \tau} \quad \text{and} \quad \lambda_R = \frac{\omega_p}{\omega}$$

The parameters with suffix '0' correspond to steady-state condition.

Substituting equation (4.8) into equation

$$\frac{\partial}{\partial \theta} \left[ \bar{g}(l_m, N, \bar{h}) \frac{\partial \bar{p}}{\partial \theta} \right] = \frac{1}{2} (1 - 2\phi) \frac{\partial \bar{h}}{\partial \theta} + \frac{\partial \bar{h}}{\partial \tau} \quad (\text{For infinitely long bearing})$$

and collecting the first order terms of  $\varepsilon_1$  and  $\varepsilon_0 \phi_1$  the following two equations are obtained

$$C_A \frac{\partial \bar{h}_0}{\partial \theta} \frac{\partial \bar{p}_1}{\partial \theta} + \{-C_A \sin \theta + (C_C \cos \theta) \frac{\partial \bar{h}_0}{\partial \theta}\} \frac{\partial \bar{p}_0}{\partial \theta} + C_B \frac{\partial^2 \bar{p}_1}{\partial \theta^2} + (C_A \cos \theta) \frac{\partial^2 \bar{p}_0}{\partial \theta^2} = -\frac{1}{2} \sin \theta + i\lambda_r \cos \theta \quad (4.12)$$

$$C_A \frac{\partial \bar{h}_0}{\partial \theta} \frac{\partial \bar{p}_2}{\partial \theta} + \{C_A \cos \theta + (C_C \sin \theta) \frac{\partial \bar{h}_0}{\partial \theta}\} \frac{\partial \bar{p}_0}{\partial \theta} + C_B \frac{\partial^2 \bar{p}_2}{\partial \theta^2} + (C_A \sin \theta) \frac{\partial^2 \bar{p}_0}{\partial \theta^2} = \frac{1}{2} \cos \theta + i \lambda_r \left( \sin \theta - \frac{1}{\epsilon_0} \frac{\partial \bar{h}_0}{\partial \theta} \right)$$

(4.13)

Where,  $C_A$  and  $C_B$  are obtained from equation (4.4).

$$C_C = \frac{\bar{h}_0}{2} + N^2 \bar{h}_0 \cos \operatorname{ech}^2 \left( \frac{N l_m \bar{h}_0}{2} \right) - \frac{N}{l_m} \coth \left( \frac{N l_m \bar{h}_0}{2} \right) - \frac{N^3 l_m \bar{h}_0^2}{4} \cos \operatorname{ech}^2 \left( \frac{N l_m \bar{h}_0}{2} \right) \coth \left( \frac{N l_m \bar{h}_0}{2} \right)$$

(4.14)

Equations (4.12) and (4.13) represent the governing differential equations for perturbed pressures.

The boundary conditions for the perturbed pressures are as follows:

1. The perturbed pressures at the ends of the bearing are zero

$$\bar{p}_1(\theta, \pm 1) = \bar{p}_2(\theta, \pm 1) = 0$$

2. The perturbed pressure distributions are symmetrical about the midplane of the bearing

$$\frac{\partial \bar{p}_1(\theta, 0)}{\partial \bar{z}} = \frac{\partial \bar{p}_2(\theta, 0)}{\partial \bar{z}} = 0$$

3. All perturbed pressure in the cavitated zone are zero

$$\bar{p}_1(\theta_1, \bar{z}) = \bar{p}_2(\theta_1, \bar{z}) = 0,$$

$$\bar{p}_1(\theta, \bar{z}) = \bar{p}_2(\theta, \bar{z}) = 0, \quad \theta \geq \theta_2$$

(4.15)

Where,  $\theta_2$  represents the angular coordinate where the film cavitates.

#### 4.2.3.1 Numerical solution for pressures

Equations (4.12) and (4.13) are solved by using finite difference method with successive over relaxation scheme to obtain the perturbed pressure distributions  $\bar{p}_1$  and  $\bar{p}_2$ , satisfying the boundary conditions as given in equation (4.15). Following the geometrical and operational symmetry of the bearing over its mid-plane, the half of the bearing length is considered and the bearing surface area is divided into a number of rectangular meshes of size  $(\Delta\theta \times \Delta z)$  each. The first and second order derivatives of pressures are approximated by central difference method as follows:

$$\left. \begin{aligned} \frac{\partial \bar{p}_n}{\partial \theta} &= \frac{(\bar{p}_n)_{i+1} - (\bar{p}_n)_{i-1}}{2(\Delta\theta)} \\ \frac{\partial^2 \bar{p}_n}{\partial \theta^2} &= \frac{(\bar{p}_n)_{i+1} - 2(\bar{p}_n)_i + (\bar{p}_n)_{i-1}}{(\Delta\theta)^2} \end{aligned} \right\} \text{Where, } n=1, 2 \quad (4.16)$$

#### 4.2.3.2 Perturbed Pressure Equations

With the help of finite difference technique as stated in equation (4.16) and the boundary conditions in equation (4.15), equations (4.12) and (4.13) are reduced to give the following pressure equations

$$(\bar{p}_1)_i = C_1(\bar{p}_1)_{i+1} + C_2(\bar{p}_1)_{i-1} + C_4(\bar{p}_0)_{i+1} + C_5(\bar{p}_0)_{i-1} + C_6(\bar{p}_0)_i + C_7 \quad (4.17)$$

$$(\bar{p}_2)_i = C_1(\bar{p}_2)_{i+1} + C_2(\bar{p}_2)_{i-1} + C_8(\bar{p}_0)_{i+1} + C_9(\bar{p}_0)_{i-1} + C_{10}(\bar{p}_0)_i + C_{11} \quad (4.18)$$

where  $C_1, C_2$  are as stated in equation (4.8) and

$$\left. \begin{aligned} C_4 &= \left( \frac{(C_A)_i}{2(C_B)_i} \cos\theta_i - \frac{(C_A)_i}{4(C_B)_i} (\Delta\theta) \sin\theta_i - \frac{(C_C)_i}{4(C_B)_i} (\Delta\theta) \varepsilon_0 \sin\theta_i \cos\theta_i \right) \\ C_5 &= \left( \frac{(C_A)_i}{2(C_B)_i} \cos\theta_i + \frac{(C_A)_i}{4(C_B)_i} (\Delta\theta) \sin\theta_i + \frac{(C_C)_i}{4(C_B)_i} (\Delta\theta) \varepsilon_0 \sin\theta_i \cos\theta_i \right) \\ C_6 &= -\frac{(C_A)_i}{(C_B)_i} \cos\theta_i \quad C_7 = \frac{(\Delta\theta)^2}{2(C_B)_i} \left( \frac{1}{2} \sin\theta_i - i\lambda_R \cos\theta_i \right) \\ C_8 &= \left( \frac{(C_A)_i}{2(C_B)_i} \sin\theta_i + \frac{(C_A)_i}{4(C_B)_i} (\Delta\theta) \cos\theta_i - \frac{(C_C)_i}{4(C_B)_i} (\Delta\theta) \varepsilon_0 \sin^2\theta_i \right) \end{aligned} \right\} \quad (4.19)$$

$$\left. \begin{aligned}
C_9 &= \left( \frac{(C_A)_i}{2(C_B)_i} \sin \theta_i - \frac{(C_A)_i}{4(C_B)_i} (\Delta \theta) \cos \theta_i + \frac{(C_C)_i}{4(C_B)_i} (\Delta \theta) \varepsilon_0 \sin^2 \theta_i \right) \\
C_{10} &= -\frac{(C_A)_i}{(C_B)_i} \sin \theta_i \quad C_{11} = -\frac{(\Delta \theta)^2}{2(C_B)_i} \left( \frac{1}{2} \cos \theta_i + 2i\lambda_R \sin \theta_i \right) \\
\theta_i &= i(\Delta \theta)
\end{aligned} \right\} \quad (4.19)$$

where,  $(C_A)_i$ ,  $(C_B)_i$  and  $(C_C)_i$  are to be evaluated by using equations (4.4) and (4.14),

in which  $\bar{h}_0 = (\bar{h}_0)_i$  and  $\frac{\partial \bar{h}_0}{\partial \theta} = \left( \frac{\partial \bar{h}_0}{\partial \theta} \right)_i$  are to be calculated corresponding to each  $\theta_i$ .

To compute the non-dimensional pressures numerically the number of divisions along  $\theta$ - and  $\bar{z}$  -axes *i.e.* along bearing circumference and bearing length, considering half of the bearing length, are taken as 44 and 12 respectively. Since the perturbed pressure distributions are also symmetrical over the midplane of the bearing, half of the bearing length is taken only. Iteration is started considering initial pressures at all mesh points as zeros and the computed grid pressures are modified through successive over-relaxation scheme. The iteration is terminated with a convergence criterion for every pressure as

$$\left| \frac{\sum \bar{p}_i^{-n+1} - \sum \bar{p}_i^{-n}}{\sum \bar{p}_i^{-n+1}} \right| \leq 0.001$$

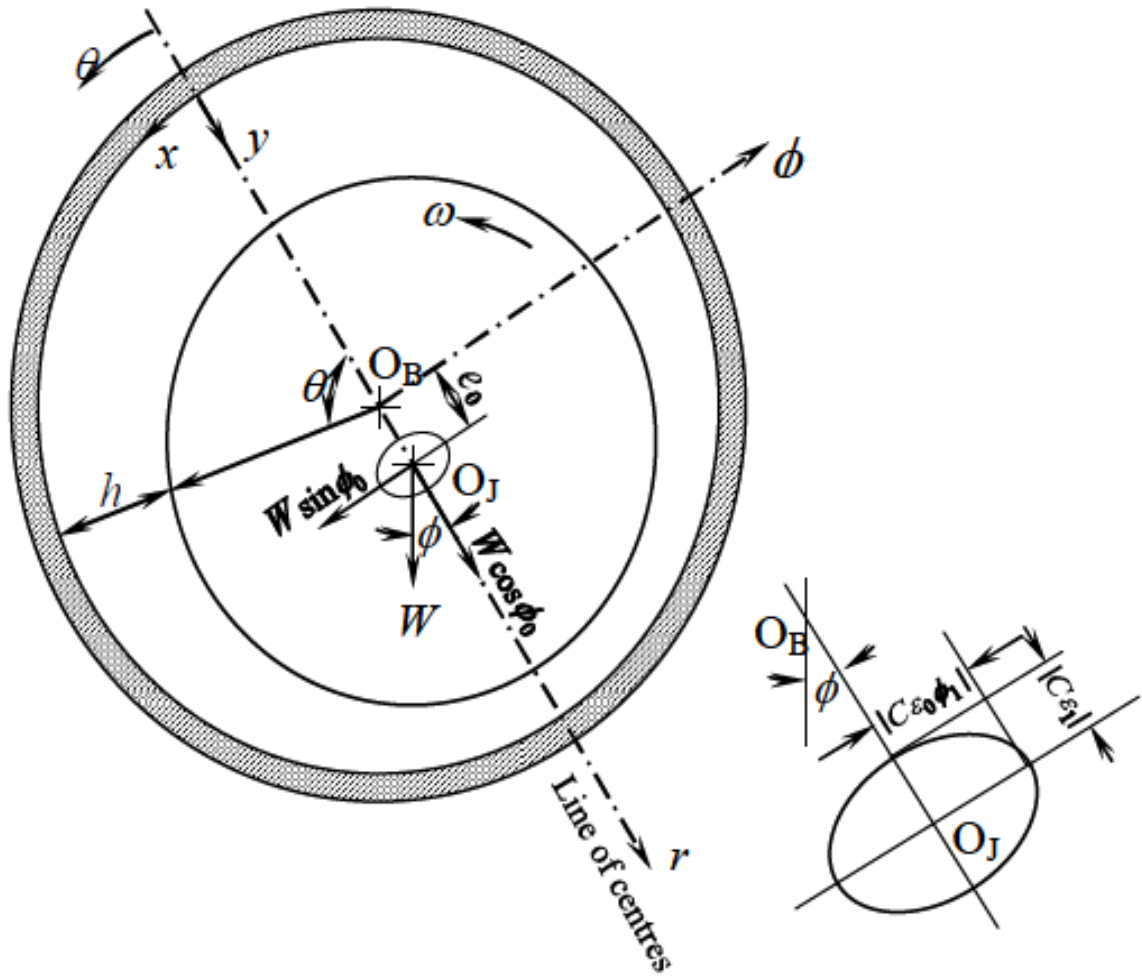


**Figure 4.2:** Schematic diagram of hydrodynamic journal bearings under dynamic operating condition

#### 4.2.4 STIFFNESS AND DAMPING COEFFICIENTS

The components of the dynamic load along the line of centers and perpendicular to the line of centers corresponding to perturbed pressure ( $p_1 \varepsilon_1 e^{i\lambda R t}$ ) in  $R$ -direction can be written as under

$$(W_d)_R e^{i\lambda R t} = -2 \int_0^{L/2} \int_{\theta_1}^{\theta_2} p_1 \cos \theta \varepsilon_1 e^{i\lambda R t} R d\theta dz \quad (4.20)$$

And

$$(W_d)_\phi e^{i\lambda R\tau} = -2 \int_0^{L/2} \int_{\theta_1}^{\theta_2} p_1 \sin \theta \varepsilon_1 e^{i\lambda R\tau} R d\theta dz \quad (4.21)$$

As the journal executes small harmonic oscillation about its steady state position in an elliptic orbit, the components of dynamic load can be expressed as a spring load and viscous damping load as

$$(W_d)_R e^{i\lambda R\tau} = S_{RR} C\varepsilon_R + D_{RR} \frac{d}{dt}(C\varepsilon_R) \quad (4.22)$$

$$(W_d)_\phi e^{i\lambda R\tau} = S_{\phi R} C\varepsilon_R + D_{\phi R} \frac{d}{dt}(C\varepsilon_R) \quad (4.23)$$

Combining equations (4.20) through (4.23), non-dimensionalising and noting that  $\varepsilon_R = \varepsilon_1 e^{i\lambda R t}$ , the following non-dimensional components of stiffness and damping coefficient result

$$\left. \begin{aligned} \bar{S}_{RR} &= -\operatorname{Re} \left[ 2 \int_0^1 \int_{\theta_1}^{\theta_2} \bar{p}_1 \cos \theta d\theta d\bar{z} \right] \\ \bar{S}_{\phi R} &= -\operatorname{Re} \left[ 2 \int_0^1 \int_{\theta_1}^{\theta_2} \bar{p}_1 \sin \theta d\theta d\bar{z} \right] \\ \bar{D}_{RR} &= -\operatorname{Im} \left[ 2 \int_0^1 \int_{\theta_1}^{\theta_2} \bar{p}_1 \cos \theta d\theta d\bar{z} \right] / \lambda_R \\ \bar{D}_{\phi R} &= -\operatorname{Im} \left[ 2 \int_0^1 \int_{\theta_1}^{\theta_2} \bar{p}_1 \sin \theta d\theta d\bar{z} \right] / \lambda_R \end{aligned} \right\} \quad (4.24)$$

Similarly, considering dynamic displacement of the journal along  $\Phi$  direction, it can be shown that

$$\left. \begin{aligned}
\bar{S}_{R\phi} &= -\operatorname{Re} \left[ 2 \int_0^1 \int_{\theta_1}^{\theta_2} \bar{p}_2 \cos \theta d\theta d\bar{z} \right] \\
\bar{S}_{\phi\phi} &= -\operatorname{Re} \left[ 2 \int_0^1 \int_{\theta_1}^{\theta_2} \bar{p}_2 \sin \theta d\theta d\bar{z} \right] \\
\bar{D}_{R\phi} &= -\operatorname{Im} \left[ 2 \int_0^1 \int_{\theta_1}^{\theta_2} \bar{p}_2 \cos \theta d\theta d\bar{z} \right] / \lambda_R \\
\bar{D}_{\phi\phi} &= -\operatorname{Im} \left[ 2 \int_0^1 \int_{\theta_1}^{\theta_2} \bar{p}_2 \sin \theta d\theta d\bar{z} \right] / \lambda_R
\end{aligned} \right\} \quad (4.25)$$

where,

$$\bar{S}_{ij} = \frac{2C^3 S_{ij}}{\mu\omega R^3 L} \text{ and } \bar{D}_{ij} = \frac{2C^3 D_{ij}}{\mu R^3 L}, \quad i = R, \phi \text{ and } j = R, \phi$$

As the dynamic pressure distributions  $\bar{p}_1$  and  $\bar{p}_2$  have been obtained by finite difference method, the above components of stiffness and damping coefficients can be easily obtained by numerical integration using Simpson's 1/3-rd rule.

#### 4.2.5. EQUATION OF MOTION

The dynamic pressure distribution  $\bar{p}_1$  &  $\bar{p}_2$  have been obtained by finite difference method and stiffness and damping co-efficient also have been calculated by numerical integration using Simpson's 1/3 rule. Stiffness and damping co-efficient thus obtained can now be employed to study the stability of the flexibility supported hydrodynamic oil journal bearing can be written as:

Equation of motion of rotor in 'r' direction is:

$$m_R \left[ A_r + \frac{d^2 e_r}{dt^2} - e_r \left( \frac{d\phi}{dt} \right)^2 \right] + S_{rr} e_r + D_{rr} \frac{de_r}{dt} + S_{r\phi} e_\phi + D_{r\phi} \frac{de_\phi}{dt} = w_0 \cos \phi \quad (4.26)$$

Equation of motion of rotor in 'Φ' direction is:

$$m_R \left[ A_\phi + \frac{d^2 e_\phi}{dt^2} + 2e_r e_\phi \right] + S_{\phi\phi} e_\phi + D_{\phi\phi} \frac{de_\phi}{dt} + S_{\phi r} e_r + D_{\phi r} \frac{de_r}{dt} = w_0 \sin \phi \quad (4.27)$$

Equation of motion of the bearing (neglecting the weight of bearing) in 'r' direction:

$$m_b [A_r] - S_{rr} e_r - D_{rr} \frac{de_r}{dt} - S_{r\phi} e_\phi - D_{r\phi} \frac{de_\phi}{dt} = - \left( Kx_b + d \frac{dx_b}{dt} \right) \sin \phi - \left( Ky_b + d \frac{dy_b}{dt} \right) \cos \phi \quad (4.28)$$

And equation of motion of bearing in 'Φ' direction is:

$$m_b [A_\phi] - S_{\phi\phi} e_\phi - D_{\phi\phi} \frac{de_\phi}{dt} - S_{\phi r} e_r - D_{\phi r} \frac{de_r}{dt} = - \left( Kx_b + d \frac{dy_b}{dt} \right) \cos \phi + \left( Ky_b + d \frac{dy_b}{dt} \right) \sin \phi \quad (4.29)$$

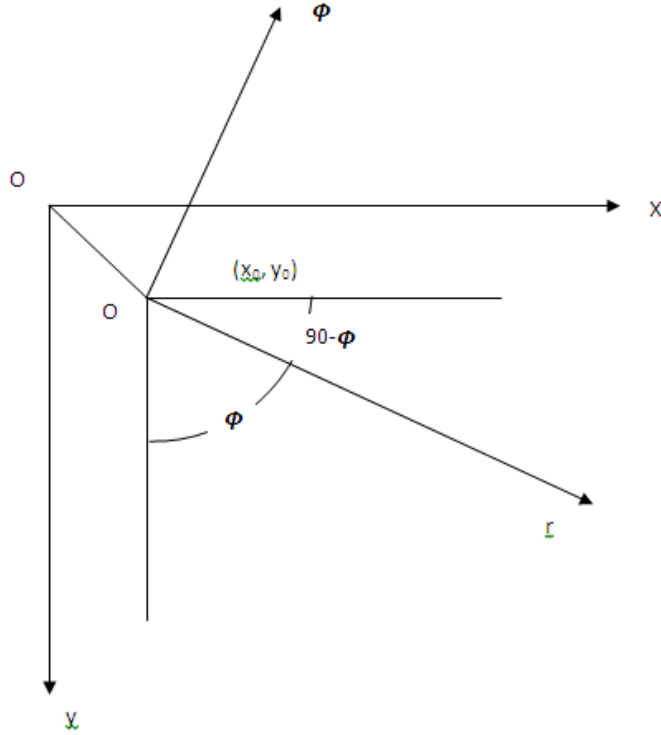


**Figure 4.3:** Schematic diagram of co-ordinate system

Where  $K$  and  $d$  are external stiffness and damping co-efficient. Here for the system

$$A_r = \ddot{x}_b \sin \phi + \ddot{y}_b \cos \phi \quad \text{And} \quad A_\phi = \ddot{x}_b \cos \phi - \ddot{y}_b \sin \phi$$

Now the following substitution are made

$$x_b = c \cdot \bar{x}_b = c (\bar{x}_0 + \bar{x}_1 e^{i\lambda_R t})$$

$$y_b = c \cdot \bar{y}_b = c (\bar{y}_0 + \bar{y}_1 e^{i\lambda_R t})$$

$$\phi = \phi_0 + \phi_1 e^{i\lambda_R t}$$

$$e_r = \bar{e}_r \cdot c = c (\epsilon_0 + \epsilon_1 e^{i\lambda_R t})$$

$$e_\phi = \bar{e}_\phi \cdot c = c (\epsilon_0 \phi_0 + \epsilon_1 \phi_1 e^{i\lambda_R t})$$

$$\cos \phi = \cos \phi_0 - \phi_1 e^{i\lambda_R t} \sin \phi_0$$

$$\sin \phi = \sin \phi_0 - \phi_1 e^{i\lambda_R t} \cos \phi_0$$

$$S_{ij} = \frac{\eta UR^2 L}{2C^3} \cdot \bar{S}_{ij}$$

$$D_{ij} = \frac{\eta R^3 L}{2C^3} \cdot \bar{D}_{ij}$$

$$w_0 = \frac{\eta UR^2 L}{2C^3} \cdot \bar{w}_0$$

$$T = \omega_p \cdot t \quad : \quad \omega_p / \omega = \lambda \quad : \quad m_b / m_R = Z$$

$$\bar{m} = \frac{MCw^2}{w_0} \text{ (Bearing stability parameter)}$$

Here  $\bar{x}_0, \bar{y}_0$  are steady state non-dimensional co-ordinates of center of bearing.

$\varepsilon_0$  = Steady state eccentricity ratio

$\phi_0$  = steady state altitude angle

$\bar{x}_1, \bar{y}_1, \varepsilon_1, \varepsilon_0$  &  $\phi_1$  are 1<sup>st</sup> order perturbation

Now using the above substitution and equation co-efficient on both sides, we have the equation of motion in the following non-dimensional form

$$-\lambda^2 \bar{m} \bar{w}_0 [\bar{x}_1 \sin \phi_0 + \bar{y}_1 \cos \phi_0] + (-\lambda^2 \bar{m} \bar{w}_0 + \bar{S}_{rr} + i\lambda \bar{D}_{rr}) \varepsilon_1 + (\bar{S}_{r\phi} \varepsilon_0 + i\lambda \bar{D}_{r\phi} \varepsilon_0 + \bar{w}_0 \sin \phi_0) \phi_1 = 0 \quad (4.30)$$

$$-\lambda^2 \bar{m} \bar{w}_0 [\bar{x}_1 \cos \phi_0 - \bar{y}_1 \sin \phi_0] + (\bar{S}_{\phi\phi} + i\lambda \bar{D}_{\phi\phi}) \varepsilon_1 + (\bar{S}_{\phi\phi} \varepsilon_0 - \lambda^2 \bar{m} \bar{w}_0 + \bar{S}_{rr} + i\lambda \bar{D}_{r\phi} \varepsilon_0 + \bar{w}_0 \cos \phi_0) \phi_1 = 0 \quad (4.31)$$

$$\begin{aligned} & (-\lambda^2 \bar{z} \bar{m} \bar{w}_0 + \bar{k} + i\lambda \bar{d}) \sin \phi_0 \bar{x}_1 + (-\lambda^2 \bar{z} \bar{m} \bar{w}_0 + \bar{k} + i\lambda \bar{d}) \cos \phi_0 \bar{y}_1 + (\bar{S}_{rr} + i\lambda \bar{D}_{rr}) \varepsilon_1 \\ & + (-\bar{S}_{r\phi} \varepsilon_0 - i\lambda \bar{D}_{r\phi} \varepsilon_0 + \bar{k} \bar{x}_0 \cos \phi_0 - \bar{k} \bar{y}_0 \sin \phi_0) \phi_1 = 0 \end{aligned} \quad (4.32)$$

$$\begin{aligned} & \left(-\lambda^2 z \overline{m w}_0 + \overline{k} + i \lambda \overline{d}\right) \cos \phi_0 \overline{x}_1 + \left(-\lambda^2 z \overline{m w}_0 - \overline{k} - i \lambda \overline{d}\right) \sin \phi_0 \overline{y}_1 + \left(-\overline{S}_{\phi r} - i \lambda \overline{D}_{\phi r}\right) \mathcal{E}_1 \\ & + \left(-\overline{S}_{\phi \phi} \mathcal{E}_0 - i \lambda \overline{D}_{\phi \phi} \mathcal{E}_0 - \overline{k} \overline{x}_0 \sin \phi_0 - \overline{k} \overline{y}_0 \cos \phi_0\right) \phi_1 = 0 \end{aligned} \quad (4.33)$$

For steady state condition

$$\overline{k} \overline{x}_0 \sin \phi_0 + \overline{k} \overline{y}_0 \cos \phi_0 = \overline{S}_{rr} \mathcal{E}_0 + \overline{S}_{r\phi} \mathcal{E}_0 \phi_0$$

And

$$\overline{k} \overline{x}_0 \cos \phi_0 - \overline{k} \overline{y}_0 \sin \phi_0 = \overline{S}_{\phi r} \mathcal{E}_0 + \overline{S}_{\phi \phi} \mathcal{E}_0 \phi_0$$

From which  $\overline{x}_0$  &  $\overline{y}_0$  are calculated as

$$\overline{x}_0 = (1/\overline{k}) \left[ \left( \overline{S}_{rr} \mathcal{E}_0 + \overline{S}_{r\phi} \mathcal{E}_0 \phi_0 \right) \sin \phi_0 + \left( \overline{S}_{\phi r} \mathcal{E}_0 + \overline{S}_{\phi \phi} \mathcal{E}_0 \phi_0 \right) \cos \phi_0 \right]$$

$$\overline{y}_0 = (1/\overline{k}) \left[ \left( \overline{S}_{rr} \mathcal{E}_0 + \overline{S}_{r\phi} \mathcal{E}_0 \phi_0 \right) \cos \phi_0 - \left( \overline{S}_{\phi r} \mathcal{E}_0 + \overline{S}_{\phi \phi} \mathcal{E}_0 \phi_0 \right) \sin \phi_0 \right]$$

Now the following substitution are imposed

$$\overline{P}_1 = (\overline{x}_1 \sin \phi_0 + \overline{y}_1 \cos \phi_0)$$

$$\overline{Q}_1 = (\overline{y}_1 \sin \phi_0 - \overline{x}_1 \cos \phi_0)$$

$$\overline{b}_1 = (\overline{x}_0 \sin \phi_0 + \overline{y}_0 \cos \phi_0)$$

$$\overline{b}_2 = (\overline{y}_0 \sin \phi_0 - \overline{x}_0 \cos \phi_0)$$

Therefore the equation of motion takes the configuration as

$$-\lambda^2 \overline{m w}_0 \overline{P}_1 + \left(-\lambda^2 \overline{m w}_0 + \overline{S}_{rr} + i \lambda \overline{D}_{rr}\right) \mathcal{E}_1 + \left(\overline{S}_{r\phi} \mathcal{E}_0 - i \lambda \overline{D}_{r\phi} \mathcal{E}_0 + \overline{w}_0 \sin \phi_0\right) \phi_1 = 0 \quad (4.34)$$

$$\lambda^2 \bar{m} \bar{w}_0 \bar{q}_1 + (\bar{S}_{\phi r} + i\lambda \bar{D}_{\phi r}) \epsilon_1 + (-\lambda^2 \bar{m} \bar{w}_0 \epsilon_0 + \bar{S}_{\phi\phi} \epsilon_0 + i\lambda \bar{D}_{\phi\phi} \epsilon_0 + \bar{w}_0 \cos \phi_0) \phi_1 = 0 \quad (4.35)$$

$$(-z\lambda^2 \bar{m} \bar{w}_0 - \bar{k} - i\lambda \bar{d}) \bar{P}_1 + (-\bar{S}_{rr} - i\lambda \bar{D}_{rr}) \epsilon_1 + (-\bar{S}_{r\phi} \epsilon_0 - i\lambda \bar{D}_{r\phi} \epsilon_0 - \bar{k} b_2) \phi_1 = 0 \quad (4.36)$$

And

$$(z\lambda^2 \bar{m} \bar{w}_0 - \bar{k} - i\lambda \bar{d}) \bar{q}_1 + (-\bar{S}_{\phi r} - i\lambda \bar{D}_{\phi r}) \epsilon_1 + (-\bar{S}_{\phi\phi} \epsilon_0 - i\lambda \bar{D}_{\phi\phi} \epsilon_0 - \bar{k} b_1) \phi_1 = 0 \quad (4.37)$$

Now for non-trivial solution, the determinant of the above equations (4.34), (4.35), (4.36), (4.37) must vanish. Equating real and imaginary parts of equation (obtained by expanding the determinant of the equations for non-trivial solution) separately to zero, the following two equations result:

$$A_{11} \bar{m}^4 + A_{12} \bar{m}^3 + A_{13} \bar{m}^2 + A_{14} \bar{m} + A_{15} = 0 \quad (4.38)$$

$$A_{12} \bar{m}^3 + A_{22} \bar{m}^2 + A_{23} \bar{m} + A_{24} = 0 \quad (4.39)$$

Where

$$A_{11} = C_{21} \cdot \lambda^8 \bar{w}_0^4 \quad (4.40)$$

$$A_{12} = C_{22} \cdot \lambda^6 \bar{w}_0^3 \quad (4.41)$$

$$A_{13} = C_{23} \cdot \lambda^6 \bar{w}_0^2 + C_{24} \cdot \lambda^4 \bar{w}_0^2 \quad (4.42)$$

$$A_{14} = C_{25} \cdot \lambda^4 \bar{w}_0 + C_{27} \cdot \lambda^2 \bar{w}_0 \quad (4.43)$$

$$A_{15} = C_{26} \cdot \lambda^4 + C_{28} \cdot \lambda^2 + C_{29} \quad (4.44)$$

$$A_{21} = C_{31} \cdot \mathcal{L}^6 \bar{w}_0^3 \quad (4.45)$$

$$A_{22} = C_{32} \cdot \mathcal{L}^4 \bar{w}_0^2 \quad (4.46)$$

$$A_{23} = C_{33} \cdot \mathcal{L}^4 \bar{w}_0 + C_{34} \cdot \mathcal{L}^2 \bar{w}_0 \quad (4.47)$$

$$A_{24} = C_{35} \cdot \mathcal{L}^2 + C_{36} \quad (4.48)$$

$$C_{21} = -Z^2 \varepsilon_0 \quad (4.49)$$

$$C_{22} = Z \bar{S}_{rr} \varepsilon_0 + Z \bar{S}_{\phi\phi} \varepsilon_0 + 2Z \bar{k} \varepsilon_0 + Z^2 \bar{S}_{\phi\phi} \varepsilon_0 + Z^2 \bar{w}_0 \cos \phi_0 + Z \bar{k} \bar{b}_1 \quad (4.50)$$

$$C_{23} = \bar{D}_{rr} \bar{D}_{\phi\phi} \varepsilon_0 - \bar{D}_{r\phi} \bar{D}_{\phi r} \varepsilon_0 - 2Z \bar{D}_{\phi r} \bar{D}_{r\phi} \varepsilon_0 + \bar{d} \bar{D}_{rr} \varepsilon_0 + 2Z \bar{D}_{rr} \bar{D}_{\phi\phi} \varepsilon_0 + \bar{d} \bar{D}_{\phi\phi} \varepsilon_0 + D^2 \bar{D}_{rr} \bar{D}_{\phi\phi} \varepsilon_0 + 2Z \bar{d} \bar{D}_{rr} \varepsilon_0 + 2Z \bar{d} \bar{D}_{\phi\phi} \varepsilon_0 - Z^2 \bar{D}_{\phi r} \bar{D}_{r\phi} \varepsilon_0 + \bar{d}^2 \varepsilon_0 \quad (4.51)$$

$$C_{24} = -\bar{S}_{rr} \bar{S}_{\phi\phi} \varepsilon_0 - \bar{S}_{rr} \bar{k} \bar{b}_1 + \bar{S}_{r\phi} \bar{S}_{\phi r} \varepsilon_0 + \bar{S}_{\phi r} \bar{k} \bar{b}_1 + 2Z \bar{S}_{r\phi} \bar{S}_{\phi r} \varepsilon_0 + Z \bar{S}_{\phi r} \bar{k} \bar{b}_2 - Z \bar{S}_{rr} \bar{w}_0 \cos \phi_0 - \bar{k} \bar{S}_{rr} \varepsilon_0 - 2Z \bar{S}_{rr} \bar{S}_{\phi\phi} \varepsilon_0 - Z \bar{k} \bar{S}_{rr} \bar{b}_1 - \bar{k} \bar{S}_{\phi\phi} \varepsilon_0 - \bar{k}^2 \bar{b}_1 + Z \bar{S}_{\phi r} \bar{w}_0 \sin \phi_0 - \bar{k}^2 \varepsilon_0 - 2Z \bar{k} \bar{S}_{rr} \varepsilon_0 - 2Z \bar{k} \bar{S}_{\phi\phi} \varepsilon_0 - Z^2 \bar{S}_{rr} \bar{S}_{\phi\phi} \varepsilon_0 - 2Z \bar{k} \bar{w}_0 \cos \phi_0 - Z^2 \bar{S}_{rr} \bar{w}_0 \cos \phi_0 + Z^2 \bar{S}_{r\phi} \bar{S}_{\phi r} \varepsilon_0 + Z^2 \bar{S}_{\phi r} \bar{w}_0 \sin \phi_0 \quad (4.52)$$

$$C_{25} = 2\bar{k} \bar{D}_{\phi r} \varepsilon_0 + 2\bar{d} \bar{D}_{\phi r} \bar{S}_{r\phi} \varepsilon_0 + \bar{d} \bar{k} \bar{b}_2 \bar{D}_{\phi r} + 2\bar{d} \bar{S}_{\phi r} \bar{D}_{r\phi} \varepsilon_0 - 2\bar{k} \bar{D}_{\phi\phi} \bar{D}_{rr} \varepsilon_0 - 2\bar{d} \bar{S}_{rr} \bar{D}_{\phi\phi} \varepsilon_0 - 2\bar{d} \bar{S}_{\phi\phi} \bar{D}_{rr} \varepsilon_0 - \bar{d} \bar{D}_{rr} \bar{w}_0 \cos \phi_0 - \bar{d} \bar{D}_{rr} \bar{k} \bar{b}_1 + \bar{d} \bar{D}_{\phi r} \bar{w}_0 \sin \phi_0 - \bar{d}^2 \bar{S}_{rr} \varepsilon_0 - \bar{d}^2 \bar{S}_{\phi\phi} \varepsilon_0 - \bar{d}^2 \bar{w}_0 \cos \phi_0 - 2Z \bar{k} \bar{D}_{\phi\phi} \bar{D}_{rr} \varepsilon_0 - 2\bar{d} \bar{k} \bar{D}_{rr} \varepsilon_0 - 2\bar{d} \bar{k} \bar{D}_{\phi\phi} \varepsilon_0 - Z \bar{d} \bar{D}_{rr} \bar{S}_{\phi\phi} \varepsilon_0 - 2Z \bar{d} \bar{D}_{rr} \bar{w}_0 \cos \phi_0 - 2Z \bar{d} \bar{S}_{rr} \bar{D}_{\phi\phi} \varepsilon_0 + 2Z \bar{k} \bar{D}_{\phi r} \bar{D}_{r\phi} \varepsilon_0 + 2Z \bar{d} \bar{S}_{r\phi} \bar{D}_{\phi r} \varepsilon_0 + 2Z \bar{d} \bar{D}_{\phi r} \bar{w}_0 \sin \varepsilon_0 + 2Z \bar{d} \bar{S}_{\phi r} \bar{D}_{r\phi} \varepsilon_0 \quad (4.53)$$

$$\begin{aligned}
C_{27} = & -2\bar{k}\bar{S}_{r\phi}\bar{S}_{\phi r}\epsilon_0 - \bar{k}^2\bar{S}_{\phi r}\bar{b}_2 + 2\bar{k}\bar{S}_{rr}\bar{S}_{\phi\phi}\epsilon_0 + \bar{k}\bar{S}_{rr}\bar{w}_0 \cos\phi_0 + \\
& \bar{k}^2\bar{S}_{rr}\bar{b}_1 - \bar{k}\bar{S}_{\phi r}\bar{w}_0 \sin\phi_0 + \bar{k}^2\bar{S}_{rr}\epsilon_0 + \bar{k}^2\bar{S}_{\phi\phi}\epsilon_0 + 2Z\bar{k}\bar{S}_{rr}\bar{S}_{\phi\phi}\epsilon_0 + \bar{k}^2\bar{w}_0 \cos\phi_0 + \\
& 2Z\bar{k}\bar{S}_{rr}\bar{w}_0 \cos\epsilon_0 - 2Z\bar{k}\bar{S}_{r\phi}\bar{S}_{\phi r}\epsilon_0 - 2Z\bar{k}\bar{S}_{\phi r}\bar{w}_0 \sin\phi_0
\end{aligned} \tag{4.54}$$

$$C_{26} = -\bar{d}^2\bar{D}_{rr}\bar{D}_{\phi\phi}\epsilon_0 + \bar{d}^2\bar{D}_{r\phi}\bar{D}_{\phi r}\epsilon_0 \tag{4.55}$$

$$\begin{aligned}
C_{28} = & -\bar{d}^2\bar{S}_{rr}\bar{S}_{\phi\phi}\epsilon_0 + \bar{d}^2\bar{S}_{rr}\bar{w}_0 \cos\phi_0 + \bar{k}^2\bar{D}_{rr}\bar{D}_{\phi\phi}\epsilon_0 + 2\bar{d}\bar{k}\bar{D}_{rr}\bar{S}_{\phi\phi}\epsilon_0 + \\
& 2\bar{d}\bar{k}\bar{D}_{rr}\bar{w}_0 \cos\phi_0 + 2\bar{d}\bar{k}\bar{D}_{\phi\phi}\bar{S}_{rr}\epsilon_0 - \bar{k}^2\bar{D}_{\phi r}\bar{D}_{r\phi}\epsilon_0 - \bar{d}^2\bar{S}_{r\phi}\bar{S}_{\phi r}\epsilon_0 - \bar{d}^2\bar{S}_{\phi r}\bar{w}_0 \sin\phi_0 - \\
& 2\bar{d}\bar{k}\bar{S}_{r\phi}\bar{D}_{\phi r}\epsilon_0 - 2\bar{d}\bar{k}\bar{D}_{\phi r}\bar{w}_0 \sin\phi_0 - 2\bar{d}\bar{k}\bar{S}_{\phi r}\bar{D}_{r\phi}\epsilon_0
\end{aligned} \tag{4.56}$$

$$C_{29} = -\bar{k}^2\bar{S}_{rr}\bar{S}_{\phi\phi}\epsilon_0 - \bar{k}^2\bar{S}_{rr}\bar{w}_0 \cos\phi_0 + \bar{k}^2\bar{S}_{r\phi}\bar{S}_{\phi r}\epsilon_0 + \bar{k}^2\bar{S}_{\phi r}\bar{w}_0 \sin\phi_0 \tag{4.57}$$

$$C_{31} = Z\bar{D}_{rr}\epsilon_0 + Z\bar{D}_{\phi\phi}\epsilon_0 + 2Z\bar{d}\epsilon_0 + Z^2\bar{D}_{rr}\epsilon_0 + Z^2\bar{D}_{\phi\phi}\epsilon_0 = 0 \tag{4.58}$$

$$\begin{aligned}
C_{32} = & -\bar{S}_{rr}\bar{D}_{\phi\phi}\epsilon_0 - \bar{D}_{rr}\bar{S}_{\phi\phi}\epsilon_0 - \bar{D}_{rr}\bar{k}\bar{b}_1 + \bar{S}_{r\phi}\bar{D}_{\phi r}\epsilon_0 + \bar{D}_{\phi r}\bar{k}\bar{b}_2 + \bar{S}_{\phi r}\bar{D}_{r\phi}\epsilon_0 + 2Z\bar{D}_{\phi r}\bar{S}_{r\phi}\epsilon_0 + \\
& Z\bar{D}_{r\phi}\bar{k}\bar{b}_2 + 2Z\bar{S}_{\phi r}\bar{D}_{r\phi}\epsilon_0 - Z\bar{D}_{rr}\bar{w}_0 \cos\phi_0 - \bar{k}\bar{D}_{rr}\epsilon_0 + Z\bar{D}_{\phi r}\bar{w}_0 \sin\phi_0 - Z\bar{d}\bar{k}\epsilon_0 - 2Z\bar{d}\bar{S}_{\phi\phi}\epsilon_0 \\
& - 2Z\bar{d}\bar{w}_0 \cos\phi_0 - Z^2\bar{S}_{\phi\phi}\bar{D}_{rr}\epsilon_0 - Z^2\bar{D}_{rr}\bar{w}_0 \cos\phi_0 - Z^2\bar{S}_{rr}\bar{D}_{\phi\phi}\epsilon_0 + Z^2\bar{D}_{\phi r}\bar{S}_{r\phi}\epsilon_0 + \\
& Z^2\bar{D}_{\phi r}\bar{w}_0 \sin\phi_0 + Z^2\bar{S}_{\phi r}\bar{D}_{r\phi}\epsilon_0 - 2Z\bar{k}\bar{D}_{rr}\epsilon_0 - 2Z\bar{k}\bar{D}_{\phi\phi}\epsilon_0
\end{aligned} \tag{4.59}$$

$$C_{33} = 2\bar{d}\bar{D}_{\phi r}\bar{D}_{r\phi}\epsilon_0 - 2\bar{d}\bar{D}_{rr}\bar{D}_{\phi\phi}\epsilon_0 - 2Z\bar{d}\bar{D}_{rr}\bar{D}_{\phi\phi}\epsilon_0 - \bar{d}^2\bar{D}_{rr}\epsilon_0 - \bar{d}^2\bar{D}_{\phi\phi}\epsilon_0 \tag{4.60}$$

$$\begin{aligned}
C_{34} = & -2\bar{D}_{\phi} \bar{S}_{r\phi} \epsilon_0 - k\bar{D}_{r\phi} \bar{b}_2 - 2k\bar{S}_{\phi} \bar{D}_{r\phi} \epsilon_0 - 2\bar{d} \bar{S}_{\phi} k\bar{b}_2 + 2k\bar{S}_{rr} \bar{D}_{\phi\phi} \epsilon_0 + 2k\bar{S}_{\phi\phi} \bar{D}_{rr} w_0 \cos\phi_0 + \\
& 2\bar{d} \bar{S}_{\phi\phi} \bar{S}_{rr} \epsilon_0 + \bar{d} \bar{S}_{rr} w_0 \cos\phi_0 + \bar{d} k \bar{b}_1 \bar{S}_{rr} + \bar{k}^2 \bar{b}_1 \bar{D}_{rr} - \bar{d} \bar{S}_{\phi} w_0 \sin\phi_0 - \bar{k} \bar{D}_{\phi} w_0 \sin\phi_0 + \\
& 2\bar{d} k \bar{S}_{rr} \epsilon_0 + 2\bar{d} k \bar{S}_{\phi\phi} \epsilon_0 + 2\bar{d} k w_0 \cos\phi_0 + 2Z\bar{d} \bar{S}_{rr} \bar{S}_{\phi\phi} \epsilon_0 + 2Z\bar{d} \bar{S}_{rr} w_0 \cos\phi_0 + \bar{k}^2 \bar{D}_{\phi\phi} \epsilon_0 + \\
& 2Zk \bar{S}_{\phi\phi} \bar{D}_{rr} \epsilon_0 + 2Zk \bar{D}_{rr} w_0 \cos\phi_0 + 2Zk \bar{S}_{rr} \bar{D}_{\phi\phi} \epsilon_0 - 2Zk \bar{D}_{\phi} w_0 \sin\phi_0 - 2Zk \bar{S}_{\phi} \bar{D}_{r\phi} \epsilon_0 - \\
& 2Z\bar{d} \bar{S}_{r\phi} \bar{S}_{\phi} \epsilon_0 - 2Z\bar{d} \bar{S}_{\phi} w_0 \sin\phi_0
\end{aligned} \tag{4.61}$$

$$\begin{aligned}
C_{35} = & 2\bar{d} k \bar{D}_{rr} \bar{D}_{\phi\phi} \epsilon_0 + \bar{d}^2 \bar{S}_{\phi\phi} \bar{D}_{rr} \epsilon_0 + \bar{d}^2 \bar{D}_{rr} \bar{w}_0 \cos\phi_0 + \bar{d}^2 \bar{S}_{rr} \bar{D}_{\phi\phi} \epsilon_0 - \bar{d}^2 \bar{S}_{r\phi} \bar{D}_{\phi} \epsilon_0 - \\
& \bar{d}^2 \bar{D}_{\phi} \bar{w}_0 \sin\phi_0 - \bar{d}^2 \bar{S}_{\phi} \bar{D}_{r\phi} \epsilon_0
\end{aligned} \tag{4.62}$$

$$\begin{aligned}
C_{36} = & 2\bar{d} k \bar{S}_{rr} \bar{S}_{\phi\phi} \epsilon_0 - 2\bar{d} k \bar{S}_{rr} \bar{w}_0 \cos\phi_0 - \bar{k}^2 \bar{S}_{\phi\phi} \bar{D}_{rr} \epsilon_0 - \bar{k}^2 \bar{D}_{rr} \bar{w}_0 \cos\phi_0 - \bar{k}^2 \bar{S}_{rr} \bar{D}_{\phi\phi} \epsilon_0 + \\
& \bar{k}^2 \bar{S}_{r\phi} \bar{D}_{\phi} \epsilon_0 + \bar{k}^2 \bar{D}_{\phi} \bar{w}_0 \sin\phi_0 + \bar{k}^2 \bar{S}_{\phi} \bar{D}_{r\phi} \epsilon_0 + 2\bar{d} k \bar{S}_{r\phi} \bar{S}_{\phi} \epsilon_0 + 2\bar{d} k \bar{S}_{\phi} \bar{w}_0 \sin\phi_0
\end{aligned} \tag{4.63}$$

The critical mass parameter & whirl ratio will be determined by satisfying the equations (4.38) & (4.39) employing Newton Raphson method.

## 4.2.6 Results and discussion

Since the dynamic characteristics expressed in terms of non-dimensional components of stiffness and damping coefficients and the critical mass parameter along with the corresponding whirl ratio, representing the stability of the journal, are dependent on the steady state and perturbed film pressures  $\bar{P}_0$ ,  $\bar{P}_1$  and  $\bar{P}_2$  and thus, in turn, depend upon the micropolar parameters ( $l_m, N$ ), eccentricity ratio  $\epsilon_o$ , detailed parametric studies are done to show their effects on the non-dimensional components of stiffness and damping coefficient and finally on critical mass parameter and whirl ratio.

### 4.2.6.1 Non-dimensional components of stiffness and damping coefficients

#### Effect of Coupling Number (N)

Figs.4.2.1 to 4.2.8 show the variation of the non-dimensional components of stiffness and damping coefficient as function of  $l_m$ , when coupling number ( $N$ ) is considered as a parameter, keeping  $\epsilon_o$  and  $L/D$  fixed at 0.5 and 1.0 respectively.

It can be observed from the figures that at any value  $l_m$ , the direct components of stiffness  $\bar{S}_{RR}$  and  $\bar{S}_{\phi\phi}$  increase with an increase in coupling number. For any of value of  $N$ ,  $\bar{S}_{RR}$  and  $\bar{S}_{\phi\phi}$  decrease with  $l_m$  and all the family of curves converge to the asymptotic value of these for Newtonian fluid as  $l_m$  becomes infinitely large. However, at  $l_m \rightarrow 0$ ,  $\bar{S}_{RR}$  and  $\bar{S}_{\phi\phi}$  are much larger compared to those of Newtonian fluids. The reason for such enhanced components of stiffness at  $l_m \rightarrow 0$  is the same as that for load parameter. Cross components of stiffness  $\bar{S}_{R\phi}$  and  $\bar{S}_{\phi R}$  follow the same trend as the direct components. Direct and cross components of damping coefficient increase with coupling number for any value of  $l_m$ , but at large  $l_m$  ( $l_m \rightarrow \infty$ ), they approach the corresponding values for Newtonian fluid.

#### **Effect of Steady State Eccentricity Ratio ( $\varepsilon_o$ )**

*Figs.4.2.9 to 4.2.16* show the variations of non-dimensional components of stiffness and damping coefficients for different values of  $\varepsilon_o$  and  $l_m$ , when other factors *viz.*,  $L/D$  and  $N$  are kept fixed. It can be observed from the referred figures that an increase in  $\varepsilon_o$  increases the magnitudes of the dynamic coefficients. It is further seen that all the curves in the micropolar fluid lubrication regime converge to those for Newtonian fluid lubrication regime at  $l_m \rightarrow \infty$ . At  $l_m \rightarrow 0$  the values of all the coefficients are more than those for Newtonian fluid because of the reason discussed in Chapter 4.1.

#### **4.2.6.2 Critical mass parameter ( $\bar{M}_c$ )**

##### **Effect of Coupling Number ( $N$ )**

*Fig.4.3.1* shows the variation of critical mass parameter representing the threshold of stability as function of  $l_m$ , when  $\varepsilon_o = 0.3$ ,  $\bar{K} = .001$ ,  $\bar{d} = .001$  and  $L/D = 1.0$  and  $N$  is considered as a parameter. It is found from the figure that the critical mass parameter increases as  $N$  is increased. Moreover, at any particular value of  $N$ , stability improves initially as  $l_m$  is increased, reaches a maximum to that for Newtonian fluid at large value of  $l_m$ .

The increase in the stability parameter in micropolar lubricant regime can be explained from the steady state analysis in which it has been shown in steady state analysis that

load parameter of a journal bearing increases in the micropolar fluid than in the Newtonian fluid. So, with the same load in a Newtonian fluid the journal will run at a higher eccentricity ratio than that in micropolar lubricant and consequently the stability parameter in micropolar lubricant regime will increase.

#### **Effect of Steady State Eccentricity Ratio ( $\varepsilon_o$ )**

The effect of variation of  $\varepsilon_o$  on  $\overline{M}_c$  for  $N^2 = 0.3$ ,  $\overline{K} = .001$ ,  $\overline{d} = .001$  and  $L/D = 1.0$  is shown in *Fig.4.3.2*. It is found from the figure that as  $\varepsilon_o$  increases and then increases irrespective of  $l_m$ . For  $\varepsilon_o \leq 0.9$ , the stability parameter is less in micropolar lubrication compared to that in Newtonian fluid. However, at higher  $\varepsilon_o$  ( $\varepsilon_o = 0.9$ ) it is found that at lower  $l_m < 60.0$ ,  $\overline{M}_c$  initially then increases with  $l_m$ . All the curves, however, show the tendency of converging to the value corresponding to the Newtonian fluid at large value of  $l_m$ . The effect of variation of  $\varepsilon_o$  on  $\overline{M}_c$  for  $N^2 = 0.1$ ,  $\overline{d} = .001$ ,  $\overline{Z} = .1$  and  $L/D = 1.0$  is shown in *Fig.4.3.3*. It is found from the figure that as  $\varepsilon_o$  decreases and then increases irrespective of  $\overline{K}$ . Threshold stability decreases with eccentricity ratio.

#### **Effect of External Damping Coefficients ( $\overline{d}$ )**

The effect of variation of  $\overline{d}$  on  $\overline{M}_c$  for  $N^2 = 0.3$ ,  $\varepsilon_o = 0.3$ ,  $\overline{Z} = .1$  and  $L/D = 1.0$  is shown in *Fig.4.3.4*. It is found from the figure that as  $\overline{d}$  increases and then increases irrespective of  $\overline{K}$ . Threshold stability increases with damping.

#### **4.2.6.3 Whirl ratio ( $\lambda_R$ )**

##### **Effect of Coupling Number ( $N$ )**

*Fig.4.3.5* shows the variation of whirl ratio with  $l_m$ , when  $N$  is taken as a parameter for  $\varepsilon_o = 0.3$  and  $L/D = 1.0$ . It can be seen from the figure that as coupling number increases, whirl ratio decreases. At a particular value of  $N$ , the whirl ratio initially decreases, reaches a minimum, then increases with further increase in  $l_m$  and ultimately converges to that for Newtonian fluid when  $l_m$  is indefinitely large. However, the variation of whirl ratio is very small.

### Effect of Steady State Eccentricity Ratio ( $\varepsilon_o$ )

The effect of  $\varepsilon_o$  on whirl ratio can be found from *Fig.4.3.6 and Fig.4.3.7* as a function of  $l_m$  for  $N^2 = 0.3$  and  $L/D = 1.0$ . It can be seen from the figure that the variation of whirl ratio is small at  $\varepsilon_o = 0.5$  i.e. within 0.3865 and 0.3903. But at higher value of  $\varepsilon_o$  ( $\varepsilon_o = 0.9$ ),  $\lambda_R$  decreases to about 0.655.

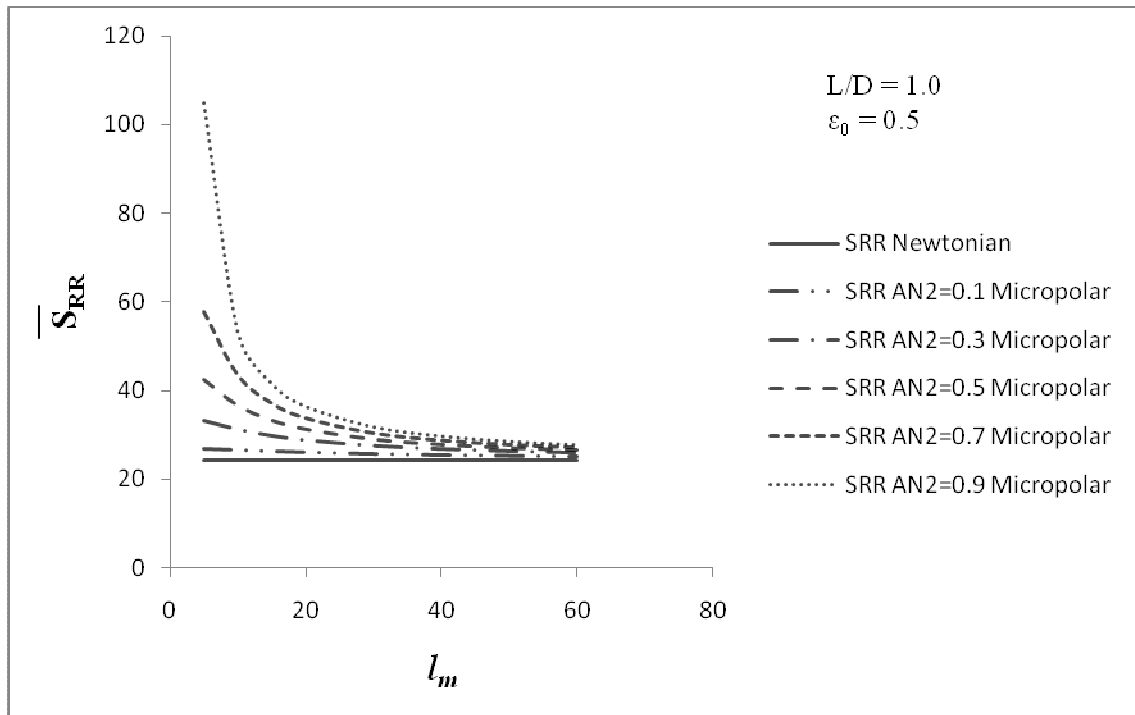


Fig.4.2.1: Variation of  $\bar{S}_{RR}$  with  $l_m$  for various values of  $N$  (AN).

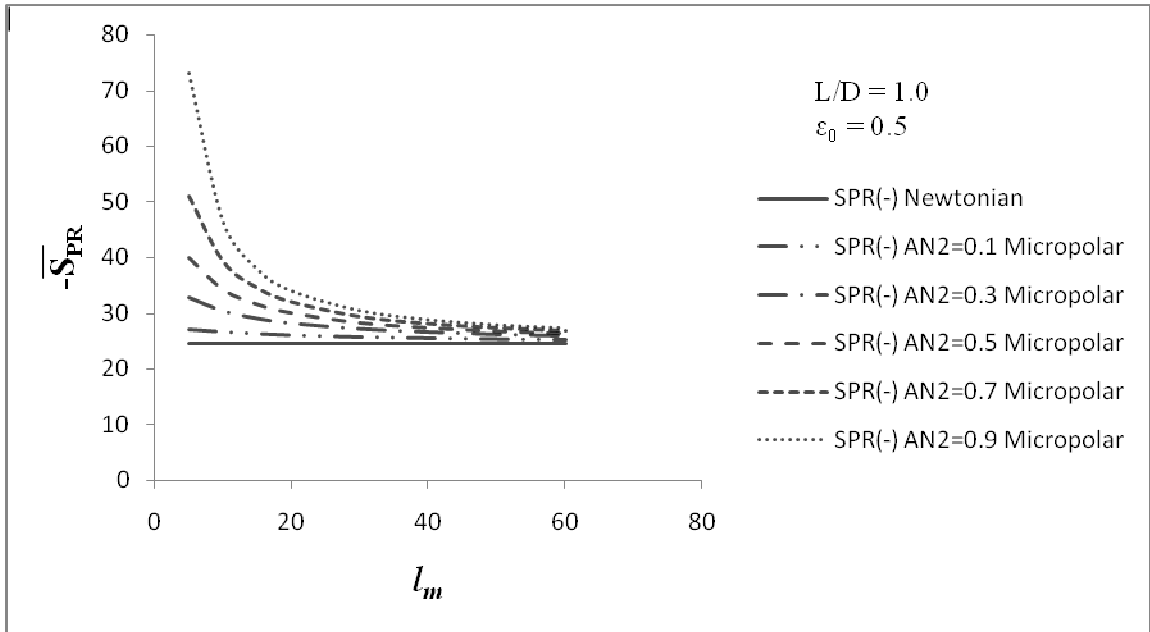


Fig.4.2.2: Variation of  $\overline{S}_{PR}$  with  $l_m$  for various values of  $N$  (AN).

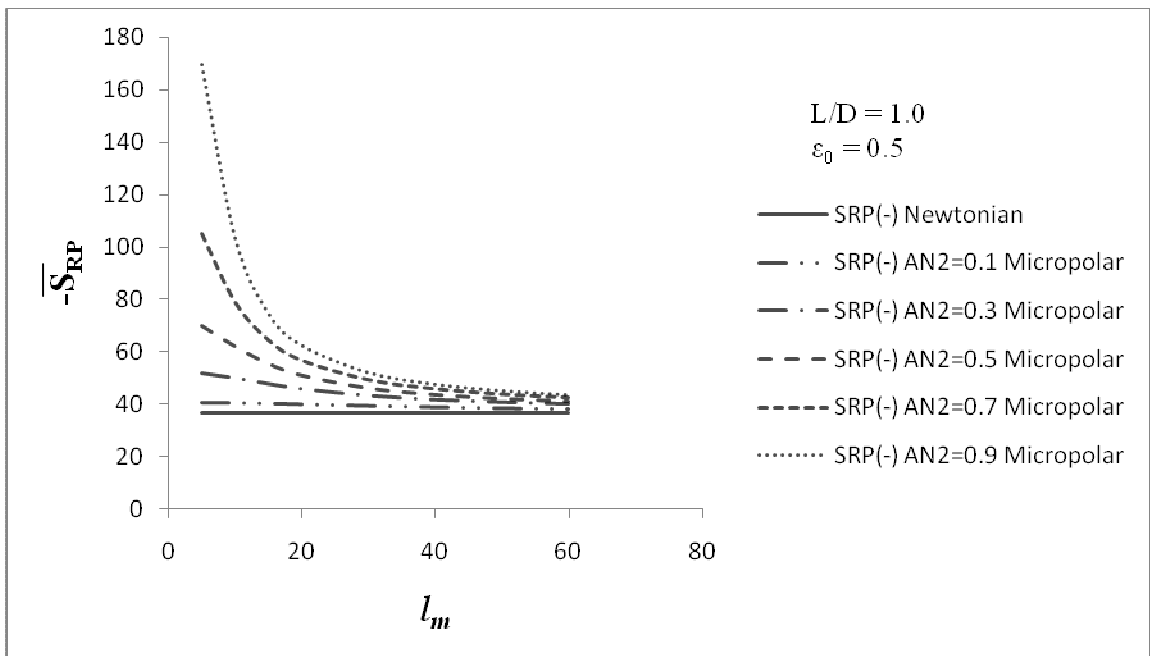


Fig.4.2.3: Variation of  $\overline{S}_{RP}$  with  $l_m$  for various values of  $N$  (AN).

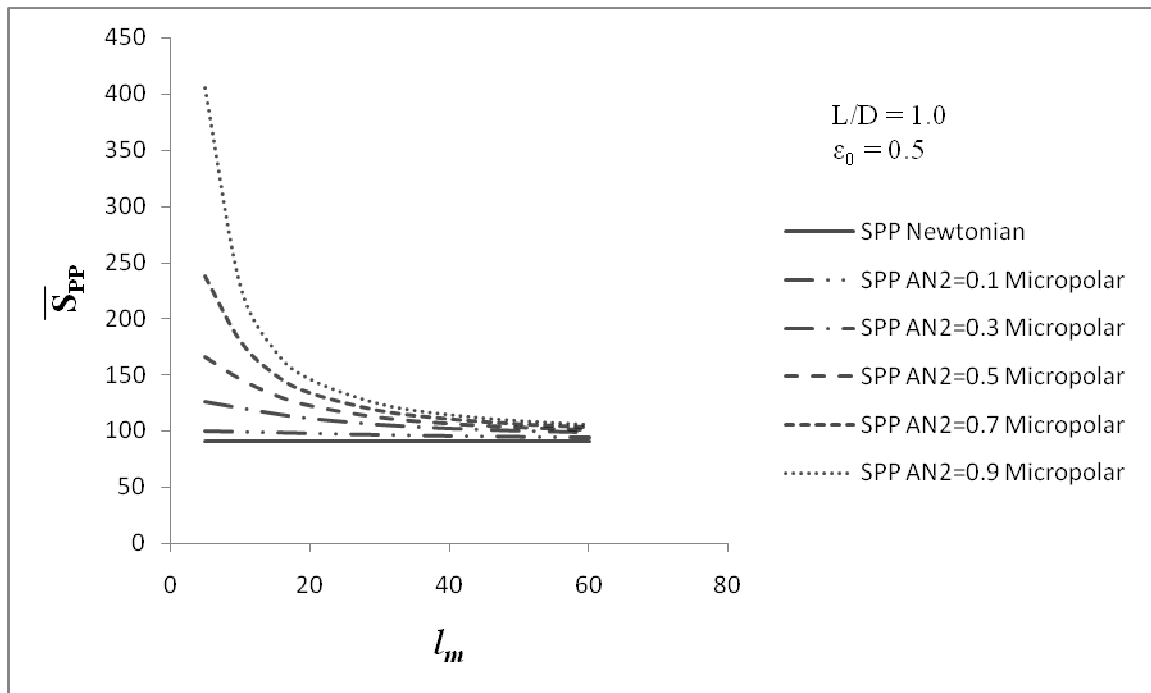


Fig.4.2.4: Variation of  $\overline{S}_{PP}$  with  $l_m$  for various values of N (AN).

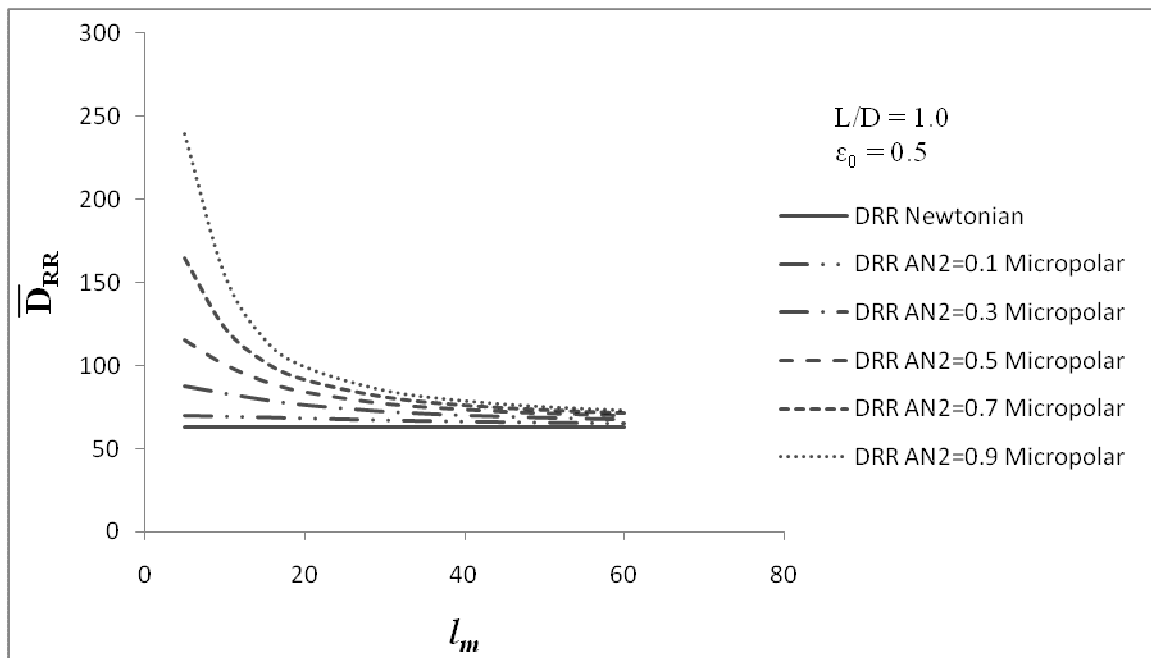


Fig.4.2.5: Variation of  $\overline{D}_{RR}$  with  $l_m$  for various values of N (AN).

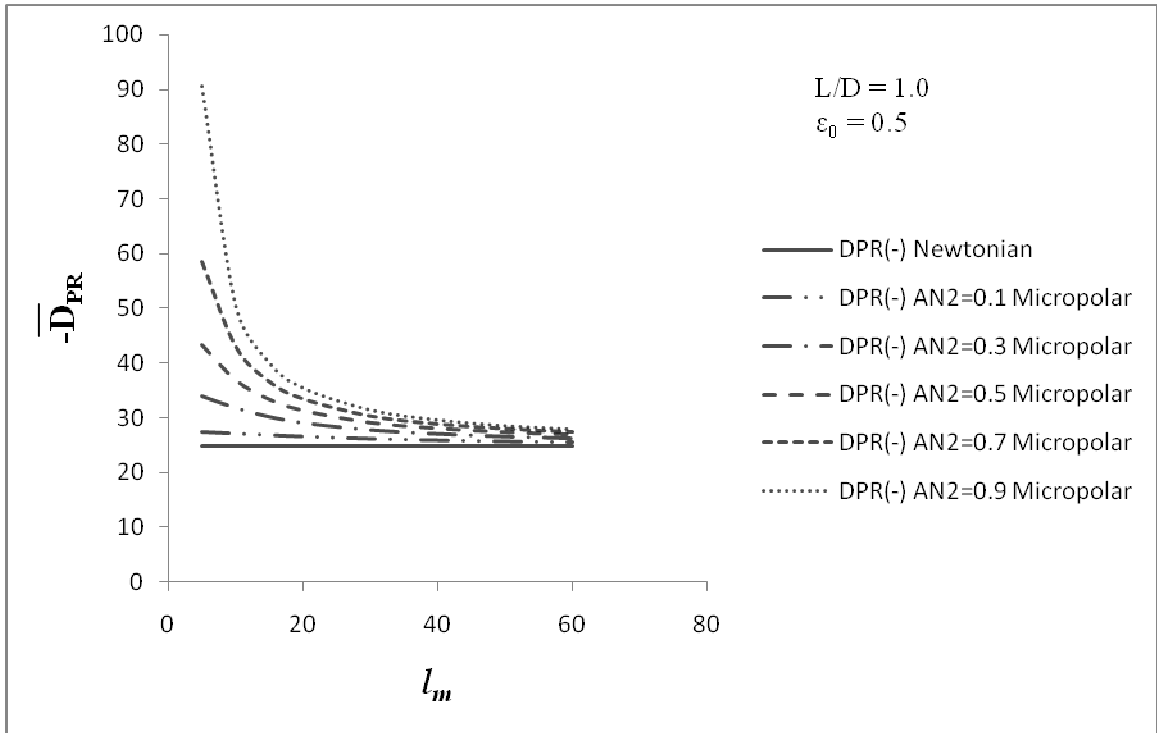


Fig.4.2.6: Variation of  $\bar{D}_{PR}$  with  $l_m$  for various values of  $N$  (AN).

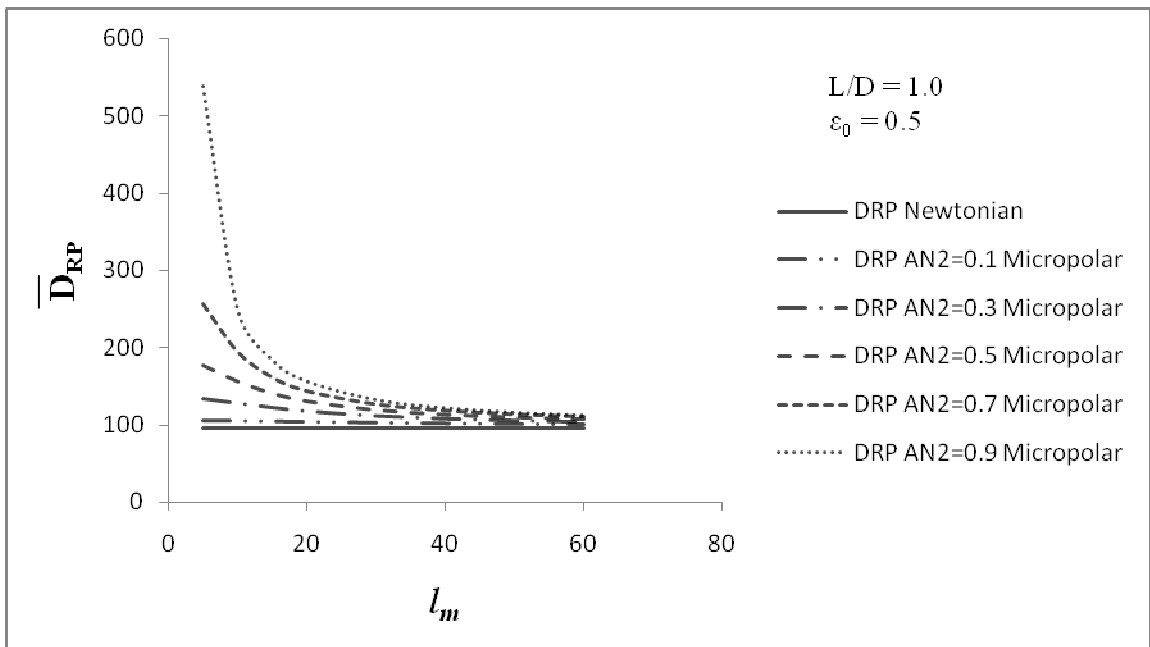


Fig.4.2.7: Variation of  $\bar{D}_{RP}$  with  $l_m$  for various values of  $N$  (AN).

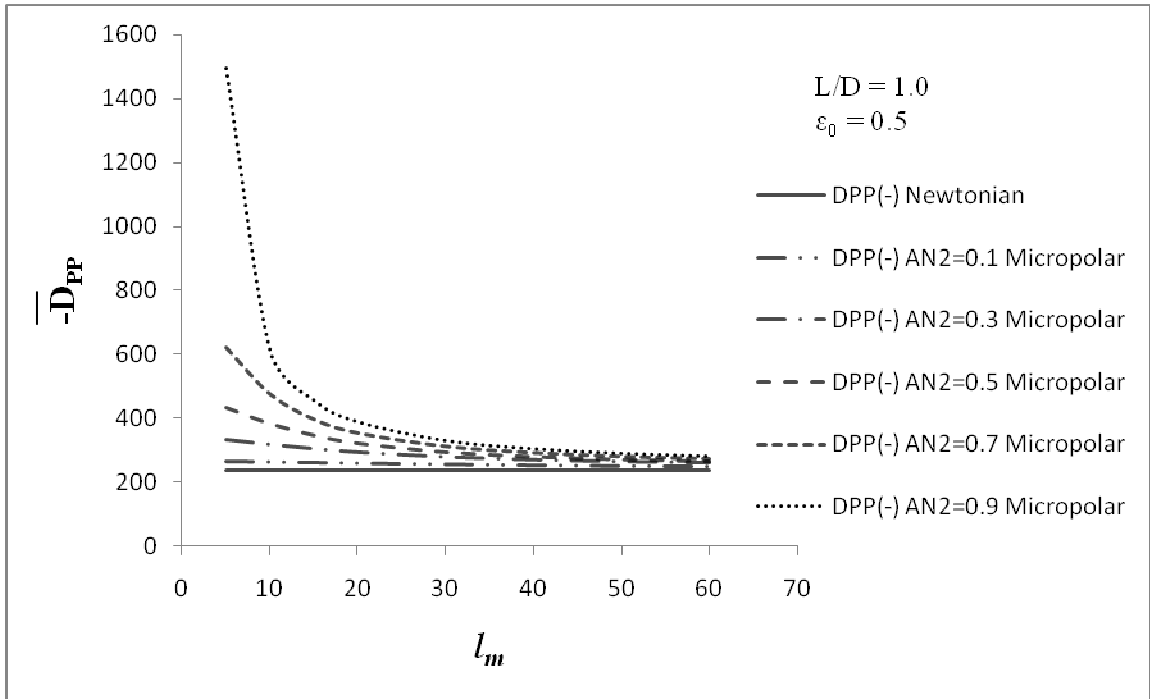


Fig.4.2.8: Variation of  $\overline{-D_{PP}}$  with  $l_m$  for various values of N (AN).

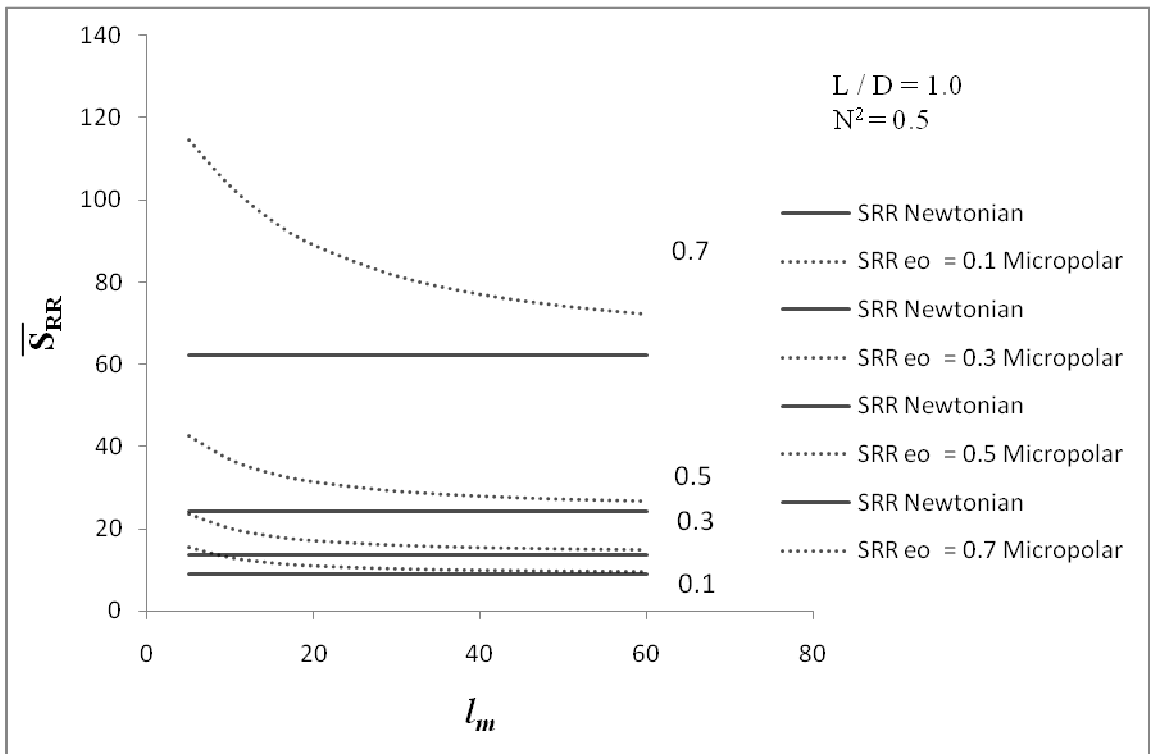


Fig.4.2.9: Variation of  $\overline{S_{RR}}$  with  $l_m$  for various values of  $\varepsilon_0$ .

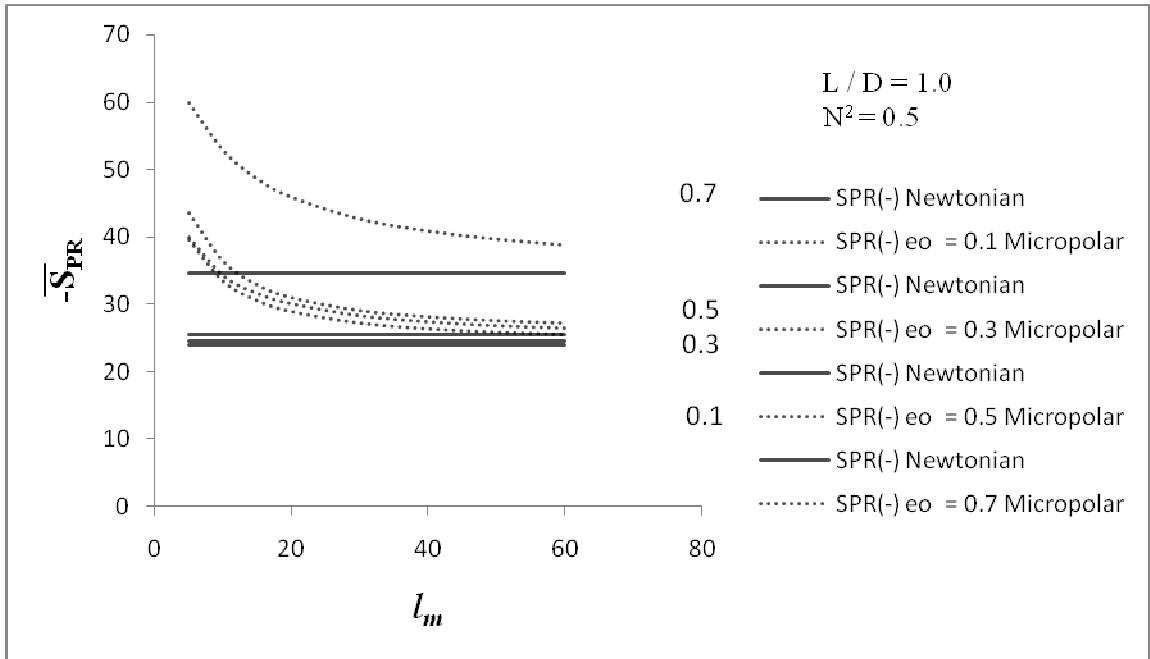


Fig.4.2.10: Variation of  $\overline{S}_{PR}$  with  $l_m$  for various values of  $\epsilon_0$ .

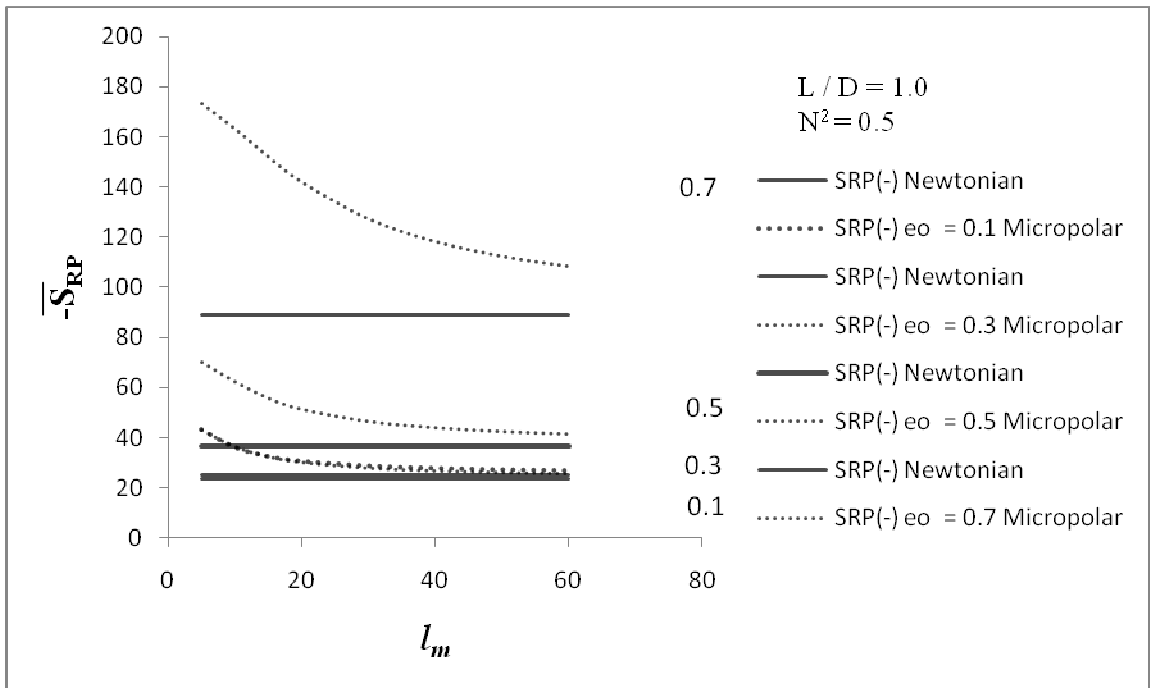


Fig.4.2.11: Variation of  $\overline{S}_{RP}$  with  $l_m$  for various values of  $\epsilon_0$ .

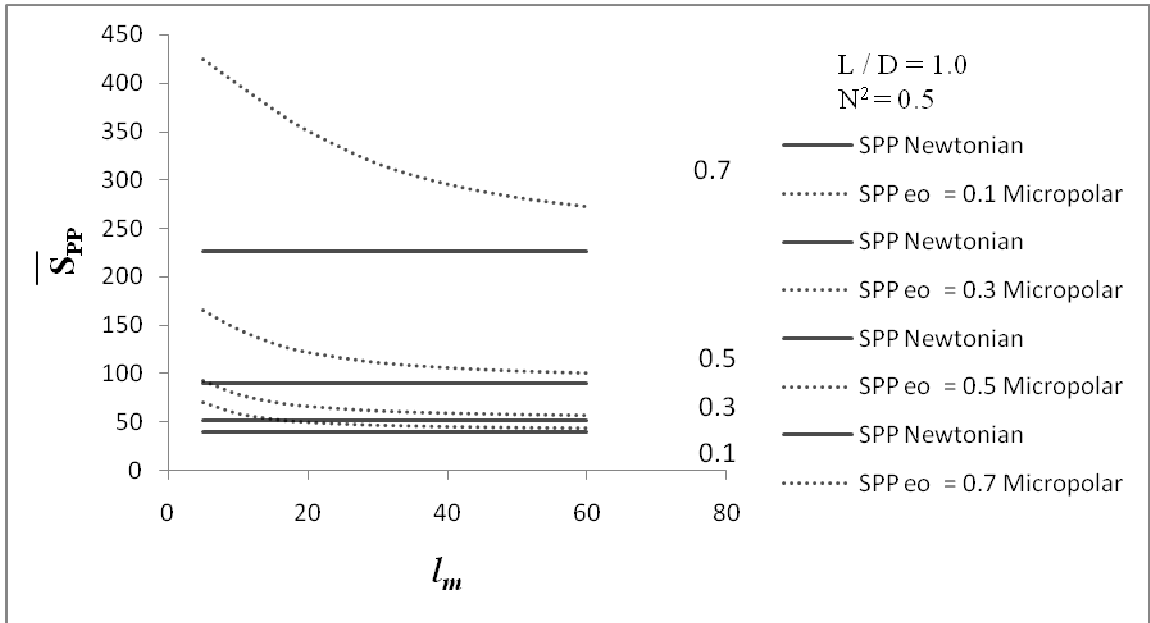


Fig.4.2.12: Variation of  $\bar{S}_{PP}$  with  $l_m$  for various values of  $\epsilon_0$ .

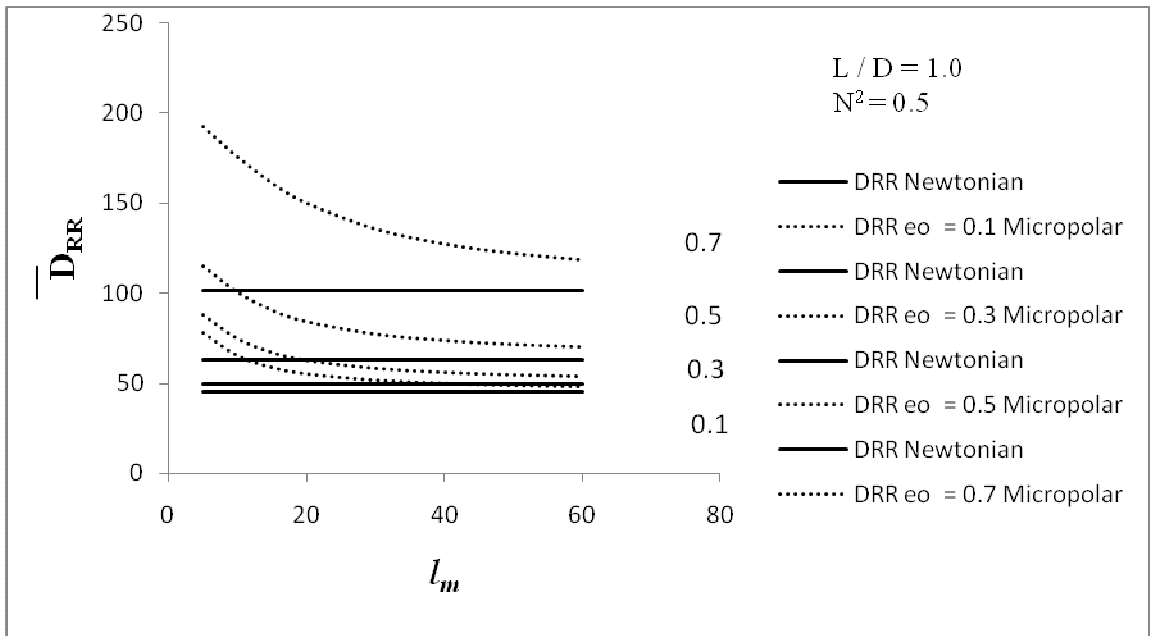


Fig.4.2.13: Variation of  $\bar{D}_{RR}$  with  $l_m$  for various values of  $\epsilon_0$ .

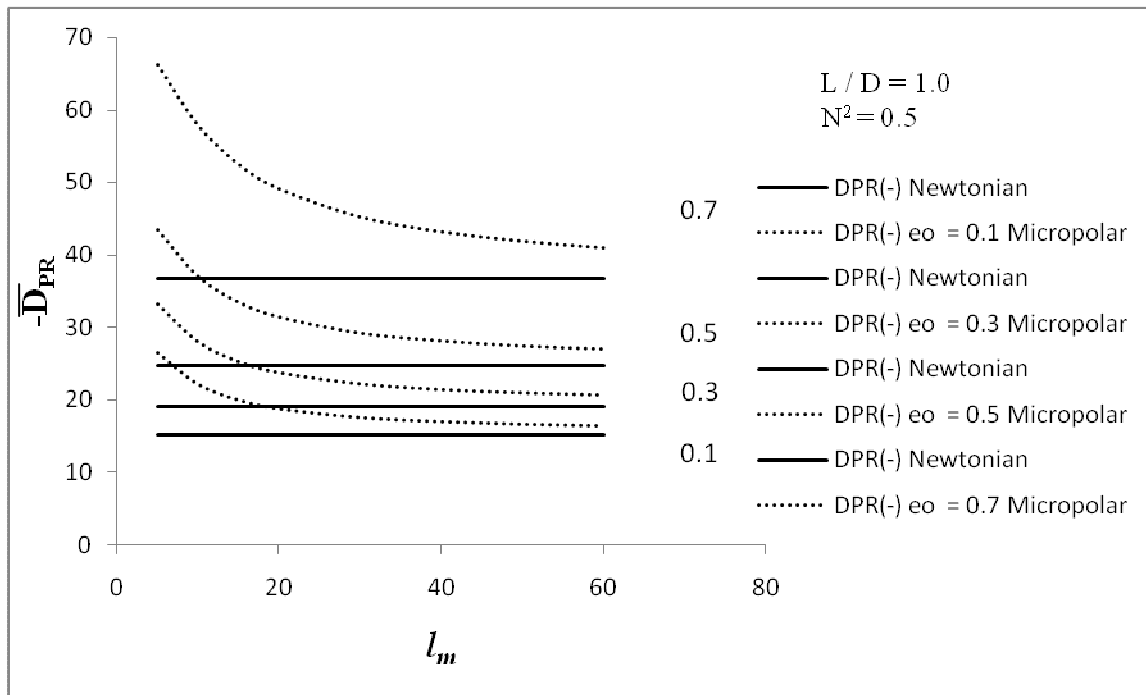


Fig.4.2.14: Variation of  $\bar{D}_{PR}$  with  $l_m$  for various values of  $\epsilon_0$ .

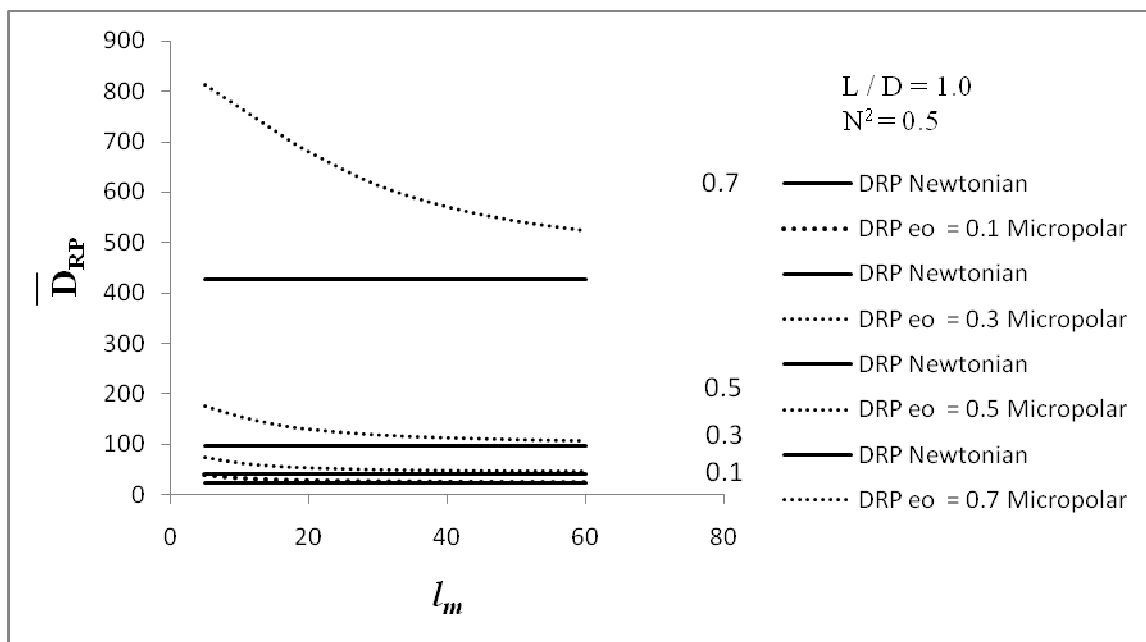


Fig.4.2.15: Variation of  $\bar{D}_{RP}$  with  $l_m$  for various values of  $\epsilon_0$ .

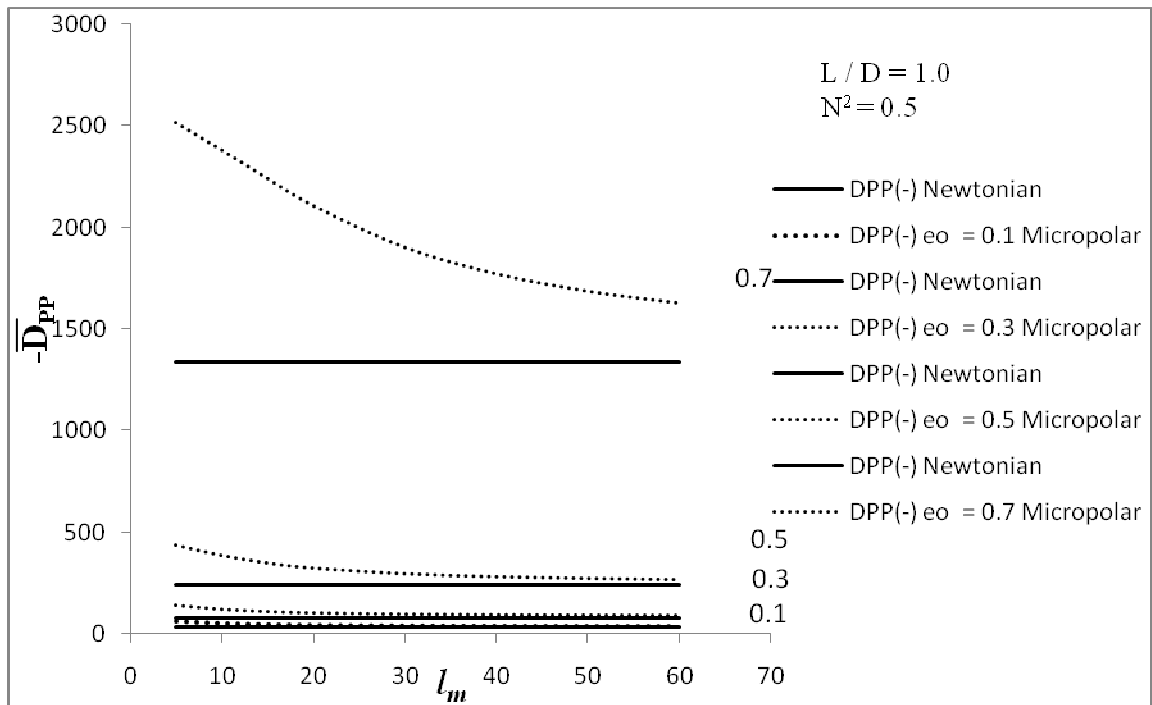


Fig.4.2.16: Variation of  $\bar{D}_{PP}$  with  $l_m$  for various values of  $\epsilon_0$ .

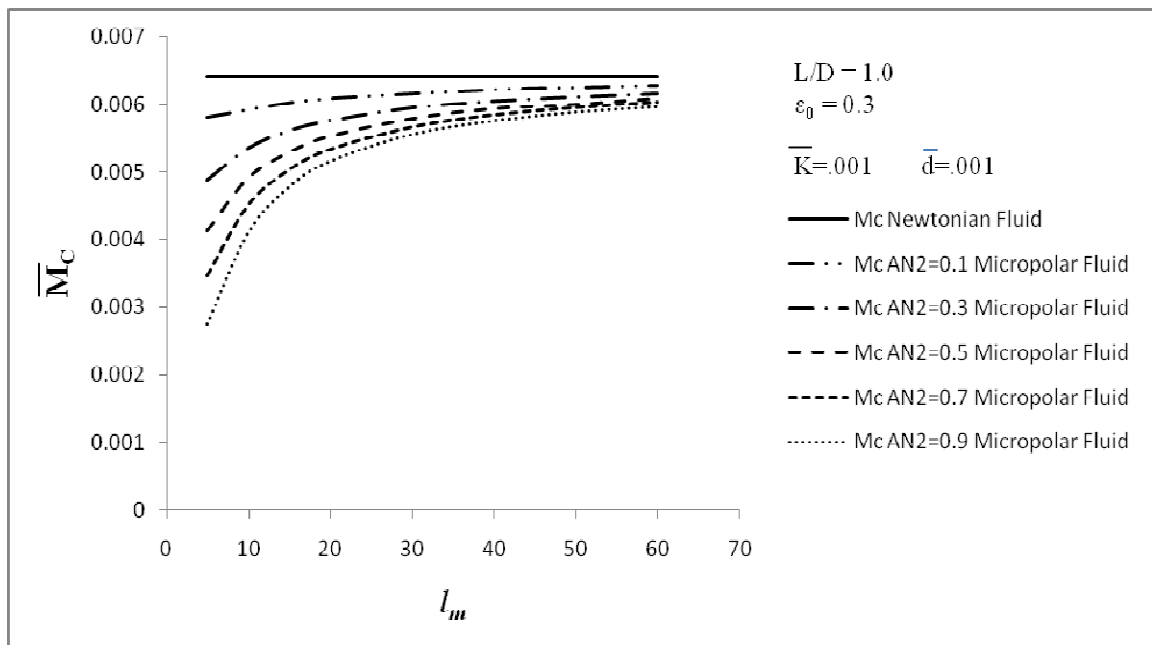


Fig.4.3.1: Variation of  $\bar{M}_C$  with  $l_m$  for various values of  $N$  (AN).

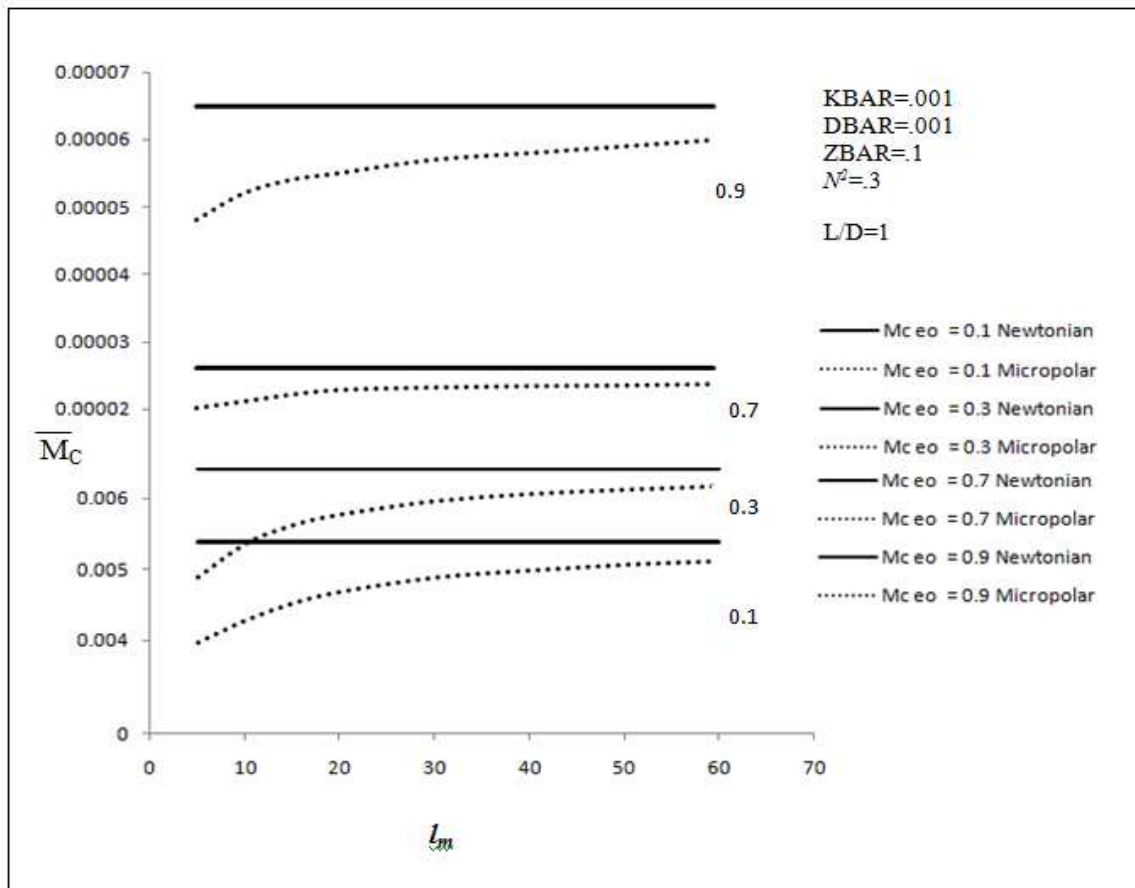


Fig.4.3.2: Variation of  $M_C$  with  $l_m$  for various values of  $\epsilon_0$ .

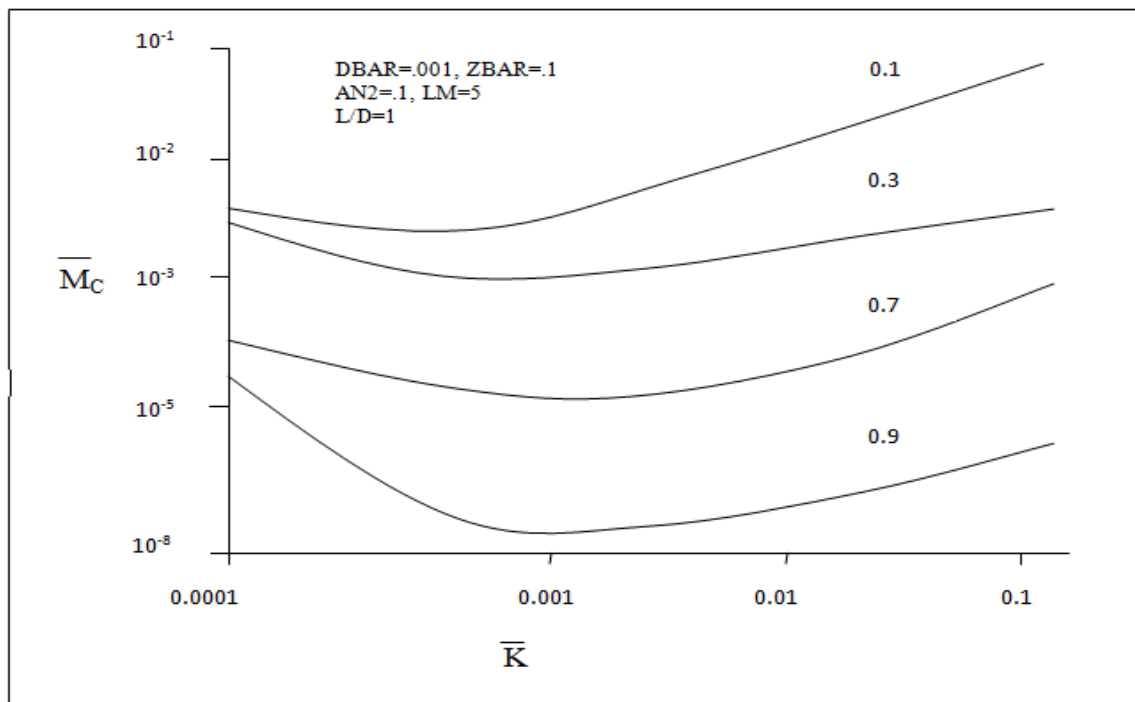


Fig.4.3.3: Variation of  $M_C$  with  $\bar{K}$  for various values of  $\epsilon_0$ .

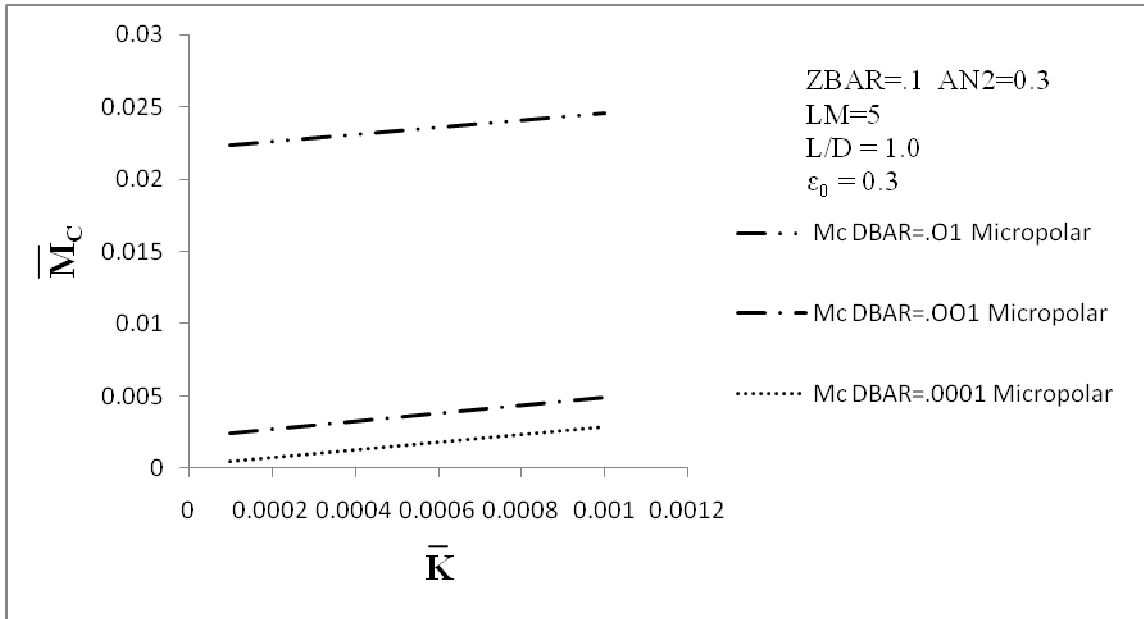


Fig.4.3.4: Variation of  $\bar{M}_C$  with  $\bar{K}$  for various values of  $\bar{d}$ .

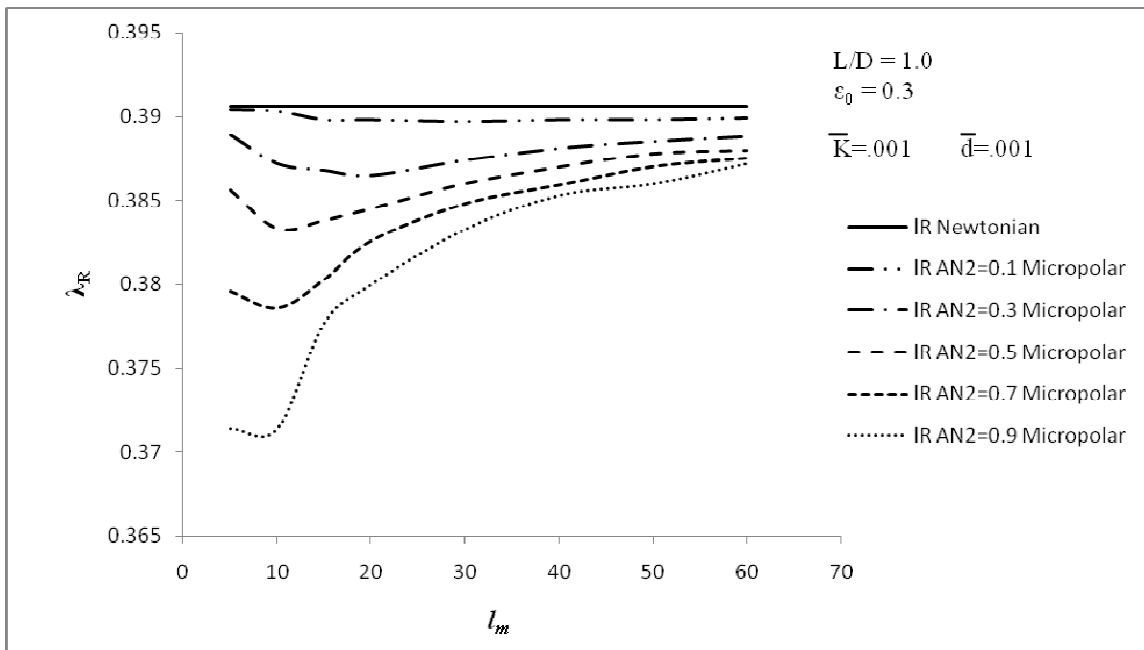


Fig.4.3.5: Variation of  $\lambda_R$  with  $l_m$  for various values of  $N$  (AN).

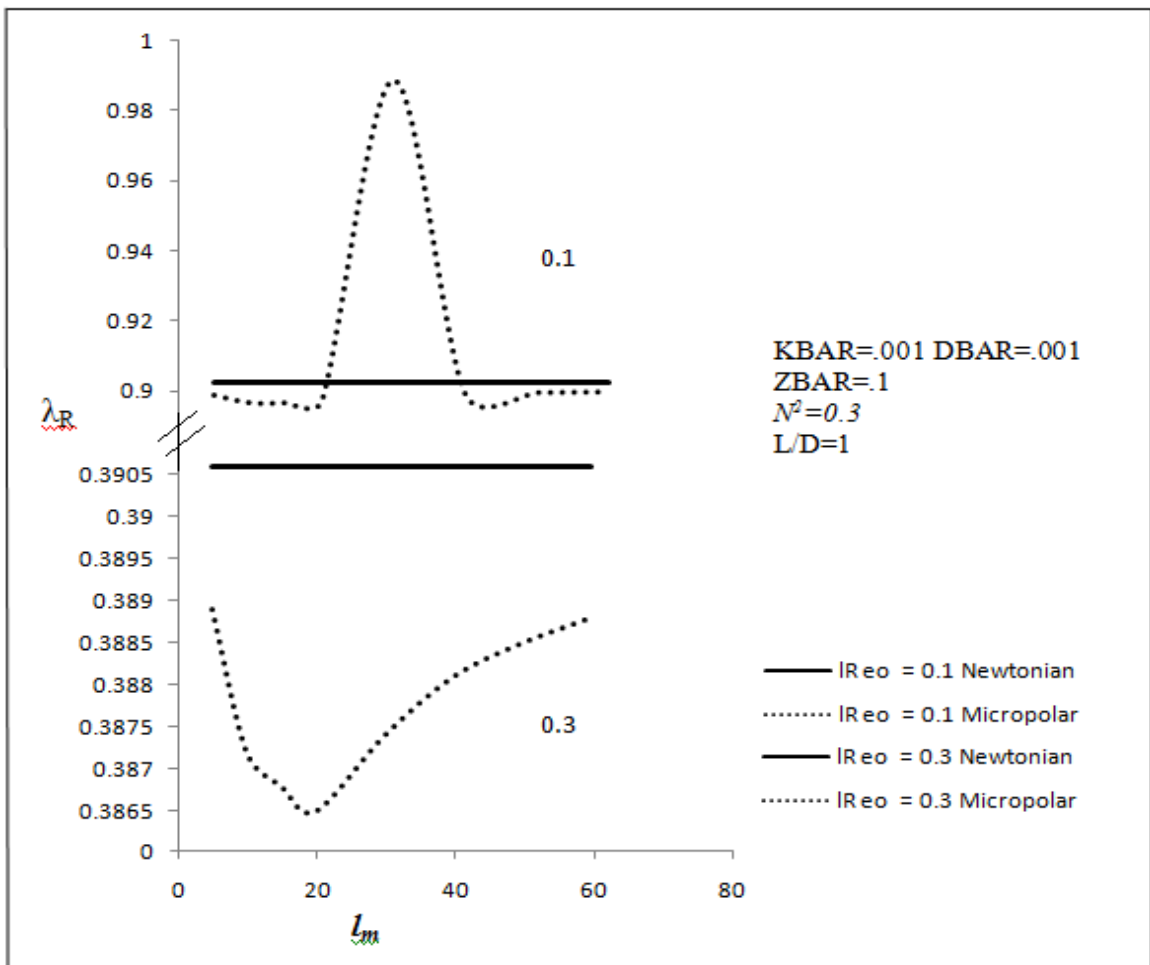


Fig.4.3.6: Variation of  $\lambda_R$  with  $l_m$  for various values of  $\epsilon_0$ .

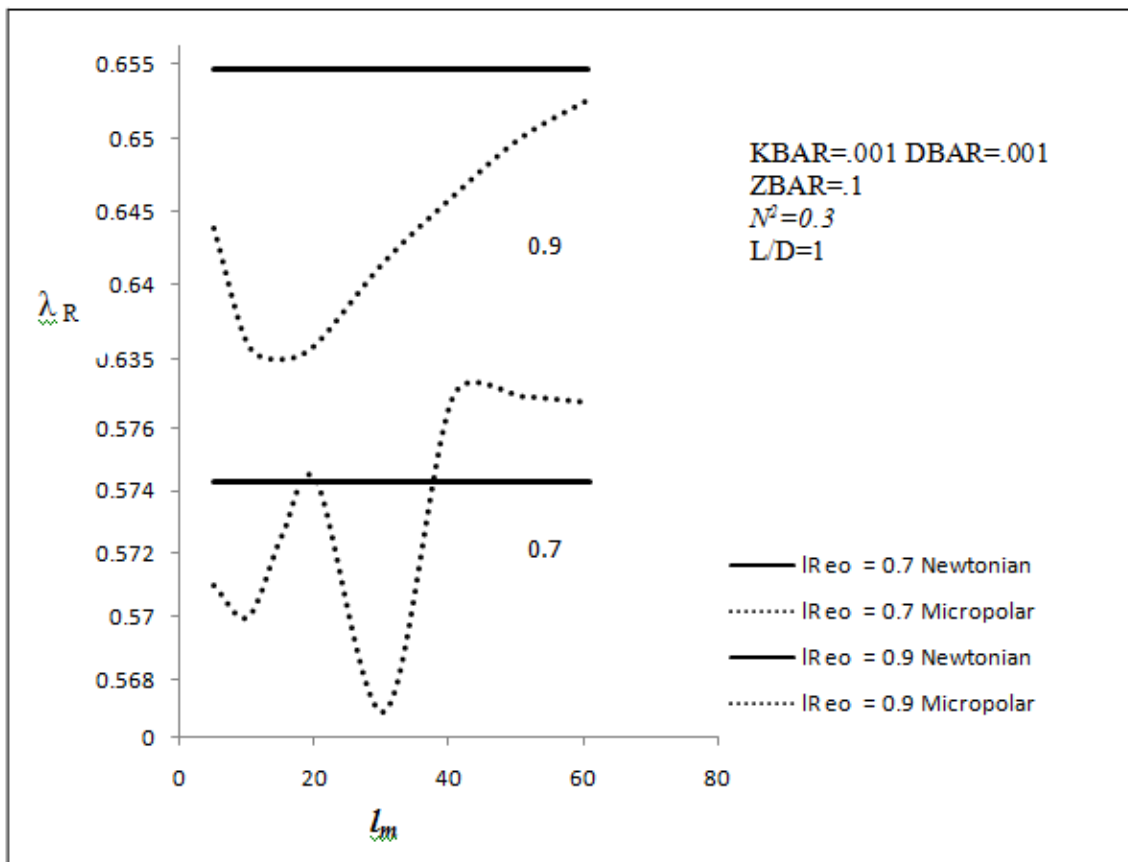


Fig.4.3.7: Variation of  $\lambda_R$  with  $l_m$  for various values of  $\epsilon_0$ .

## 5. CONCLUSION AND SCOPE FOR FUTURE WORK

### 5.1 Conclusion

In the present dissertation, the steady state and dynamic analysis of infinitely long flexibly supported hydrodynamic journal bearings under micropolar lubrication are studied theoretically. Bearing characteristics have been studied and presented for a wide range of micropolar lubrication parameters as well as bearing parameters, so as to provide a guideline for the design of such bearings. From the studies and the results reported in the previous chapters, the following conclusions may be drawn.

1. The non-dimensional load carrying capacity increases as the coupling number increases and non-dimensional characteristic length decreases. The load parameter converges to the Newtonian value as  $N \rightarrow 0$  and  $l_m \rightarrow \infty$ .
2. Other parameters remaining the same, the load parameter increases in both types of lubrication with the increase in eccentricity ratio. The load parameter remains always higher in the micropolar fluid than that in the Newtonian fluid.
3. The values of the attitude angle decrease as micropolar effect increases. The attitude angle also decreases as eccentricity ratio increases. The micropolar effect on  $\phi_0$  is also increased with the increase in  $\varepsilon_o$ .
4. All non-dimensional components of direct and cross stiffness and damping coefficients exhibit the similar relationship with the micropolar parameters as that of dimensionless steady state load.
5. At a certain value of  $l_m$ , all dimensionless response coefficients increase as the eccentricity ratio increases when other parameters remain the same.
6. The values of the whirl ratio always remain around 0.8.
7. Threshold stability increases with damping.
8. Threshold stability decreases with eccentricity ratio ( $\varepsilon_o$ ).

## **5.2 Scope for future work**

The present work is purely a theoretical work on the dynamic of flexibly supported infinitely long hydrodynamic journal bearings. The theoretical results could not be compared with the experimental data as there were no facilities of the kind required for conducting such an experimental to collect the data. So, there is a great scope for comparison of the present study of the bearings with the test results, if done carefully.

Furthermore, the present analysis is based on cylindrical journal bearings, although bearings of different geometries exist now-a-days. So, analysis of different shaped bearings on flexibly support could be done and compared with the present results.

Only a selected set of variables have considered in analyzing different parameters for time shortage. So, there is ample scope for similar analysis of the bearings considering wider range of variables.

A non linear analysis of this same problem could be of more use and this will indicate that the actual growth of orbit and also the limit cycles, if any.

## 6. REFERENCES

### 6.1 References

SL.N0.	JOURNALS
1.	<b>Newton, I.</b> “Mathematical Principles”, <i>London, 1668, Cajori’s revision of Motle’s translation, Univ. of California Press, 1946.</i>
2.	<b>Petroff, N.</b> “Friction in Machines and the Effect of Lubrication” ( <i>In Russian</i> ) <i>Engng. J. St.Petersburg, Nos. 1,2,3,4, 1883, pp.71,228,377,530.</i>
3.	<b>Tower, B.</b> “First Report on Friction Experiments”, <i>Proc. Inst. Mech. Engrs., London, Vol.34,Nov., 1883, pp.632-666</i> ; “Second Report on Friction Experiments”, <i>Proc. Inst. Mech. Engrs. London, Vol.36, 1885, pp.58-70</i> ; “Third Report on Friction Experiments”, <i>Proc. Inst. Mech. Engrs., London, 1888, pp.173-205</i> ; “Fourth Report on Friction Experiments”, <i>Proc. Inst. Mech. Engrs., London, 1891, pp.111-140.</i>
4.	<b>Reynolds, O.</b> “On the Theory of Lubrication and Its Application to Mr. Beuchamp Tower’s Experiments, including An Experimental Determination of the Viscosity of Olive Oil”, <i>Phil.Trans. Roy. Soc., London, Vol.177, Pt.1, 1886, pp. 157-234.</i>
5.	<b>Kingsbury, A.</b> “Experiments with an Air Lubricated Journal”, <i>J. American Soc. Naval Engrs., Vol.9, 1897, pp.267-292</i>
6.	<b>Sommerfeld, A.</b> “Zur Hydrodynamischen Theorie der Schmiermittelneibung” <i>Z. Maths. u.Physik, Vol.50, 1904, pp.97-155</i>
7.	<b>Harrison, W. J.</b> “The Hydrodynamical Theory of Lubrication with Special Reference to Air as a Lubricant”, <i>Trans. Cambridge. Phil. Soc., Vol.22, No.III, 1913, pp.39-54.</i>
8.	<b>Rayleigh, L.</b> “Notes on the Theory of Lubrication”, <i>Phil. Mag., Vol.35, No.1, 1918, pp.1-12.</i>
9.	<b>Christopherson, D. G.</b> “A New Mathematical Method for the Solution of Film Lubrication Problems”, <i>Proc. Inst. Mech. Engrs., London, Vol.146, 1941, pp.126-135.</i>
10.	<b>Cameron, A. and Wood, L. (Mrs.)</b> “The Full Journal Bearing”, <i>Proc. Inst. Mech. Engrs., London, Vol.161, 1949, pp.59-64.</i>

11.	<b>Vogelpohl, G.</b> “Zur Integration der Reynoldschen Gleichung für des Zapfenlager Endlicher Breite”, <i>Ingenieur Archiv., Band.XIV, 1943, pp.192-212.</i>
12.	<b>Ocvirk, F. W.</b> “Short Bearing Approximation for Full Journal Bearings”, <i>NACA TN 2808.</i>
13.	<b>Harrison, W.J.</b> “The Hydrodynamic Theory of Lubrication of Cylindrical Bearings under variable Load”, <i>Trans. Cambridge. Phil.Soc., Vol.22, 1913, p.373.</i>
14.	<b>Kahlert, W.</b> “Der Einfluss der Tragheitskräfte bei der Hydrodynamischen Schmiermitteltheorie”, <i>Ingenieur Archiv., Band XVI, 1948, pp.321-342.</i>
15.	<b>Osterle, F. and Saibel, E.</b> “On the Effect of Lubricant Inertia in Hydrodynamic Lubrication”, <i>Z. Maths. u. Physik, Vol.6, 1955, pp.334-339.</i>
16.	<b>Coles, J. A. and Hughes, C. J.</b> “Oil Flow and Film extend in Complete Journal Bearings”, <i>Proc. Inst. Mech. Engrs., Vol.170, 1956, pp.499-510.</i>
17.	<b>Jacobson, B. and Floberg, L.</b> “The Finite Journal Bearing considering Vaporization”, <i>Trans.Chalmers Univ., Tech. Gothenburg. 189 &amp; 190.</i>
18.	<b>Kingsbury, A.</b> “A New Oil Testing Machine and Some of Its Results”, <i>Trans. ASME, Vol.24, 1903, p.144.</i>
19.	<b>Cosserat, E. and Cosserat, F.</b> “Théorie des Corps Deformables”, <i>Hermann et Fils, Paris, 1909.</i>
20.	<b>Jeffery, G. B.</b> “The Motion of Ellipsoidal Particles Immersed in A Viscous Fluid”, <i>Proc. Roy. Soc., London, Ser. A., Vol.102, 1922, pp.171-179.</i>
21.	<b>Hardy, W. and Nottage, M.</b> “Studies in Adhesion – I”, <i>Proc. Roy. Soc., London, Ser. A., Vol.112, 1926, p.64.</i>
22.	<b>Needs, S. J.</b> “Boundary Film Investigations”, <i>Trans. ASME, Vol.62, 1940, pp.331-345.</i>
23.	<b>Buckley, R.</b> “Viscous Flow and Surface Films” <i>U.S. Bureau of Standards Journal of Research, Research Paper No. 264, Vol.6, 1931, p.89.</i>
24.	<b>Anzelius, A.</b> <i>The Annual of the Univ. of Uppsala, 1931.</i>
25.	<b>Henniker, J. C.</b> “The depth of the Surface Zone of a Liquid”, <i>Revs. Modern Physics, Vol.21, 1949, pp.322-341</i>

26.	<b>Fuks, G. I.</b> “The Properties of Solutions of Organic Acids in Liquid Hydrocarbons at Solid Surfaces”, <i>Research in Surface Forces, ed. B. V. Deryagin, Vol.1, 1960, p.79.</i>
27.	<b>Fuks, G. I.</b> “The Polymolecular Component of the Lubricating Boundary Layer”, <i>ibid, Vol.2, 1964, p.159.</i>
28.	<b>Needs, S. J.</b> “Boundary Film Investigations”, <i>Trans. ASME, Vol.62, 1940, pp.331-345.</i>
29.	<b>Hoyt, J. W. and Fabula, A. G.</b> “The Effect of Additives on Fluid Friction”, <i>U.S. Naval Ordnance Test Station Report, 1964</i>
30.	<b>Vogel, W. M. and Patterson, A. M.</b> “An Experimental Investigation of the Effect of Additives Injected into the Boundary Layer of A Underwater Body”, <i>Pacific Naval Lab., Defence Research Board of Canada, Report 64-2.</i>
31.	<b>Eringen, A. C.</b> “Simple Microfluids”, <i>Int. J. Engng. Sci., Vol. 2, 1964, pp.205-217.</i>
32.	<b>Eringen, A. C.</b> “Mechanics of Micromorphic Materials”, <i>Proc. XI, Int. Cong. of Appl. Mech., Springer-Verlag, 1965.</i>
33.	<b>Eringen, A. C.</b> “Theory of Micropolar Continua”, <i>Dev. in Mech., Vol. 3, Pt.1, 1965, pp.23-40.</i>
34.	<b>Eringen, A. C.</b> “Theory of Micropolar Continua”, <i>Dev. in Mech., Vol. 3, Pt.1, 1965, pp.23-40.</i>
35.	<b>Eringen, A. C.</b> “Linear Theory of Micropolar Elasticity”, <i>J. Math. Mech., Vol.15, No.1, 1965, pp.909-923.</i>
36.	<b>Eringen, A. C.</b> “Theory of Micropolar Fluids”, <i>J. Math. Mech., Vol.16, No.1, 1966, pp.1-18.</i>
37.	<b>Eringen, A. C.</b> “Theory of Micropolar Fluids”, <i>J. Math. Mech., Vol.16, No.1, 1966, pp.1-18.</i>
38.	<b>Balaram, M.</b> “Micropolar Squeeze Films”, <i>J. Lub. Technol., Trans. ASME, Oct., 1975, pp.635-637.</i>
39.	<b>Prakash, J. and Christensen, H.</b> “Rheological Anomalies in Thin Hydrodynamic Films — A Microcontinuum View”, <i>Symposium on Lubricant Properties in Thin Lubricating Films, American Chem. Soc., NY Meet., Apr. 4-9, 1976, pp.79-90.</i>

40.	<b>Prakash, J. and Sinha, P.</b> “A Study of Squeezing Flow in Micropolar Fluid Lubricated Journal Bearings”, <i>Wear</i> , Vol.38, 1976, pp.17-28.
41.	<b>Prakash, J. and Sinha, P.</b> “Cyclic Squeeze Films in Micropolar Fluid Lubricated Journal Bearings”, <i>J. Lub. Technol., Trans. ASME</i> , 1975, 76-Lub-E.
42.	<b>Zaheeruddin, Kh. and Isa, Md.</b> “Micropolar Fluid Lubrication of One-Dimensional Journal Bearings”, <i>Wear</i> , Vol.50, 1978, pp.211-220.
43.	<b>Zaheeruddin, Kh.</b> “The Dynamic Behavior of Squeeze Films in One-Dimensional Porous Journal Bearings Lubricated by a Micropolar Fluid”, <i>Wear</i> , Vol.71, 1981, pp.139-152.
44.	<b>Singh, C. and Sinha, P.</b> “The Three-Dimensional Reynolds Equation for Micropolar Fluid Lubricated Bearings”, <i>Wear</i> , Vol.76, No.2, 1982, pp.199-209.
45.	<b>Huang, T-W. and Weng, C-I.</b> “Dynamic Characteristics of Finite-Width Journal Bearings with Micropolar Fluids”, <i>Wear</i> , Vol.141, No.1, 1990, pp.23-33.
46.	<b>Chaturani, P. and Narasimman, S.</b> “Numerical Solution of a Micropolar Fluid Flow between Two Rotating Coaxial Disks”, <i>Acta Mech.</i> , Vol.89, No.1-4, 1991, pp.133-145.
47.	<b>Chattopadhyay. A.K., Karmakar, S., in 1997</b> Non linear analysis of flexibly supported finite turbulent flow oil journal bearings, <i>Applied mechanics and engineering</i> , vol.2,No.4, 557-568.
48.	<b>Das, s., Guha, S.K., and Chattopadhyay,A.K.</b> Theoretical analysis of stability characteristic of hydrodynamic journal bearings lubricated with micropolar fluid.Proc. Instn Mech. Engrs., Part J:J.Engineering Tribology, 2004,218,45-56.
49.	<b>Tipei, N.</b> “Lubrication with Micropolar Liquids and Its Application to Short Bearings”, <i>J. Lub.Technol., Trans. ASME</i> , Vol.101, Jul., 1979, pp.356-363.
50.	<b>Tipei, N.</b> “Theory of Lubrication”, <i>Stanford Univ. Press, Stanford</i> , 1962.
51.	<b>Huang, T-W.; Weng, C-I and Chen, C-K.</b> “Analysis of Finite Width Journal Bearings with Micropolar Fluids”, <i>Wear</i> , Vol.123, 1988, pp.1-12.
52.	<b>Khonsari, M. M. and Brewe, D. E.</b> “On the Performance of Finite Journal Bearings Lubricated with Micropolar Fluids”, <i>STLE, Tribology Trans.</i> , Vol.32, No.2, 1989, pp.155-160.

53.	<b>Marsh,H.</b> , The Stability of Aerodynamics Gas Bearings. <i>Part 2: Non-circular Bearings. Report for Ministry of Aviation , 1964.</i>
54.	<b>Kerr, J.</b> “The onset and cessation of Half-speed whirl in Air-lubricated Self Pressurized Journal Bearings”. <i>Proc. Inst, Mech. Engrs. Vol.180, 1966 (4<sup>th</sup> Convention of Lubrication and Wear Group, Paper Number.221.</i>
55.	<b>D.A.Boffey</b> , The stability of a rigid rotor in a flexibility supported Self-acting Gas Journal Bearings. <i>Univ. Southampton , Gas Bearing Symposium, April1969, Paper No.12, 1-15.</i>

## 7. APPENDICES

### 7.1 APPENDIX-I:

***Programme For Calculating Load Carrying Capacity, Attitude Angle, Stiffness & Damping Of Infinitely Long Hydrodynamic Journal Bearings With Micropolar Lubricants.***

```
=====
COMPLEX P1(55),P2(55),TERM11,TERM21,SPO1,SPO2,SPN1,SPN2
COMPLEX AM11,AM12,AM21,AM22,F11(55),F12(55),F21(55),F22(55)
COMPLEX CA9,CA15,WDX1,WDY1,WDX2,WDY2,DEV1,DEV2
INTEGER PRECAV
REAL LM, LM2
DIMENSION P(55),THETA(55),HH0(55)
DIMENSION RLM(10),CC1(55),CC2(55),CC3(55)
OPEN(3,FILE='RESULT.DAT')
OPEN(2,FILE='VALR.DAT')
OPEN(1,FILE='VALLM.DAT')
C
PI=4.0*ATAN(1.0)
WRITE(*,*)'IPT = ? (=44), JPT = ? (=12) '
READ(*,*)IPT,JPT
C WRITE(*,*)'GIVE VALUES FOR: RLAMDA (=WHIRL RATIO) (Given as 1.0) '
C READ(*,*)RLAMDA
C WRITE(*,*)'MICROPOLAR CHARACTERISITCS LM, AN2 (=N2) '
C READ(*,*)LM,AN2
C WRITE(*,*)'GIVE VALUES FOR: EPH0 '
C READ(*,*)EPH0
WRITE(*,*)'GIVE VALUE FOR: ORF (1.05) '
READ(*,*)ORF
C
KNT=1
AN2=0.1
READ(1,*)(RLM(ILM),ILM=1,8)
450 IF(AN2.GT.0.9) GOTO 460
ILM=1
430 IF(ILM.GT.8) GOTO 440
LM=RLM(ILM)
WRITE(3,1510)LM,AN2
1510 FORMAT(/32X,'MICROPOLAR FLUID CHARACTERISTICS:',3X,'LM =',F10.3,
#3X,'N^2 =',F7.4/)
C
RLAMDA=1.0
EPH0=0.1
WRITE(3,1520)RLAMDA
1520 FORMAT(5X,'RLAMDA =',F4.1/)
WRITE(3,1010)
1010 FORMAT('EPH0',1X,'ITER',2X,'SS LOAD',2X,'ATT ANGLE',5X,'SN',
#3X,'IP1',1X,'IP2',8X,'WDX1(Cos:P1)',15X,'WDY1(Sin:P1)',15X,
#'WDX2(Cos:P2)',15X,'WDY2(Sin:P2)',12X,'SRR',10X,'SPR',10X,'DRR',
#10X,'DPR',10X,'SRP',10X,'SPP',10X,'DRP',10X,'DPP',4X,'STABILITY',
#2X,'WH RATIO',2X,'MASS PARA'/)
410 IF(EPH0.GE.1.0) GOTO 420
```

```

C
WRITE(*,1220)KNT,RLAMDA,LM,AN2,R,EPH0
1220 FORMAT(/4X,'KNT=',I8,4X,'RLAMDA=',F4.2,3X,'LM=',F7.2,3X,
#'AN2=',F6.3,3X,'R=',F3.1,3X,'EPH0=',F5.2)
C
I5=IPT+2
I6=I5+1
I4=I5-1
I3=I4-1
I2=I3-1
AI3=I3
DELTH=2.0*PI/AI3
DELTH2=DELTH*DELTH
LM2=LM*LM
AN=SQRT(AN2)
AN3=AN2*AN
C
ITER=1
SPO=0.
C
C
CALCULATION OF FILM THICKNESS AND THE FUNTIONS F1=COTH(N*LM*H0/2)
C
AND F2={COSECH(N*LM*H0/2)}^2
C
DO 10 I=2,I5
AI=I-2
THETA=AI*DELTH
THETA(I)=THETA
H0=1.0+EPH0*COS(THETA)
HH0(I)=H0
A=0.5*AN*LM*H0
TANHA=TANH(A)
COTHA=1.0/TANHA
SINHA=SINH(A)
CSCHA=1.0/SINHA
CSCHA2=CSCHA*CSCHA
H02=H0*H0
H03=H02*H0
CC1(I)=H02/4.+1./LM2-AN*H0*COTHA/LM+AN2*H02*CSCHA2/4.
CC2(I)=H03/12.+H0/LM2-0.5*AN*H02*COTHA/LM
CC3(I)=H0/2.+AN2*H0*CSCHA2-AN*COTHA/LM-AN3*LM*H02*CSCHA2*COTHA/4.
10 CONTINUE
C
INITIALISATION OF PRESSURE
C
DO 20 I=1,I6
P(I)=0.0
P1(I)=CMPLX(0.,0.)
P2(I)=CMPLX(0.,0.)
20 CONTINUE
C
SETTING OF BOUNDARY CONDITIONS
C
60 IF(I.EQ.2) THEN
P(I)=0.0
ENDIF
C
SOLUTION OF REYNOLDS' EQUATION
C
DO 30 I=2,I5
THETA=THETA(I)

```

```

C
  CC1I=CC1(I)
  CC2I=CC2(I)
  CC3I=CC3(I)
  CA=0.25*CC1I*EPH0*DELTH*SIN(THETAI)/CC2I
  CA1=(0.5-CA)
  CA2=(0.5+CA)
  CA3=0.25*EPH0*DELTH2*SIN(THETAI)/CC2I
  TERM=CA1*P(I+1)+CA2*P(I-1)+CA3
  ERR=TERM-P(I)
C
  P(I)=P(I)+ORF*ERR
  IF(P(I).LT.0.0) P(I)=0.0
  IF(I.EQ.2) THEN
    P(I5)=P(2)
      ELSEIF(I.EQ.I4) THEN
        P(1)=P(I4)
          ELSE
            GOTO 30
      ENDIF
30  CONTINUE
C
C  TEST FOR CONVERGENCE
C
  SPN=0.0
  DO 40 I=2,I5
    SPN=SPN+P(I)
40  CONTINUE
  ERR=1.0-SPO/SPN
  IF(ABS(ERR).LE.0.001.OR.ITER.GE.500) GOTO 50
  ITER=ITER+1
  SPO=SPN
  GOTO 60
50  IF(ITER.GE.500) THEN
  GOTO 70
    ELSE
      GOTO 80
  ENDIF
70  WRITE(*,*)'GIVE NEW VALUE FOR: ORF'
  READ(*,*)ORF
  ITER=1
  GOTO 60
C
C  TEST FOR CAVITATION
C
80  I=5
120 IF(P(I))90,90,100
100 IF(I.EQ.I5) GOTO 110
  I=I+1
  GOTO 120
110 WRITE(*,*)'NO CAVITATION IN THE BEARING'
90  NCAVI=I
  PRECAV=NCAVI-1
  THETA0=(NCAVI-2)*360.0/AI3
C
C  EVALUATION OF LOAD AND ATTITUDE ANGLE
C
  WX=0.0
  WY=0.0
  DO 130 I=2,PRECAV,2

```

```

IF(I.EQ.PRECAV) GOTO 140
AI=I-2
TH1=AI*DELTH
TH2=TH1+DELTH
TH3=TH2+DELTH
TERM1=P(I)*COS(TH1)+4.*P(I+1)*COS(TH2)+P(I+2)*COS(TH3)
TERM2=P(I)*SIN(TH1)+4.*P(I+1)*SIN(TH2)+P(I+2)*SIN(TH3)
WX=WX+TERM1*DELTH/3.
WY=WY+TERM2*DELTH/3.
GOTO 130
140 M=PRECAV-1
AI=M-2
TH1=AI*DELTH
TH2=TH1+DELTH
TH3=TH2+DELTH
TERM1=-P(M)*COS(TH1)+8.*P(M+1)*COS(TH2)+5.*P(M+2)*COS(TH3)
TERM2=-P(M)*SIN(TH1)+8.*P(M+1)*SIN(TH2)+5.*P(M+2)*SIN(TH3)
WX=WX+TERM1*DELTH/12.
WY=WY+TERM2*DELTH/12.
130 CONTINUE
C
W=2*SQRT(WX*WX+WY*WY)
ATTRAD=ATAN(-WY/WX)
ATT=ATTRAD*180./PI
SN=1./(PI*W)
C
C CALCULATION OF THE PERTURBED FILM PRESSURE, P2
C
210 ITERP1=1
SPO1=CMPLX(0.,0.)
180 DO 150 I=2,PRECAV
THETAI=THETA(I)
CC1I=CC1(I)
CC2I=CC2(I)
CC3I=CC3(I)
C
C CALCULATION OF THE COEFFICIENTS RELATED WITH THE EXPRESSION OF
C THE PERTURBED FILM PRESSURE, P1
C
CA=0.25*CC1I*EPH0*DELTH*SIN(THETAI)/CC2I
CAA=0.25*CC1I*SIN(THETAI)*DELTH/CC2I
CAB=0.25*CC3I*EPH0*SIN(THETAI)*COS(THETAI)*DELTH/CC2I
CAC=0.5*CC1I*COS(THETAI)/CC2I
CA4=(0.5-CA)
CA5=(0.5+CA)
CA6=(-CAA-CAB+CAC)
CA7=-CC1I*COS(THETAI)/CC2I
CA8=(CAA+CAB+CAC)
CA9A=0.25*SIN(THETAI)*DELTH2/CC2I
CA9B=-0.5*RLAMDA*COS(THETAI)*DELTH2/CC2I
CA9=CMPLX(CA9A,CA9B)
C
C CALCULATION OF PERTURBED FILM PRESSURE, P1
C
TERM11=CA4*P1(I+1)+CA5*P1(I-1)+CA6*P(I+1)+CA7*P(I)+CA8*P(I-1)+CA9
DEV1=TERM11-P1(I)
P1(I)=P1(I)+ORF*DEV1
IF(I.EQ.2) THEN
P1(I5)=P1(2)
ELSEIF(I.EQ.I4) THEN

```

```

                P1(1)=P1(I4)
                ELSE
                GOTO 150
ENDIF
150 CONTINUE
C
C TEST FOR CONVERGENCE OF P1
C
SPN1=CMPLX(0.,0.)
DO 160 I=2,NCAVI
SPN1=SPN1+P1(I)
160 CONTINUE
DEV1=1.-SPO1/SPN1
IF((CABS(DEV1).LE.0.001).OR.ITERP1.GE.500) GO TO 170
ITERP1=ITERP1+1
SPO1=SPN1
GOTO 180
170 IF(ITERP1.GE.500) THEN
GOTO 190
ELSE
GOTO 200
ENDIF
190 WRITE(*,*)'GIVE NEW VALUE OF ORF FOR COMPUTATION OF P1'
READ(*,*)ORF
GOTO 210
C
C CALCULATION OF THE PERTURBED FILM PRESSURE, P2
C
200 ITERP2=1
SPO2=CMPLX(0.,0.)
250 DO 220 I=2,PRECAV
THETA I=THETA(I)
CC1 I=CC1(I)
CC2 I=CC2(I)
CC3 I=CC3(I)
C
C CALCULATION OF THE COEFFICIENTS RELATED WITH THE EXPRESSION OF
C THE PERTURBED FILM PRESSURE, P2
C
CA=0.25*CC1 I*EPH0*DELTH*SIN(THETA I)/CC2 I
CBA=0.25*CC1 I*COS(THETA I)*DELTH/CC2 I
CBB=0.25*CC3 I*EPH0*SIN(THETA I)*SIN(THETA I)*DELTH/CC2 I
CBC=0.5*CC1 I*SIN(THETA I)/CC2 I
CA10=(0.5-CA)
CA11=(0.5+CA)
CA12=(CBA-CBB+CBC)
CA13=-CC1 I*SIN(THETA I)/CC2 I
CA14=(-CBA+CBB+CBC)
CA15A=-0.25*COS(THETA I)*DELTH2/CC2 I
CA15B=-RLAMDA*SIN(THETA I)*DELTH2/CC2 I
CA15=CMPLX(CA9A,CA9B)
C
C CALCULATION OF PERTURBED FILM PRESSURE, P2
C
TERM21=CA10*P2(I+1)+CA11*P2(I-1)+CA12*P(I+1)+CA13*P(I)+CA14*P(I-1)
#+CA15
DEV2=TERM21-P2(I)
P2(I)=P2(I)+ORF*DEV2
IF(I.EQ.2) THEN

```

```

P2(I5)=P2(2)
      ELSEIF(I.EQ.I4) THEN
        P2(1)=P2(I4)
      ELSE
        GOTO 220
      ENDIF
220  CONTINUE
C
C    TEST FOR CONVERGENCE OF P2
C
      SPN2=CMPLX(0.,0.)
      DO 230 I=2,NCAVI
        SPN2=SPN2+P2(I)
230  CONTINUE
      DEV2=1.-SPO2/SPN2
      IF((CABS(DEV2).LE.0.001).OR.ITERP2.GE.500) GO TO 240
      ITERP2=ITERP2+1
      SPO2=SPN2
      GOTO 250
240  IF(ITERP2.GE.500) THEN
      GOTO 260
      ELSE
        GOTO 300
      ENDIF
260  WRITE(*,*)'GIVE NEW VALUE OF ORF FOR COMPUTATION OF P2'
      READ(*,*)ORF
      GOTO 200
C
C    EVALUATION OF STIFFNESS
C
300  WDX1=CMPLX(0.,0.)
      WDY1=CMPLX(0.,0.)
      WDX2=CMPLX(0.,0.)
      WDY2=CMPLX(0.,0.)

      IF(NCAVI.EQ.I5) THEN
        NMOD=I3
      ELSE
        NMOD=PRECAV
      ENDIF
      DO 310 I=2,NMOD,2
        IF(I.EQ.PRECAV) GOTO 320
        AI=I
        TH1=(AI-2.0)*DELTH
        TH2=TH1+DELTH
        TH3=TH2+DELTH
C
        AM11=P1(I)*COS(TH1)+4.*P1(I+1)*COS(TH2)+P1(I+2)*COS(TH3)
        AM12=P1(I)*SIN(TH1)+4.*P1(I+1)*SIN(TH2)+P1(I+2)*SIN(TH3)
        WDX1=WDX1+AM11*DELTH/3.0
        WDY1=WDY1+AM12*DELTH/3.0
C
        AM21=P2(I)*COS(TH1)+4.*P2(I+1)*COS(TH2)+P2(I+2)*COS(TH3)
        AM22=P2(I)*SIN(TH1)+4.*P2(I+1)*SIN(TH2)+P2(I+2)*SIN(TH3)
        WDX2=WDX2+AM21*DELTH/3.0
        WDY2=WDY2+AM22*DELTH/3.0
        GOTO 310
C
320  M=PRECAV-1
      AI=M-2

```

```

TH1=AI*DELTH
TH2=TH1+DELTH
TH3=TH2+DELTH
C
AM11=-P1(M)*COS(TH1)+8.*P1(M+1)*COS(TH2)+5.*P1(M+2)*COS(TH3)
AM12=-P1(M)*SIN(TH1)+8.*P1(M+1)*SIN(TH2)+5.*P1(M+2)*SIN(TH3)
WDX1=WDX1+AM11*DELTH/12.
WDY1=WDY1+AM12*DELTH/12.
C
AM21=-P2(M)*COS(TH1)+8.*P2(M+1)*COS(TH2)+5.*P2(M+2)*COS(TH3)
AM22=-P2(M)*SIN(TH1)+8.*P2(M+1)*SIN(TH2)+5.*P2(M+2)*SIN(TH3)
WDX2=WDX2+AM21*DELTH/12.
WDY2=WDY2+AM22*DELTH/12.
310 CONTINUE
C
C STIFFNESS AND DAMPING COEFFICIENTS FOR THE PERTURBED FILM
C PRESSURE, P1
C
RWDX1=REAL(WDX1)
RWDY1=REAL(WDY1)
WDX1A=AIMAG(WDX1)
WDY1A=AIMAG(WDY1)
SRR=-2.0*RWDX1
SPR=-2.0*RWDY1
DRR=-2.0*WDX1A/RLAMDA
DPR=-2.0*WDY1A/RLAMDA
C
C STIFFNESS AND DAMPING COEFFICIENTS FOR THE PERTURBED FILM
C PRESSURE, P2
C
RWDX2=REAL(WDX2)
RWDY2=REAL(WDY2)
WDX2A=AIMAG(WDX2)
WDY2A=AIMAG(WDY2)
SRP=-2.0*RWDX2
SPP=-2.0*RWDY2
DRP=-2.0*WDX2A/RLAMDA
DPP=-2.0*WDY2A/RLAMDA
C
C CALCULATION OF WHIRL RATIO AND CRITICAL MASS PARAMETER
C
TRM1=( (SRR*DPP+SPP*DRR) - (SPR*DRP+SRP*DPR) - (DPR*W*SIN(ATTRAD) - DRR*
#W*COS(ATTRAD)) / EPH0) / (DPP+DRR)
TRM2=SRR+SPP+(W*COS(ATTRAD)) / EPH0
TRM3=DPP*DRR-DRP*DPR
TRM4=SPP*SRR-SRP*SPR+(SRR*W*COS(ATTRAD) - SPR*W*SIN(ATTRAD)) / EPH0
WRSQ=(TRM1*(TRM1-TRM2)+TRM4) / TRM3
IF (WRSQ.LT.0.0) THEN
GOTO 350
ELSE
WR=SQRT(WRSQ)
EM=TRM1 / (WRSQ*W)
GOTO 360
ENDIF
C
350 WRITE(3,1020)EPH0,ITER,W,ATT,ITERP1,ITERP2,RWDX1,WDX1A,RWDY1,
#WDY1A,RWDX2,WDX2A,RWDY2,WDY2A,SRR,SPR,DRR,DPR,SRP,SPP,DRP,DPP

```

```

1020  FORMAT(F4.2,1X,I4,1X,F8.2,1X,F8.2,9X,I3,1X,I3,1X,F11.2,'+ i ',
#F11.2,1X,F11.2,'+ i ',F11.2,1X,F11.2,'+ i ',F11.2,1X,F11.2,'+ i ',
#F11.2,1X,F12.2,1X,F12.2,1X,F12.2,1X,F12.2,1X,F12.2,1X,F12.2,1X,
#F12.2,1X,F12.2,2X,'INFINITE')
      GOTO 370
360  WRITE(3,1030)EPH0,ITER,W,ATT,SN,ITERP1,ITERP2,SRR,SPR,DRR,DPR,SRP,
#WDY1A,RWDX2,WDX2A,RWDY2,WDY2A,SRR,SPR,DRR,DPR,SRP,SPP,DRP,DPP,WR,
#EM
1030  FORMAT(F4.2,1X,I4,2X,F8.2,2X,F8.2,9X,I3,1X,I3,1X,F11.2,'+ i ',
#F11.2,1X,F11.2,'+ i ',F11.2,1X,F11.2,'+ i ',F11.2,1X,F11.2,'+ i ',
#F11.2,1X,F12.2,1X,F12.2,1X,F12.2,1X,F12.2,1X,F12.2,1X,F12.2,1X,
#F12.2,1X,F12.2,2X,'FINITE',2X,F10.2,3X,F8.2)
C
370  KOUNT=3
      IF(KOUNT-2)180,380,390
C
380  WRITE(*,*)'NEW VALUE OF ORF ='
      READ(*,*)ORF
      ITER=1
      DO 400 I=1,I6
      P1(I)=CMPLX(0.,0.)
      P2(I)=CMPLX(0.,0.)
400  CONTINUE
      GO TO 210
C
390  EPH0=EPH0+0.1
      KNT=KNT+1
      GOTO 410
420  ILM=ILM+1
      GOTO 430
440  AN2=AN2+0.2
      GOTO 450
460  WRITE(*,*)'PROGRAM TERMINATED'
C420 WRITE(*,*)'PROGRAM TERMINATED'
      STOP
      END

```

## 7.2 APPENDIX-II:

### *Programme For Calculating Load Carrying Capacity, Attitude Angle, Stiffness & Damping Of Infinitely Long Hydrodynamic Journal Bearings With Newtonian Fluids.*

```
COMPLEX P1(55),P2(55),TERM11,TERM21,SPO1,SPO2,SPN1,SPN2
COMPLEX AM11,AM12,AM21,AM22,F11(55),F12(55),F21(55),F22(55)
COMPLEX CA9,CA15,WDX1,WDY1,WDX2,WDY2,DEV1,DEV2
INTEGER PRECAV
REAL LM, LM2
DIMENSION P(55),THETA(55),HH0(55)
DIMENSION RLM(10),CC1(55),CC2(55),CC3(55)
OPEN(3,FILE='RESULTN.DAT')
WRITE(*,*)'LM=?','AN2=?'
READ(*,*)LM,AN2
RLAMDA=1.0
EPH0=0.1
WRITE(3,1520)RLAMDA
1520 FORMAT(5X,'RLAMDA =',F4.1/)
WRITE(3,1010)
1010 FORMAT('EPH0',1X,'ITER',2X,'SS LOAD',2X,'ATT ANGLE',5X,'SN',
#3X,'IP1',1X,'IP2',8X,'WDX1(Cos:P1)',15X,'WDY1(Sin:P1)',15X,
#'WDX2(Cos:P2)',15X,'WDY2(Sin:P2)',12X,'SRR',10X,'SPR',10X,'DRR',
#10X,'DPR',10X,'SRP',10X,'SPP',10X,'DRP',10X,'DPP',4X,'STABILITY',
#2X,'WH RATIO',2X,'MASS PARA'/)
410 IF (EPH0.GE.1.0) STOP
C
WRITE(*,1220)KNT,RLAMDA,LM,AN2,R,EPH0
1220 FORMAT(/4X,'KNT=',I8,4X,'RLAMDA=',F4.2,3X,'LM=',F7.2,3X,
#'AN2=',F6.3,3X,'R=',F3.1,3X,'EPH0=',F5.2)
C
IPT=44
PI=4.*ATAN(1.0)
I5=IPT+2
I6=I5+1
I4=I5-1
I3=I4-1
I2=I3-1
AI3=I3
DELTH=2.0*PI/AI3
DELTH2=DELTH*DELTH
LM2=LM*LM
AN=SQRT(AN2)
AN3=AN2*AN
C
ITER=1
SPO=0.
C
C CALCULATION OF FILM THICKNESS AND THE FUNTIIONS F1=COTH(N*LM*H0/2)
C AND F2={COSECH(N*LM*H0/2)}^2
C
DO 10 I=2,I5
AI=I-2
THETA=AI*DELTH
THETA(I)=THETA
H0=1.0+EPH0*COS(THETA)
HH0(I)=H0
```

```

A=0.5*AN*LM*H0
TANHA=TANH(A)
COTHA=1.0/TANHA
SINHA=SINH(A)
CSCHA=1.0/SINHA
CSCHA2=CSCHA*CSCHA
H02=H0*H0
H03=H02*H0
CC1(I)=H02/4.+1./LM2-AN*H0*COTHA/LM+AN2*H02*CSCHA2/4.
CC2(I)=H03/12.+H0/LM2-0.5*AN*H02*COTHA/LM
CC3(I)=H0/2.+AN2*H0*CSCHA2-AN*COTHA/LM-AN3*LM*H02*CSCHA2*COTHA/4.
10 CONTINUE
C
C INITIALISATION OF PRESSURE
C
DO 20 I=1,I6
P(I)=0.0
P1(I)=CMPLX(0.,0.)
P2(I)=CMPLX(0.,0.)
20 CONTINUE
C
C SETTING OF BOUNDARY CONDITIONS
C
60 IF(I.EQ.2) THEN
P(I)=0.0
ENDIF
C
C SOLUTION OF REYNOLDS' EQUATION
C
DO 30 I=2,I5
THETA=THETA(I)
C
CC1I=CC1(I)
CC2I=CC2(I)
CC3I=CC3(I)
CA=0.25*CC1I*EPH0*DELTH*SIN(THETA)/CC2I
CA1=(0.5-CA)
CA2=(0.5+CA)
CA3=0.25*EPH0*DELTH2*SIN(THETA)/CC2I
TERM=CA1*P(I+1)+CA2*P(I-1)+CA3
ERR=TERM-P(I)
C
P(I)=P(I)+ORF*ERR
IF(P(I).LT.0.0) P(I)=0.0
IF(I.EQ.2) THEN
P(I5)=P(2)
ELSEIF(I.EQ.I4) THEN
P(1)=P(I4)
ELSE
GOTO 30
ENDIF
30 CONTINUE
C
C TEST FOR CONVERGENCE
C
SPN=0.0
DO 40 I=2,I5
SPN=SPN+P(I)
40 CONTINUE
ERR=1.0-SPO/SPN

```

```

IF(ABS(ERR).LE.0.001.OR.ITER.GE.500) GOTO 50
ITER=ITER+1
SPO=SPN
GOTO 60
50 IF(ITER.GE.500) THEN
GOTO 70
ELSE
GOTO 80
ENDIF
70 WRITE(*,*)'GIVE NEW VALUE FOR: ORF'
READ(*,*)ORF
ITER=1
GOTO 60

C
C TEST FOR CAVITATION
C
80 I=5
120 IF(P(I))90,90,100
100 IF(I.EQ.I5) GOTO 110
I=I+1
GOTO 120
110 WRITE(*,*)'NO CAVITATION IN THE BEARING'
90 NCAVI=I
PRECAV=NCAVI-1
THETA0=(NCAVI-2)*360.0/AI3

C
C EVALUATION OF LOAD AND ATTITUDE ANGLE
C
WX=0.0
WY=0.0
DO 130 I=2,PRECAV,2
IF(I.EQ.PRECAV) GOTO 140
AI=I-2
TH1=AI*DELTH
TH2=TH1+DELTH
TH3=TH2+DELTH
TERM1=P(I)*COS(TH1)+4.*P(I+1)*COS(TH2)+P(I+2)*COS(TH3)
TERM2=P(I)*SIN(TH1)+4.*P(I+1)*SIN(TH2)+P(I+2)*SIN(TH3)
WX=WX+TERM1*DELTH/3.
WY=WY+TERM2*DELTH/3.
GOTO 130
140 M=PRECAV-1
AI=M-2
TH1=AI*DELTH
TH2=TH1+DELTH
TH3=TH2+DELTH
TERM1=-P(M)*COS(TH1)+8.*P(M+1)*COS(TH2)+5.*P(M+2)*COS(TH3)
TERM2=-P(M)*SIN(TH1)+8.*P(M+1)*SIN(TH2)+5.*P(M+2)*SIN(TH3)
WX=WX+TERM1*DELTH/12.
WY=WY+TERM2*DELTH/12.
130 CONTINUE
C
W=2*SQRT(WX*WX+WY*WY)
ATTRAD=ATAN(-WY/WX)
ATT=ATTRAD*180./PI
SN=1./(PI*W)

C
C CALCULATION OF THE PERTURBED FILM PRESSURE, P2
C
210 ITERP1=1

```

```

SPO1=CMPLX(0.,0.)
180 DO 150 I=2,PRECAV
    THETA I=THETA(I)
    CC1I=CC1(I)
    CC2I=CC2(I)
    CC3I=CC3(I)
C
C   CALCULATION OF THE COEFFICIENTS RELATED WITH THE EXPRESSION OF
C   THE PERTURBED FILM PRESSURE, P1
C
CA=0.25*CC1I*EPH0*DELTH*SIN(THETA I)/CC2I
CAA=0.25*CC1I*SIN(THETA I)*DELTH/CC2I
CAB=0.25*CC3I*EPH0*SIN(THETA I)*COS(THETA I)*DELTH/CC2I
CAC=0.5*CC1I*COS(THETA I)/CC2I
CA4=(0.5-CA)
CA5=(0.5+CA)
CA6=(-CAA-CAB+CAC)
CA7=-CC1I*COS(THETA I)/CC2I
CA8=(CAA+CAB+CAC)
CA9A=0.25*SIN(THETA I)*DELTH2/CC2I
CA9B=-0.5*RLAMDA*COS(THETA I)*DELTH2/CC2I
CA9=CMPLX(CA9A,CA9B)
C
C   CALCULATION OF PERTURBED FILM PRESSURE, P1
C
TERM11=CA4*P1(I+1)+CA5*P1(I-1)+CA6*P(I+1)+CA7*P(I)+CA8*P(I-1)+CA9
DEV1=TERM11-P1(I)
P1(I)=P1(I)+ORF*DEV1
IF(I.EQ.2) THEN
P1(I5)=P1(2)
    ELSEIF(I.EQ.I4) THEN
    P1(1)=P1(I4)
    ELSE
    GOTO 150
ENDIF
150 CONTINUE
C
C   TEST FOR CONVERGENCE OF P1
C
SPN1=CMPLX(0.,0.)
DO 160 I=2,NCAVI
SPN1=SPN1+P1(I)
160 CONTINUE
DEV1=1.-SPO1/SPN1
IF((CABS(DEV1).LE.0.001).OR.ITERP1.GE.500) GO TO 170
ITERP1=ITERP1+1
SPO1=SPN1
GOTO 180
170 IF(ITERP1.GE.500) THEN
GOTO 190
    ELSE
    GOTO 200
ENDIF
190 WRITE(*,*)'GIVE NEW VALUE OF ORF FOR COMPUTATION OF P1'
    READ(*,*)ORF
    GOTO 210
C
C   CALCULATION OF THE PERTURBED FILM PRESSURE, P2
C
200 ITERP2=1

```

```

SPO2=CMPLX(0.,0.)

250 DO 220 I=2,PRECAV
    THETA I=THETA(I)
    CC1 I=CC1(I)
    CC2 I=CC2(I)
    CC3 I=CC3(I)

C
C   CALCULATION OF THE COEFFICIENTS RELATED WITH THE EXPRESSION OF
C   THE PERTURBED FILM PRESSURE, P2
C
    CA=0.25*CC1 I*EPH0*DELTH*SIN(THETA I)/CC2 I
    CBA=0.25*CC1 I*COS(THETA I)*DELTH/CC2 I
    CBB=0.25*CC3 I*EPH0*SIN(THETA I)*SIN(THETA I)*DELTH/CC2 I
    CBC=0.5*CC1 I*SIN(THETA I)/CC2 I
    CA10=(0.5-CA)
    CA11=(0.5+CA)
    CA12=(CBA-CBB+CBC)
    CA13=-CC1 I*SIN(THETA I)/CC2 I
    CA14=(-CBA+CBB+CBC)
    CA15A=-0.25*COS(THETA I)*DELTH2/CC2 I
    CA15B=-RLAMDA*SIN(THETA I)*DELTH2/CC2 I
    CA15=CMPLX(CA9A,CA9B)

C
C   CALCULATION OF PERTURBED FILM PRESSURE, P2
C
    TERM21=CA10*P2(I+1)+CA11*P2(I-1)+CA12*P(I+1)+CA13*P(I)+CA14*P(I-1)
    #+CA15
    DEV2=TERM21-P2(I)
    P2(I)=P2(I)+ORF*DEV2
    IF(I.EQ.2) THEN
        P2(I5)=P2(2)
        ELSEIF(I.EQ.I4) THEN
            P2(1)=P2(I4)
        ELSE
            GOTO 220
    ENDIF

220 CONTINUE

C
C   TEST FOR CONVERGENCE OF P2
C
    SPN2=CMPLX(0.,0.)
    DO 230 I=2,NCAVI
        SPN2=SPN2+P2(I)
230 CONTINUE
    DEV2=1.-SPO2/SPN2
    IF((CABS(DEV2).LE.0.001).OR.ITERP2.GE.500) GO TO 240
    ITERP2=ITERP2+1
    SPO2=SPN2
    GOTO 250

240 IF(ITERP2.GE.500) THEN
    GOTO 260
    ELSE
    GOTO 300
ENDIF

260 WRITE(*,*)'GIVE NEW VALUE OF ORF FOR COMPUTATION OF P2'
    READ(*,*)ORF
    GOTO 200

C
C   EVALUATION OF STIFFNESS

```

```

C
300  WDX1=CMPLX(0.,0.)
      WDY1=CMPLX(0.,0.)
      WDX2=CMPLX(0.,0.)
      WDY2=CMPLX(0.,0.)

      IF(NCAVI.EQ.I5) THEN
        NMOD=I3
      ELSE
        NMOD=PRECAV
      ENDIF
      DO 310 I=2,NMOD,2
        IF(I.EQ.PRECAV) GOTO 320
        AI=I
        TH1=(AI-2.0)*DELTH
        TH2=TH1+DELTH
        TH3=TH2+DELTH

C
        AM11=P1(I)*COS(TH1)+4.*P1(I+1)*COS(TH2)+P1(I+2)*COS(TH3)
        AM12=P1(I)*SIN(TH1)+4.*P1(I+1)*SIN(TH2)+P1(I+2)*SIN(TH3)
        WDX1=WDX1+AM11*DELTH/3.0
        WDY1=WDY1+AM12*DELTH/3.0

C
        AM21=P2(I)*COS(TH1)+4.*P2(I+1)*COS(TH2)+P2(I+2)*COS(TH3)
        AM22=P2(I)*SIN(TH1)+4.*P2(I+1)*SIN(TH2)+P2(I+2)*SIN(TH3)
        WDX2=WDX2+AM21*DELTH/3.0
        WDY2=WDY2+AM22*DELTH/3.0
        GOTO 310

C
320  M=PRECAV-1
      AI=M-2
      TH1=AI*DELTH
      TH2=TH1+DELTH
      TH3=TH2+DELTH

C
        AM11=-P1(M)*COS(TH1)+8.*P1(M+1)*COS(TH2)+5.*P1(M+2)*COS(TH3)
        AM12=-P1(M)*SIN(TH1)+8.*P1(M+1)*SIN(TH2)+5.*P1(M+2)*SIN(TH3)
        WDX1=WDX1+AM11*DELTH/12.
        WDY1=WDY1+AM12*DELTH/12.

C
        AM21=-P2(M)*COS(TH1)+8.*P2(M+1)*COS(TH2)+5.*P2(M+2)*COS(TH3)
        AM22=-P2(M)*SIN(TH1)+8.*P2(M+1)*SIN(TH2)+5.*P2(M+2)*SIN(TH3)
        WDX2=WDX2+AM21*DELTH/12.
        WDY2=WDY2+AM22*DELTH/12.
310  CONTINUE

C
C      STIFFNESS AND DAMPING COEFFICIENTS FOR THE PERTURBED FILM
C      PRESSURE, P1
C
      RDX1=REAL(WDX1)
      RDY1=REAL(WDY1)
      WDX1A=AIMAG(WDX1)
      WDY1A=AIMAG(WDY1)

      SRR=-2.0*RDX1
      SPR=-2.0*RDY1
      DRR=-2.0*WDX1A/RLAMDA
      DPR=-2.0*WDY1A/RLAMDA

C
C      STIFFNESS AND DAMPING COEFFICIENTS FOR THE PERTURBED FILM

```

```

C      PRESSURE, P2
C
      RWDX2=REAL(WDX2)
      RWDY2=REAL(WDY2)
      WDX2A=AIMAG(WDX2)
      WDY2A=AIMAG(WDY2)

      SRP=-2.0*RWDX2
      SPP=-2.0*RWDY2
      DRP=-2.0*WDX2A/RLAMDA
      DPP=-2.0*WDY2A/RLAMDA

C
C      CALCULATION OF WHIRL RATIO AND CRITICAL MASS PARAMETER
C
      TRM1=( (SRR*DPP+SPP*DRR) - (SPR*DRP+SRP*DPR) - (DPR*W*SIN(ATTRAD) -DRR*
#W*COS(ATTRAD)) /EPH0) / (DPP+DRR)
      TRM2=SRR+SPP+(W*COS(ATTRAD)) /EPH0
      TRM3=DPP*DRR-DRP*DPR
      TRM4=SPP*SRR-SRP*SPR+(SRR*W*COS(ATTRAD) -SPR*W*SIN(ATTRAD)) /EPH0
      WRSQ=(TRM1*(TRM1-TRM2)+TRM4) /TRM3
      IF (WRSQ.LT.0.0) THEN
      GOTO 350
          ELSE
          WR=SQRT(WRSQ)
          EM=TRM1/(WRSQ*W)
          GOTO 360
      ENDIF

C
350  WRITE(3,1020)EPH0,ITER,W,ATT,ITERP1,ITERP2,RWDX1,WDX1A,RWDY1,
#WDY1A,RWDX2,WDX2A,RWDY2,WDY2A,SRR,SPR,DRR,DPR,SRP,SPP,DRP,DPP

1020  FORMAT(F4.2,1X,I4,1X,F8.2,1X,F8.2,9X,I3,1X,I3,1X,F11.2,'+ i ',
#F11.2,1X,F11.2,'+ i ',F11.2,1X,F11.2,'+ i ',F11.2,1X,F11.2,'+ i ',
#F11.2,1X,F12.2,1X,F12.2,1X,F12.2,1X,F12.2,1X,F12.2,1X,F12.2,1X,
#F12.2,1X,F12.2,2X,'INFINITE')
      GOTO 370

360  WRITE(3,1030)EPH0,ITER,W,ATT,SN,ITERP1,ITERP2,SRR,SPR,DRR,DPR,SRP,
#WDY1A,RWDX2,WDX2A,RWDY2,WDY2A,SRR,SPR,DRR,DPR,SRP,SPP,DRP,DPP,WR,
#EM

1030  FORMAT(F4.2,1X,I4,2X,F8.2,2X,F8.2,9X,I3,1X,I3,1X,F11.2,'+ i ',
#F11.2,1X,F11.2,'+ i ',F11.2,1X,F11.2,'+ i ',F11.2,1X,F11.2,'+ i ',
#F11.2,1X,F12.2,1X,F12.2,1X,F12.2,1X,F12.2,1X,F12.2,1X,F12.2,1X,
#F12.2,1X,F12.2,2X,'FINITE',2X,F10.2,3X,F8.2)

C
370  KOUNT=3
      IF(KOUNT-2)180,380,390

C
380  WRITE(*,*)'NEW VALUE OF ORF ='
      READ(*,*)ORF
      ITER=1
      DO 400 I=1,I6
      P1(I)=CMPLX(0.,0.)
      P2(I)=CMPLX(0.,0.)

400  CONTINUE
      GO TO 210

C
390  EPH0=EPH0+0.1
      KNT=KNT+1
      GOTO 410
      END

```

### 7.3 APPENDIX-III:

#### *Programme For Calculating Bearing Stability Parameter of Infinitely Long Flexibly Supported Hydrodynamic Journal Bearings.*

```
      IMPLICIT REAL*8(A-H,O-Z)
C      DIMENSION A(5),XR(3),F(3)
      PARAMETER (PI=3.1415927)
C      OPEN(5,FILE='STD1.DAT')
C      OPEN(7,FILE='STO.DAT')
C      WRITE(*,2)
C2     FORMAT(1X,3H$K,2HD,1HZ)
14     WRITE(*,*) 'K$AR,D,Z'
      READ(*,*)SK,D,Z
      WRITE(*,*) 'EPH0=', 'W=', 'ATT=', 'SRR=', 'SPR=', 'DRR=', 'DPR='
      #, 'SRP=', 'SPP=', 'DRP=', 'DPP='
      READ(*,*)EPH0,W,ATT,SRR,SPR,DRR,DPR,SRP,SPP,DRP,DPP
      PHI=ATT*PI/180.
      X=((SRR+SRP*PHI)*DSIN(PHI)+(SPR+SPP*PHI)*DCOS(PHI))*EPH0/SK
      Y=((SRR+SRP*PHI)*DCOS(PHI)-(SPR+SPP*PHI)*DSIN(PHI))*EPH0/SK
      B1=(X*DSIN(PHI)+Y*DCOS(PHI))
      B2=(Y*DSIN(PHI)-X*DCOS(PHI))

      A1=-(Z**2)*EPH0*(W**4)

      A2=(Z*SRR*EPH0+Z*SPP*EPH0+Z*(SK*B1+2.*SK*EPH0)+(Z**2)*(SRR*EPH0+
      #SPP*EPH0+W*DCOS(PHI)))*(W**3)

      A31=((DRR*DPP-DPR*DRP)*EPH0+2.*Z*(DRR*DPP-DRP*DPR)*EPH0+D*EPH0*
      # (DRR+DPP)+2.*Z*D*EPH0*(DRR+DPP)+(Z**2)*(DRR*DPP-DRP*DPR)*EPH0+
      # (D**2)*EPH0)*(W**2)

      A32=((SRP*SPR-SRR*SPP)*EPH0+2.*Z*(SRP*SPR-SRR*SPP-SK*SRR-SK*SPP)*
      #EPH0-SK*(SRR+SPP)*EPH0-Z*W*SRR*DCOS(PHI)*(1.+Z)+Z*W*SPR
      #*DSIN(PHI)*(1.+Z)+(Z**2)*(SRP*SPR-SRR*SPP)*EPH0-2.*Z*SK*
      #W*DCOS(PHI)-(SK**2)*EPH0-SK*B1*(SRR-SPR+Z*SRR+SK)+Z*SK*B2*SPR)
      #*(W**2)

      A42=(2.*SK*(DPR*DRP-DPP*DRR)*EPH0+2.*D*(DPR*SRP-SRR*DPP)*EPH0
      #+D*SK*B2*DPR+2.*D*(SPR*DRP-SPP*DRR)*EPH0-D*W*DRR*(1.+2.*Z)
      #*DCOS(PHI)-(D**2)*W*DCOS(PHI)-D*SK*B1*DRR+D*W*DPR*DSIN(PHI)*
      # (1.+2.*Z)-(D**2)*EPH0*(SRR+SPP)+2.*Z*SK*(DPR*DRP-DPP*DRR)*EPH0-
      #2.*D*SK*(DRR+DPP)*EPH0-2.*Z*D*(DRR*SPP+SRR*DPP-SRP*DPR-SPR*DRP)
      #*EPH0)*W

      A51=(D**2)*(DRP*DPR-DRR*DPP)*EPH0

      A41=(2.*SK*(SRR*SPP-SRP*SPR)*EPH0+(SK**2)*(SRR+SPP)*EPH0+SK*W*SRR*
      #DCOS(PHI)*(1.+2.*Z)-SK*W*SPR*DSIN(PHI)*(1.+2.*Z)+(SK**2)*W*
      #DCOS(PHI)+2.*Z*SK*(SRR*SPP-SPR*SRP)*EPH0-(SK**2)*B2*SPR+
      # (SK**2)*B1*SRR)*W

      A52=(D**2)*(SRR*SPP-SPR*SRP)*EPH0+(SK**2)*(DRR*DPP-DRP*DPR)*EPH0
      #+2.*D*SK*(DRR*SPP+SRR*DPP-SRP*DPR-SPR*DRP)*EPH0+W*D*COS(PHI)*
      # (D*SRR+2.*SK*DRR)-D*W*DSIN(PHI)*(D*SPR+2.*SK*DPR)

      A53=(SK**2)*(SRP*SPR-SRR*SPP)*EPH0+(SK**2)*W*(SPR*DSIN(PHI)-SRR*
```

#DCOS(PHI))

BB1=(Z\*(DRR+DPP+2.\*D)\*EPH0+(Z\*\*2)\*(DRR+DPP)\*EPH0)\*(W\*\*3)

BB2=((SRP\*DPR+SPR\*DRP-SRR\*DPP-DRR\*SPP)\*EPH0+2.\*Z\*(DPR\*SRP+SPR\*DRP-  
#SRR\*DPP-SPP\*DRR)\*EPH0-D\*(SRR+SPP)\*EPH0-Z\*W\*DRR\*DCOS(PHI)\*(1.+Z)+  
#Z\*W\*DPR\*DSIN(PHI)\*(1.+Z)-2.\*Z\*D\*W\*DCOS(PHI)-(Z\*\*2)\*(SPP\*DRR+SRR  
#\*DPP-DPR\*SRP-SPR\*DRP)\*EPH0-2.\*Z\*SK\*(DRR+DPP)\*EPH0-2.\*Z\*D\*(SPP+SRR  
#)\*EPH0-SK\*(DPP+DRR)\*EPH0-D\*B1\*SK-Z\*D\*SK\*EPH0-B1\*DRR\*SK\*(1.+Z)+  
#SK\*B2\*(DPR+Z\*DRP))\*(W\*\*2)

BB32=(2.\*D\*DPR\*DRP\*EPH0-2.\*D\*DRR\*DPP\*EPH0-2.\*Z\*D\*DRR\*DPP\*EPH0-  
#(D\*\*2)\*(DRR+DPP)\*EPH0)\*W

BB31=(2.\*SK\*(SRR\*DPP+SPP\*DRR-DPR\*SRP-SPR\*DRP)\*EPH0+2.\*D\*(SPP\*SRR-  
#SRP\*SPR)\*EPH0+SK\*W\*DRR\*DCOS(PHI)\*(1.+2.\*Z)-D\*W\*SPR\*DSIN(PHI)\*  
#(1.+2.\*Z)+D\*W\*SRR\*DCOS(PHI)\*(1.+2.\*Z)-SK\*W\*DPR\*DSIN(PHI)\*  
#(1.+2.\*Z)+2.\*D\*SK\*W\*DCOS(PHI)+2.\*D\*SK\*(SRR+SPP)\*EPH0+  
#(SK\*\*2)\*(DRR+DPP)\*EPH0+2.\*SK\*Z\*(SPP\*DRR+SRR\*DPP-SRP\*DPR-SPR\*DRP)\*  
#EPH0+2.\*Z\*D\*(SRR\*SPP-SRP\*SPR)\*EPH0-SK\*B2\*(SK\*DRP-D\*SPR)+  
#SK\*B1\*(D\*SRR+SK\*DRR))\*W

BB41=2.\*D\*SK\*DRR\*DPP\*EPH0+(D\*\*2)\*(SPP\*DRR+SRR\*DPP-SRP\*DPR-SPR\*DRP)  
#\*EPH0+(D\*\*2)\*W\*(DRR\*DCOS(PHI)-DPR\*DSIN(PHI))

BB42=2.\*SK\*D\*(SRP\*SPR-SRR\*SPP)\*EPH0+(SK\*\*2)\*(SRP\*DPR+SPR\*DRP-  
#SPP\*DRR-SRR\*DPP)\*EPH0-SK\*W\*DCOS(PHI)\*(2.\*D\*SRR+SK\*DRR)+  
#SK\*W\*DSIN(PHI)\*(SK\*DPR+2.\*D\*SPR)

C SIMULTANEOUS SOLUTION BY NEWTON RAPHSON-METHOD

```
401 ITER=1
WRITE(*,*)'LAMDA, SM, '
READ(*,*)SL, SM
S=SL**2*SM
V=SL**2
200 F1=A1*S**4+A2*S**3+(A31*V+A32)*S**2+(A42*V+A41)*S+
#(A51*V**2+A52*V+A53)
F2=BB1*S**3+BB2*S**2+(BB32*V+BB31)*S+(BB41*V+BB42)
IF(ITER.NE.1) GO TO 20
WRITE(*,*) 'F1=', F1, 'F2=', F2
WRITE(*,*) 'FURTHER INITIALIZE? IF YESS PRESS 1 '
READ(*,*) LOGIC
IF(LOGIC.EQ.1) GO TO 401
20 DF1S=4.*A1*S**3+3.*A2*S**2+2.*(A31*V+A32)*
#S+(A42*V+A41)
DF2S=3.*BB1*S**2+2.*BB2*S+(BB32*V+BB31)
DF1V=A31*S**2+A42*S+2*A51*V+A52
DF2V=BB32*S+BB41
DEN=DF1S*DF2V-DF2S*DF1V
H=(F2*DF1V-F1*DF2V)/DEN
AK=-(F2*DF1S-F1*DF2S)/DEN
WRITE(*,*) 'K=', AK, 'H=', H, 'ERR1=', ERR1, 'ERR2=', ERR2
WRITE(*,*) 'V=', V, 'M=', S/V
AS=S+H
AV=V+AK
C ERR1=1.-S/AS
C ERR2=1.-V/AV
ERR1=DABS(S-AS)
ERR2=DABS(V-AV)
```

```

        IF((ERR1).GT.1.0E-08) GO TO 100
        IF((ERR2).GT.1.0E-08) GO TO 100
        WRITE(*,*)S,V
        IF(V) 400,400,2000
400    WRITE(*,*) 'INFINTELY STABLE'
        GO TO 2001
2000   SL=SQRT(V)
        SM=S/V
        WRITE(*,*) 'WHIRL RATIO=',SL,'CRITICAL MASS=',SM
        WRITE(*,*)SRR,SPR,DRR,DPR
2001   WRITE(*,*)'INDEX=?,INDEX=1 IMPLIES GOING FOR NEXT CALCULATION'
        READ(*,*) INDEX
        IF (INDEX.EQ.1) GO TO 310
        STOP
100    IF(ITER.GT.100) GO TO 300
        S=AS
        V=AV
        ITER=ITER+1
        GO TO 200
300    WRITE(*,*)'MODIFY THE INITIAL VALUES AS ITER IS >100'
        GO TO 401
310    GO TO 14
C      WRITE(7,26)EPH0,SM,SL
C26    FORMAT(1X,'R=',F7.1,2X,'EPH0=',F3.1,2X,'SM='F12.9,2X,'SL=',F12.9)
C      WRITE(*,27)EPH0,SM,SL
C27    FORMAT(1X,'R=',F7.1,2X,'EPH0=',F3.1,2X,'SM='F12.9,2X,'SL=',F12.9)
C14    CONTINUE
        END

```

## 7.4 Appendix-IV: *Additional Literature Review*

---

**Sinha[56]** derived the generalized Reynolds equation for a dynamically loaded journal bearing, considering the presence of both wedge and squeeze films, in which the load and speed of rotation varied with time in magnitude and direction. The bearing characteristics for an infinitely long journal bearing were obtained and the dynamic behaviour of squeeze films in a half journal bearing under a fluctuating load with no journal rotation was studied in detail.

**Yousif and Ibrahim[57]** analyzed numerically the characteristics of conventional infinitely long thrust bearings for the steady laminar flow of an incompressible micropolar fluid, which showed the enhancement of the bearing performance in micropolar fluids over the Newtonian fluid.

**Bessonov[58]** derived the generalized Reynolds equation that would be applicable to the cases of all possible variations in boundary viscosity and microrotations near the friction surface. The slider bearing performance was studied as an example. Sufficient decrease in the friction coefficient of the bearing without a noticeable change in its load capacity was found to be obtained by varying the interaction between a micropolar lubricant and friction surfaces.

**Tomantschger[59]** reported an analysis of the motion of a micropolar suspension between two coaxial cylinders. The general and special solutions of two coupled ordinary second-order differential equations were derived. These solutions were found to be modified forms of Bessel functions of the first and second kind, and powers of the variable.

A numerical analysis of a finite journal bearing under micropolar lubrication was presented by **Wang and Zhu[60]**, considering both thermal and cavitation effects. The modified Reynolds equation was derived along with the energy equation and was solved using the Elord's cavitation algorithm. The effects of micropolarity on the thermohydrodynamic performance of the bearing were investigated. The results exhibited the increase in load capacity and temperature, but the decrease in coefficient of friction and side leakage flow in the micropolar fluids, when compared with Newtonian fluids. It was observed that in the full film region, non-dimensional density was increased with the degree of micropolarity, while in the cavitated region, both micropolar fluids and Newtonian fluids yielded the same values of the fractional film content.

**Suresh Verma, Vijay Kumar, K. D. Gupta [61]** presents a theoretical study of the performance characteristics of a constant flow valve compensated multirecess hydrostatic journal bearings operating with micropolar lubricant. The finite element method and iterative procedure have been used to solve the modified Reynolds equation governing the micropolar lubricant flow in the bearing. The performance characteristics are presented for a wide range of nondimensional load, lubricant flow, and micropolar parameters. It has been observed that the micropolar parameters significantly influence the performance characteristics of the bearing.

**K. Prabhakaran Nair, Mohammed Shabbir Ahmed, Saed Thamer Al-qahtani [62]** presents the static and dynamic analysis of hydrodynamic journal bearing operating under nanolubricants are presented. The load carrying capacity of journal bearing mainly depends upon the viscosity of the lubricant. The addition of nano particles on commercially available lubricant may enhance the viscosity of lubricant and in turn changes the performance characteristics. In the proposed work, to obtain pressure distribution in the clearance space of the journal bearing, modified Reynolds equation is used. An iterative procedure is used to establish the film extent of the bearing. The modified Reynolds equation is solved by using the powerful numerical technique, finite element method. The static characteristics in terms of load capacity, attitude angle and end leakage and dynamic characteristics in terms of stiffness coefficients, damping coefficients, threshold speed and damped frequency of whirl are evaluated for different eccentricity ratios.

**Ravindra R. Navthar, Dr. N.V. Halegowda [63]** presents, journal bearings are widely applied in different rotating machineries. These bearings allow for transmission of large loads at mean speed of rotation. These bearings are susceptible to large amplitude lateral vibration due to self excited instability which is known as oil whirl or Synchronous whirl. This paper presents a method to determine the Synchronous whirl i.e. Stability of hydrodynamic Journal bearings by using dynamic characteristics such as stiffness coefficients. Analysis shows that Bearing operating at a speed of 800 rpm and 150N load remains stable up to a speed of 1666rpm. This is verified experimentally on journal bearing test rig by operating the bearing up to 1666 rpm and observing the pressure distribution plot. Different journal speeds and loads are considered for the analysis.

#### 7.4 Appendix-V: *Reference of Additional Literature Review*

SL.NO.	JOURNALS
56	<b>Sinha, P.</b> “Dynamically loaded micropolar fluid lubricated journal bearings with special reference to squeeze films under fluctuating loads”, <i>Wear, Vol. 45, Issue 3, Dec. 1977, pp. 279- 292.</i>
57	<b>Yousif, A. E. and Ibrahim T. M.</b> “Lubrication of infinitely long thrust bearings with micropolar fluids”, <i>Wear, Vol. 89, Issue 2, 15 Aug. 1983, pp. 137-150.</i>
58	<b>Bessonov, N. M.</b> “A new generalization of the Reynolds equation for a micropolar fluid and its application to bearing theory”, <i>Tribol. Int., Vol. 27, Issue 2, Apr. 1994, pp. 105-108.</i>
59	<b>Tomantschger, K. W.</b> “A boundary value problem in the micropolar theory”, <i>ZAMM, Vol. 82, Issue 6, 18 Apr. 2002, pp. 421-422.</i>
60	<b>Wang, X-L. and Zhu, K-Q.</b> “Numerical analysis of journal bearings lubricated with micropolar fluids including thermal and cavitating effects”, <i>Tribol. Int., In Press.</i>
61	<b>Suresh Verma, Vijay Kumar, K. D. Gupta</b> “Analysis of Multirecess Hydrostatic Journal Bearing Operating With Micropolar Lubricant.” <i>J. Tribol - April 2009--Volume 131, Issue 2, 021103 (9 pages).</i>
62	<b>K. Prabhakaran Nair, Mohammed Shabbir Ahmed, Saed Thamer Al-qahtani</b> “Static and dynamic analysis of hydrodynamic journal bearing operating under nano lubricants”, <i>Volume 2, Number 1-6 / 2009 Pages: 251 – 262</i>
63	<b>Ravindra R. Navthar ,Dr. N.V. Halegowda</b> “Stability Analysis of Hydrodynamic Journal Bearing using Stiffness Coefficients” <i>International Journal of Engineering Science and Technology Vol.2 (2), 2010, 87-93</i>